Declassified in Part - Sanitized Copy Approved for Release @ 50-Yr 2013/09/03 : CIA-RDP81-01043R002500170003-9

STAT

Page Denied

Next 1 Page(s) In Document Denied

Declassified in Part - Sanitized Copy Approved for Release @ 50-Yr 2013/09/03 : CIA-RDP81-01043R002500170003-9

Declassified in Part - Sanitized Copy Approved for Release @ 50-Yr 2013/09/03 : CIA-RDP81-01043R002500170003-9

STAT

TRANSISTOR CIRCUIT APPLICATIONS

A STUDY OF TRANSISTOR VIDEO AMPLIFIERS

By

HERBERT HELLERMAN

CARL ZIMMER

Sponsored by
ROME AIR DEVELOPMENT CENTER
Contract No AF30(602)-929

SYRACUSE UNIVERSITY RESEARCH INSTITUTE

ELECTRICAL ENGINEERING DEPARTMENT

Report No EE278 5611F

Declassified in Part - Sanitized Copy Approved for Release @ 50-Yr 2013/09/03 : CIA-RDP81-01043R002500170003-9

Declassified in Part - Sanitized Copy Approved for Release @ 50-Yr 2013/09/03 : CIA-RDP81-01043R002500170003-9

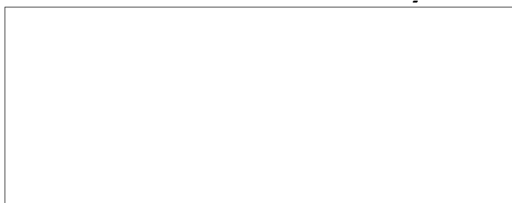

STAT

A STUDY OF TRANSISTOR VIDEO AMPLIFIERS

Final Report

November 1, 1956

AF 30(602)-929

by

Herbert Hellerman

Carl R. Zimmer

This report was produced under a sponsored contract. The conclusions and recommendations expressed are those of the Author(s) and are not necessarily endorsed by the Sponsor. Reproduction of this report, or any portion thereof, must bear reference to the original source and Sponsor.

SYRACUSE UNIVERSITY RESEARCH INSTITUTE

Approved by:

Glenn M. Glasford
Project Director

Sponsored by:

Rome Air Development Center
Griffiss Air Force Base
Rome, New York

S.U.R.I. Report No.

EE278-5611F

Date:

November 1, 1956

Declassified in Part - Sanitized Copy Approved for Release @ 50-Yr 2013/09/03 : CIA-RDP81-01043R002500170003-9

Declassified in Part - Sanitized Copy Approved for Release @ 50-Yr 2013/09/03 : CIA-RDP81-01043R002500170003-9

PREFACE

This report is concerned with the theoretical and experimental results of a study begun in the Fall of 1955 on the general subject of transistor low pass amplifiers. Since the work is still in progress, interim results are reported here.

Most of the effort has been concentrated on wide band response through the use of linear networks to extend the bandwidth beyond that obtainable using the transistors alone. This approach which is usually called equalization requires as a basic starting point the specification of the network to be equalized. In the case at hand a reasonably accurate transistor equivalent circuit must be found before the design of the compensating networks can proceed on a systematic basis. For this reason a good deal of effort has been expended on the small signal equivalent circuit of the junction transistor from both the theoretical and experimental points of view. The theoretical work on this important subject has been first to review and check the results reported in the literature and second, to simplify the general equivalent circuit to fit the impedance conditions met in the video interstage. The representation used has for the most part been the common emitter h parameters and experimental checks have been made on alloy junction, grown junction and surface barrier transistors. Two measurement techniques have been employed. One is a high accuracy bridge which can give precise results for driving point immittances However, since the bridge is rather cumbersome from the point of view of auxilliary equipment needed and numerical work necessary to obtain the final results, a simpler direct reading type of measuring set-up has been developed which can be calibrated against the bridge initially and thereafter give important parameters to a fair degree of accuracy with a maximum of convenience.

Declassified in Part - Sanitized Copy Approved for Release @ 50-Yr 2013/09/03 : CIA-RDP81-01043R002500170003-9

Declassified in Part - Sanitized Copy Approved for Release @ 50-Yr 2013/09/03 : CIA-RDP81-01043R002500170003-9

TABLE OF CONTENTS

PAGE

PREFACE . . . .

CHAPTER 1. PRINCIPLES OF WIDE BAND TRANSISTOR EQUALIZATION 1

CHAPTER 2. THEORETICAL EQUIVALENT CIRCUITS 4

2-1. Alloy- or Fused-Junction Transistors. 4
2-2. Effect of the Base Spreading Resistance r_b' 8
2-3. Approximation for the Grounded-Base Parameters. 12
2-4. Transistor Parameters in the Grounded-Emitter Connection. . . 16
2-5. Approximating the Parameters as Functions of Frequency. . . . 20
2-6. Summary 40

CHAPTER 3. MEASUREMENT OF TRANSISTOR PARAMETERS. 41

3-1. Measurement Techniques. 41
3-2. Measurement of Transistor Parameters using Bridge techniques. 48
3-3. Results for a Fused-Junction Transistor 60
3-4. Results for the Grown-Junction Transistor 74

CHAPTER 4. COMPENSATION USING RC NETWORKS. 80
4-1. Compensation using RC Networks. 80
4-2. Wide Band Response Utilizing Local RC Feedback. 88
4-3. Effect of Load Capacitance. 94
4-4. Experimental Results with RC Local Feedback Equalization. . . 96
4-5. Common Emitter-Common Base Circuit. 99

CHAPTER 5. COMPENSATION USING RL NETWORKS. 103

5-1. Compensated Amplifiers using Simple RL Networks 103
5-2. Single Stage Amplifier with RL Network in Output Circuit. . . 104
5-3. Experimental Single Stage Amplifiers. 110
5-4. Experimental Results. 113
5-5. Interstage Equalization 117
5-6. Two-Stage Amplifier with Interstage and Output Equalization . 119
5-7. Summary 122

APPENDIX . SOME CHARACTERISTICS OF TRANSISTORS UNDER HUSHED BIASING CONDITIONS. 123

Declassified in Part - Sanitized Copy Approved for Release @ 50-Yr 2013/09/03 : CIA-RDP81-01043R002500170003-9

Declassified in Part - Sanitized Copy Approved for Release @ 50-Yr 2013/09/03 : CIA-RDP81-01043R002500170003-9

CHAPTER 1

Principles of Wide Band Transistor Equalization

The purpose of this section is to point out some of the limits on the solution of the problem imposed by the characteristics of realizable networks. It is usually true in low pass amplifier practice that midband gain is exchangeable for bandwidth. The efficiency with which the trade can be accomplished and the limit to which this efficiency may be extended by the use of suitable networks are important fundamental problems. In general it has been found in vacuum tube circuits that the ultimate gain-bandwidth figure of merit of the simplest configuration consisting of a tube working into a shunt capacitance C_o, transconductance g_m and a load resistance interstage R_o is

$$K_o \times f_o = \frac{g_m}{2\pi C_o} \qquad (1\text{-}1)$$

where K_o = midband voltage gain ratio f_o = 3 db bandwidth
Since the minimum value of C_o is the shunt output capacitance of the tube, the ultimate limitation on the figure of merit is dependent on tube parameters only, the interstage resistance R_o just determines the division of gain and bandwidth within the product which has a maximum value that is a constant for a given tube.

Since Eq. (1-1) holds for the specified amplifier structure it is reasonable to inquire into the possibility of obtaining a larger bandwidth for a given gain by employing a more complicated interstage network. The simplest general class of such networks is a two terminal shunt interstage. Bode has shown* that if the gain is to be flat over the desired band the best that can

* "Network Analysis and Feedback Amplifier Design" p. 408 by H. Bode (D. Van Nostrand, 1946)

Declassified in Part - Sanitized Copy Approved for Release @ 50-Yr 2013/09/03 : CIA-RDP81-01043R002500170003-9

Declassified in Part - Sanitized Copy Approved for Release @ 50-Yr 2013/09/03 : CIA-RDP81-01043R002500170003-9

be done with any two terminal interstage limited by a specified shunt capacitance is only a factor of two higher in the figure of merit than for the simplest case of Eq. (1-1). The next step in complexity beyond the simple resistance interstage is the shunt peaking circuit (series L and R across the output). If this is adjusted for no rise in response above the midband value the figure of merit is about 1.8 times the product of Eq. (1-1) or within 20% of the ultimate.

The four terminal interstage can give further improvements although here the design often imposes a restriction on the division of input and output capacitances which is not necessarily the way these capacitances normally appear in practical circuits. However, even neglecting this difficulty it is found that the gain-bandwidth figure of merit for a four terminal interstage is not improved beyond a factor of about 3 over the very simplest case of Eq. (1-1) without considerable complexity in circuit design, construction and adjustment.

Although the above discussion dealt with the tube circuit problem, it is well to summarize the general conclusions which can serve as a guide to what one can look for in the corresponding transistor case. These are:

1. The constraints on video amplifier design are principally due to the parameters of the active device.

2. The parameters of importance as well as an order of magnitude idea of the bandwidth obtainable for a specified midband gain (or vica versa) can be found by an analysis of the simplest configuration.

3. The use of equalizing networks can give improvements in performance over the simplest circuits but the point of diminishing returns is reached very rapidly with regard to circuit complexity unless the amplifier must be designed to give ultimate performance regardless of cost and other factors.

The above discussion outlined the broad aspects of the problem. The logical first step in the consideration of the specific case of transistor low pass amplifiers is the derivation of a suitable transistor equivalent circuit.

Declassified in Part - Sanitized Copy Approved for Release @ 50-Yr 2013/09/03 : CIA-RDP81-01043R002500170003-9

Declassified in Part - Sanitized Copy Approved for Release @ 50-Yr 2013/09/03 : CIA-RDP81-01043R002500170003-9

Using the results of the equivalent circuit investigations, the problem of wide band response has been studied using two distinct approaches. One has utilized interstage networks to obtain the necessary equalization while the other has been to employ local feedback using R-C networks to obtain the desired bandwidth. Preliminary results using both techniques are described in this report.

It is felt that the initial aims of the study have been accomplished. Transistor video amplifiers having voltage gains of about 26 db and bandwidths of 4 Mc. have been constructed using conventional triode transistors. The most important parameters of the transistor intended for use in a video amplifier can now be specified. Future work on extending the response and a study of output circuit limitations will be carried on in the next period.

Declassified in Part - Sanitized Copy Approved for Release @ 50-Yr 2013/09/03 : CIA-RDP81-01043R002500170003-9

Declassified in Part - Sanitized Copy Approved for Release @ 50-Yr 2013/09/03 : CIA-RDP81-01043R002500170003-9

CHAPTER 2

Theoretical Equivalent Circuits

2-1. Alloy - or Fused-Junction Transistor:

For the derivation of an equivalent circuit for the alloy - or fused-junction transistor, we start with the analytical expressions for the y-system parameters of an idealized one-dimensional transistor, as obtained by Early[1]. The geometry of the situation is shown in Figure 2-1 for the case of a PNP transistor, where the boundaries of the regions are plane, parallel, and of infinite extent. The solution is also applicable to an NPN transistor with the roles of holes and electrons interchanged.

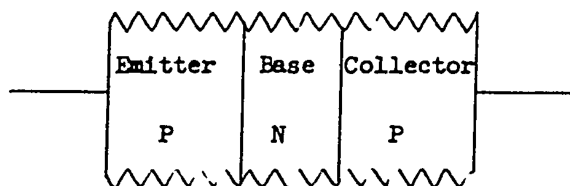

Fig. 2-1. Idealized Transistor Structure.

The parameters are obtained from a solution of the diffusion equation for minority carriers in the base region which satisfies the boundary conditions imposed by the instantaneous collector and emitter potentials, the "one dimension" which enters into the solution being that normal to the boundaries of the regions.

The parameters, for the reference directions and circuit configuration shown in Figure 2-2, are as follows:

[1] "Design Theory of Junction Transistors", by J. M. Early, BSTJ, Vol. 32, pp. 1271-1312, Nov. 1953.

Declassified in Part - Sanitized Copy Approved for Release @ 50-Yr 2013/09/03 : CIA-RDP81-01043R002500170003-9

Declassified in Part - Sanitized Copy Approved for Release @ 50-Yr 2013/09/03 : CIA-RDP81-01043R002500170003-9

$$y_{11}{}^{d} = \left.\frac{I_1'}{E_1'}\right|_{E_2'=0} = \frac{q}{kT}\left| I_e \frac{u_p \tanh \frac{w_o}{L}}{\tanh\left[\frac{w_o}{L} u_p\right]} \right| \qquad (2\text{-}1)$$

$$y_{12}{}^{d} = \left.\frac{I_1'}{E_1'}\right|_{E_1'=0} = -\frac{\partial w}{\partial V_c}\left| I_{pc} \frac{u_p}{L \sinh\left[\frac{w_o}{L} u_p\right]} \right| \qquad (2\text{-}2)$$

$$y_{21}{}^{d} = \left.\frac{I_2'}{E_1'}\right|_{E_2'=0} = -\frac{q}{kT}\left| I_e \frac{u_p \tanh \frac{w_o}{L}}{\sinh\left[\frac{w_o}{L} u_p\right]} \right| \qquad (2\text{-}3)$$

$$y_{22}{}^{d} = \left.\frac{I_2'}{E_2'}\right|_{E_1'=0} = \frac{\partial w}{\partial V_c}\left| I_{pc} \frac{u_p}{L \tanh\left[\frac{w_o}{L} u_p\right]} \right| \qquad (2\text{-}4)$$

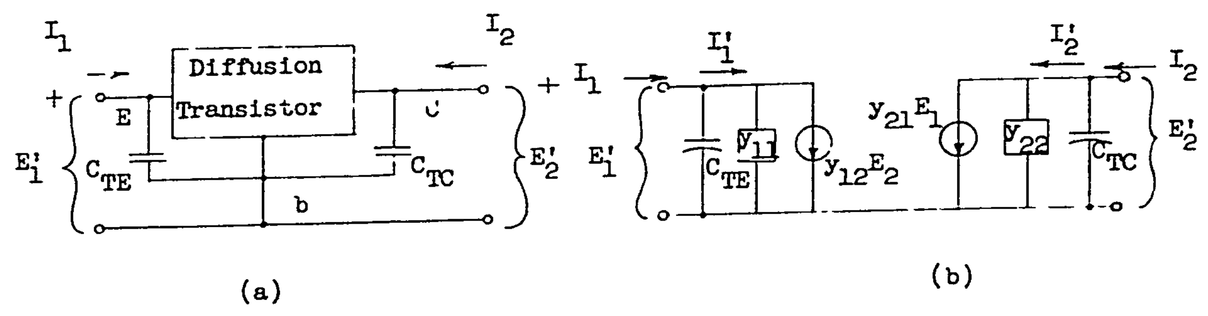

Fig. 2-2(a). Reference Directions for small-signal currents and voltages, grounded-base connection. (b). Circuit representation of the y-system equations. Note that I_1 and I_2' do not include the currents flowing into C_{TE} and C_{TC}, respectively.

Declassified in Part - Sanitized Copy Approved for Release @ 50-Yr 2013/09/03 : CIA-RDP81-01043R002500170003-9

Declassified in Part - Sanitized Copy Approved for Release @ 50-Yr 2013/09/03 : CIA-RDP81-01043R002500170003-9

The quantities involved in Eqs. (2-1) thru (2-4) are:

q = electronic charge

k = Boltzmann's constant

T = absolute temperature

w = width of base region

w_o = time average width of base region

$L = D_p \tau_p$ diffusion length of minority carriers in base region

V_c = collector voltage

τ_p = lifetime of minority carrier in base region

I_{pc} = collector hole bias current

I_e = emitter bias current

and, in addition, the quantity u_p as a function of complex frequency s is given by

$$u_p = \sqrt{1 + s\tau_p} \qquad (2\text{-}5)$$

For steady-state sinusoidal excitation $s = j\omega$ and $u_p = \sqrt{1 + \omega\tau_p}$

If we define g_{11}, g_{12}, etc. as the low frequency (i. e., $s = 0$) values of y_{11}, y_{12}, etc., then:

$$g_{11} = \frac{qI_e}{kT} \left. \frac{u_p \tanh \frac{w_o}{L}}{\tanh \frac{w_o}{L} u_p} \right|_{s=0} = \frac{qI_e}{kT} \qquad (2\text{-}6)$$

$$g_{12} = \frac{\partial w}{\partial V_c} \; Ipc \left. \frac{u_p}{L \sinh \frac{w_o}{L} u_p} \right|_{s=0} = \frac{\partial w}{\partial V_c} \frac{I_{pc}}{L \sinh \frac{w_o}{L}} \qquad (2\text{-}7)$$

$$g_{21} = \frac{qI_e}{kT} \left. \frac{u_p \tanh \frac{w_o}{L}}{\sinh \frac{w_o}{L} u_p} \right|_{s=0} = \frac{qI_e}{kT} \frac{1}{\cosh \frac{w_o}{L}} \qquad (2\text{-}8)$$

Declassified in Part - Sanitized Copy Approved for Release @ 50-Yr 2013/09/03 : CIA-RDP81-01043R002500170003-9

Declassified in Part - Sanitized Copy Approved for Release @ 50-Yr 2013/09/03 : CIA-RDP81-01043R002500170003-9

$$g_{22} = \frac{\partial w}{\partial V_c} I_{pc} \left. \frac{u_p \cosh \frac{w_o}{L} u_p}{L \sinh \frac{w_o}{L} u_p} \right|_{s=0} = \frac{\partial w}{\partial V_c} I_{pc} \frac{\cosh \frac{w_o}{L}}{w_o}$$

Here, the minus signs which are associated with y_{12} and y_{21} have been retained, as these result from our choice of current and voltage reference directions and not from a consideration of the low frequency values. We note that, in the right hand sides of Eqs. (2-6) thru (2-9), all quantities are readily measured with the exception of $\frac{\partial w}{\partial V_c}$, w_o and $\frac{w_o}{L}$. On the other hand, there are four equations, so that the measurement of the low-frequency values enables us to check the validity of the theoretical results. This point will be discussed in detail later.

Referring to Figure 2-2(b), we show the C_{TE} and C_{TC}, the emitter and collector junction capacitances, respectively. The effects of these are not included in the parameters above, so that the next step in the analysis is to take them into account. The impedance level on the emitter side is generally low enough so that C_{TE} may be neglected, even at relatively high frequencies; on the other hand, C_{TC} is important, due to the much higher impedance level in the collector circuit. Thus we have

$$y'_{11} = \frac{E'_1}{I_1} = y_{11}{}^d + sC_{TE} \cong y_{11}{}^d \qquad (2\text{-}10)$$

$$y'_{22} = \frac{E'_2}{I_2} = y_{22}{}^d + sC_{TE} \qquad (2\text{-}11)$$

To summarize, the y-system equations including the effects of C_{TC} and C_{TE} are:

$$I_1 = y_{11}{}^d E'_1 + y_{12}{}^d E'_2 \qquad (2\text{-}12)$$

$$I_2 = y_{21}{}^d E'_1 + (y_{22}{}^d + sC_{TC}) E'_2 \qquad (2\text{-}13)$$

Declassified in Part - Sanitized Copy Approved for Release @ 50-Yr 2013/09/03 : CIA-RDP81-01043R002500170003-9

Declassified in Part - Sanitized Copy Approved for Release @ 50-Yr 2013/09/03 : CIA-RDP81-01043R002500170003-9

2.2 Effect of the Base Spreading Resistance r_b'

One of the assumptions in the one-dimensional analysis previously described is that the base is everywhere at the same potential, i.e. that there is no current flow in the base region parallel to the junctions In the actual transistor, however, the emitter and collector currents are different, and the current flow in the base region produces a transverse voltage drop.

For a transistor structure similar to that of Figure 2-1 but having finite boundaries, the most important effect of this on the equivalent circuit, especially at high frequencies, appears to be the addition of a base spreading resistance r_b' between the base terminal of the diffusion transistor and that of the actual transistor.[3] More complicated physical structures[4] require further additions to the basic equivalent circuit which make it quite difficult to analyze. For this reason our attention will be focused upon the effects of adding r_b' to the equivalent circuit for the diffusion transistor.

In order to find the y-system parameters of the actual transistor, which we denote by y_{11}, y_{12}, etc., it is most convenient to consider the problem as one of two networks connected in series, one of them being the diffusion transistor and the other being the simple network represented by r_b' itself. The z-system parameters of the overall network, i.e., the actual transistor, are then the sum of the corresponding parameters for the two networks. The manipulations involved may be handled through the use of matrices[5], as transformations from the y-system to the z-system, and vice versa, are necessary.

The y-matrix for the diffusion transistor, denoted by $[y]_d$, is

3,4. See, for example, the paper by Early previously cited.

5. Matrix methods applicable to this type of problem are described in Chapter 15 of "Principles of Transistor Circuits", John Wiley and Sons (1953).

Declassified in Part - Sanitized Copy Approved for Release @ 50-Yr 2013/09/03 : CIA-RDP81-01043R002500170003-9

Declassified in Part - Sanitized Copy Approved for Release @ 50-Yr 2013/09/03 : CIA-RDP81-01043R002500170003-9

$$[y]_d = \begin{bmatrix} y_{11}^d & y_{12}^d \\ y_{21}^d & y_{22}^d + sC_{TC} \end{bmatrix} \qquad (2\text{-}14)$$

The z-matrix for the diffusion transistor, $|z|_d$, is expressed in terms of the y's for the diffusion transistor as

$$|z|_d = \begin{bmatrix} z_{11}^d & z_{12}^d \\ z_{21}^d & z_{22}^d \end{bmatrix} = \frac{1}{\Delta_y^d} \begin{bmatrix} y_{22}^d + sC_{TC} & -y_{12}^d \\ -y_{21}^d & y_{11}^d \end{bmatrix} \qquad (2\text{-}15)$$

where

$$\Delta_y^d = \begin{bmatrix} y_{11}^d & y_{12}^d \\ y_{21}^d & y_{22}^d + sC_{TC} \end{bmatrix} = y_{11}^d \,(y_{22}^d + sC_{TC}) - y_{12}^d\, y_{21}^d \qquad (2\text{-}16)$$

Referring to Figure 3, the z-matrix for the network consisting of r_b' is simply

$$[z]_{r_b'} = \begin{bmatrix} r_b' & r_b' \\ r_b' & r_b' \end{bmatrix} \qquad (2\text{-}17)$$

and $|Z|$, the z-matrix for the actual transistor, is

$$[Z] = [Z]_d + [Z]r_b' = \begin{bmatrix} \dfrac{y_{22}^d + sC_{TC}}{\Delta_y^d} + r_b' & \dfrac{-y_{12}^d}{} + r_b'\ \Delta y^d \\ \dfrac{-y_{21}^d}{\Delta_y^d} + r_b' & \dfrac{y_{11}^d}{\Delta_y^d} + r_b' \end{bmatrix} \qquad (2\text{-}18)$$

Declassified in Part - Sanitized Copy Approved for Release @ 50-Yr 2013/09/03 : CIA-RDP81-01043R002500170003-9

Declassified in Part - Sanitized Copy Approved for Release @ 50-Yr 2013/09/03 : CIA-RDP81-01043R002500170003-9

The final step is to convert from the z-system for the actual transistor to the y-system, as the latter are more accurately measured in the laboratory. The y-matrix for the actual transistor is

$$[y] = \frac{1}{\Delta_z}\begin{bmatrix} z_{22} & -z_{12} \\ -z_{21} & z_{11} \end{bmatrix} \tag{2-19}$$

We next evaluate Δ_z as

$$\Delta_z = \begin{bmatrix} z_{11} & z_{12} \\ z_{21} & z_{22} \end{bmatrix} = z_{11}\, z_{22} - z_{12}\, z_{21}$$

$$= \left(\frac{1}{\Delta_y{}^d}\right)^2 (y_{22}{}^d + sC_{TC} + r_b'\,\Delta_y{}^d)(y_{11}{}^d + r_b'\,\Delta_y{}^d) - (y_{12}{}^d + r_b'\,\Delta_y{}^d)(y_{21}{}^d + r_b'\,\Delta_y{}^d)$$

$$= \left(\frac{1}{\Delta_y{}^d}\right)^2 y_{11}{}^d\,(y_{22}{}^d + sC_{TC}) - y_{12}{}^d\, y_{21}{}^d + \Delta_y{}^d\, r_b'\,(y_{22}{}^d + sC_{TC} + y_{11}{}^d - y_{12}{}^d - y_{21}{}^d)$$

$$= \frac{1}{\Delta_y{}^d}\; 1 + r'_b\,(y_{22}{}^d + sC_{TC} + y_{11}{}^d - y_{12}{}^d - y_{21}{}^d) \tag{2-20}$$

The result for y_{11} of the actual transistor becomes

$$y_{11} = \frac{z_{22}}{\Delta_z} = \frac{\frac{1}{\Delta_y{}^d}\; y_{11}{}^d + r_b'\,\Delta_y{}^d}{\frac{1}{\Delta_y{}^d}\; 1 + r_b'\,(y_{11}{}^d + y_{22}{}^d + sC_{TC} - y_{12}{}^d - y_{21}{}^d)}$$

Declassified in Part - Sanitized Copy Approved for Release @ 50-Yr 2013/09/03 : CIA-RDP81-01043R002500170003-9

Declassified in Part - Sanitized Copy Approved for Release @ 50-Yr 2013/09/03 : CIA-RDP81-01043R002500170003-9

$$= \frac{y_{11}{}^{d} + r_b' \, \Delta_y{}^{d}}{1 + r_b' \, (y_{11}{}^{d} + y_{22}{}^{d} + sC_{TC} - y_{12}{}^{d} - y_{21}{}^{d}} \qquad (2\text{-}21)$$

We note that, for the case where r_b' is zero, this expression reduces to $y_{11}{}^{d}$, as it should. The other y parameters are

$$y_{12} = \frac{-z_{12}}{\Delta_z} = \frac{y_{12}{}^{d} - r_b' \, \Delta_y{}^{d}}{D} \qquad (2\text{-}22)$$

$$y_{21} = \frac{-z_{21}}{\Delta_z} = \frac{y_{21}{}^{d} - r_b' \, \Delta_y{}^{d}}{D} \qquad (2\text{-}23)$$

$$y_{22} = \frac{z_{11}}{\Delta_z} = \frac{y_{22}{}^{d} + sC_{TC} + r_b' \, \Delta_y{}^{d}}{D} \qquad (2\text{-}24)$$

$$\text{where } D = 1 + r_b' \left| \, y_{11}{}^{d} + y_{22}{}^{d} + sC_{TC} + y_{12}{}^{d} + y_{21}{}^{d} \, \right| \qquad (2\text{-}25)$$

Of these, the ones with which we will mainly be concerned are y_{11}, y_{21} and y_{22} - the first two because they determine α, the short-circuit current gain in the grounded-base connection for the actual transistor, and y the latter because it is the same as y_{22} for the actual transistor in the grounded-emitter connection.

Declassified in Part - Sanitized Copy Approved for Release @ 50-Yr 2013/09/03 : CIA-RDP81-01043R002500170003-9

Declassified in Part - Sanitized Copy Approved for Release @ 50-Yr 2013/09/03 : CIA-RDP81-01043R002500170003-9

2-3. Approximations for the grounded-base parameters

Due to our assumption of unity collector and emitter efficiencies, the y-parameters for the diffusion transistor (with consideration of C_{TE} and C_{TC} neglected) are not all independent. Referring to Eqs. (2-1) thru (2-4), we form the ratio

$$\frac{y_{21}^{d}}{y_{11}^{d}} = \frac{\dfrac{-qI_e}{kT}\,\dfrac{u_p \tanh \frac{w_o}{L}}{\sinh \frac{w_o}{L} u_p}}{\dfrac{qI_e}{kT}\,\dfrac{u_p \tanh \frac{w_o}{L}}{\tanh \frac{w_o}{L} u_p}} = -\frac{1}{\cosh \frac{w_o}{L} u_p} \qquad (2\text{-}26)$$

Similarly, forming

$$\frac{-\dfrac{\partial w}{\partial V_c} I_{pc} \dfrac{u_p}{L \sinh \frac{w_o}{L} u_p}}{\dfrac{\partial w}{\partial V} I_{pc} \dfrac{u_p}{L \tanh \frac{w_o}{L} u_p}} = -\frac{1}{\cosh \frac{w_o}{L} u_p} \qquad (2\text{-}27)$$

Thus we have the useful relationship $y_{21}^{d}/y_{11}^{d} = y_{11}^{d}/y_{22}^{d}$, which simplifies the preceeding derivations considerably. For example, the quantity Δy^{d} becomes

$$\Delta y^{d} = y_{11}^{d}\, y_{22}^{d} - y_{12}^{d}\, y_{21}^{d} + sC_{TC}\, y_{11}^{d}$$

$$= y_{11}^{d}\, y_{12}^{d} \left\{ \frac{y_{22}^{d}}{y_{12}^{d}} - \frac{y_{21}^{d}}{y_{11}^{d}} \right\} + sC_{TC}\, y_{11}^{d}$$

Declassified in Part - Sanitized Copy Approved for Release @ 50-Yr 2013/09/03 : CIA-RDP81-01043R002500170003-9

Declassified in Part - Sanitized Copy Approved for Release @ 50-Yr 2013/09/03 : CIA-RDP81-01043R002500170003-9

$$= y_{11}^d \, y_{12}^d \left\{ \frac{1}{y_{21}^d} - \frac{y_{21}^d}{y_{11}^d} \right\} + sC_{TC} \, y_{11}^d \quad \text{since} \quad \frac{y_{12}^d}{y_{22}^d} = \frac{y_{21}^d}{y_{11}^d} \tag{2-28}$$

$$= y_{11}^d \, y_{12}^d \left\{ \frac{1}{-\alpha_d} + \alpha_d \right\} + sC_{TC} \, y_{11}^d = - y_{11}^d \, y_{12}^d \, \frac{1 - \alpha_d^2}{\alpha_d} \pm sC_{TC} \, y_{11}^d$$

The quantity $\alpha_d = -\frac{y_{21}^d}{y_{11}^d}$ which was introduced in Eq. (2-28) is of considerable importance. This is the short circuit current gain (for the diffusion transistor) in the grounded-base connection, the frequency dependence of which is given by Eq. (2-26). The minus sign in (2-26) is due to our choice of current reference directions, and indicates that current flow is out of the collector terminal when current flows into the emitter terminal. Also, since w_o/L is typically in the range 0.14-0.30, the low-frequency value of α_d is very close to, but slightly less than, unit.

This means that Δ_y^d as given by Eq. (2-28) is approximately equal to $2(1 - \alpha_d) \, g_{11}^d \, g_{12}^d$.

Since g_{12} is on the order of 10^{-3} times g_{11}, and $(1 - \alpha_d)$ is on the order of 0.05 at the most for representative transistors, the quantity $r_b' \, \Delta_y^d$ can usually be neglected in the expressions for y_{11} and y_{21}. This gives us

$$y_{11} = \frac{y_{11}^d}{D} \tag{2-29}$$

$$y_{21} = \frac{y_{21}^d}{D} \tag{2-30}$$

together with the very important result that, since α for the actual transistor is given by $- y_{21}/y_{11}$, it is, to a good approximation, the same as α_d. This is considered in detail in Section 2-4.

Declassified in Part - Sanitized Copy Approved for Release @ 50-Yr 2013/09/03 : CIA-RDP81-01043R002500170003-9

Declassified in Part - Sanitized Copy Approved for Release @ 50-Yr 2013/09/03 : CIA-RDP81-01043R002500170003-9

Before discussing the frequency dependence of α, we will express the quantity $D = 1 + r_b' \left| sC_{TC} + y_{11}^d + y_{12}^d + y_{21}^d + y_{22}^d \right|$ in a simpler form which involves α. This is done by rewriting it as

$$D = 1 + sr_b' C_{TC} + y_{11}^d \left(1 + \frac{y_{21}^d}{y_{11}^d}\right) + y_{22}^d \left(1 + \frac{y_{12}^d}{y_{22}^d}\right)$$

$$= 1 + sr_b' C_{TC} + r_b' (y_{11}^d + y_{22}^d) (1 - \alpha) \qquad (2\text{-}31)$$

$$\text{since } \alpha_d = -\frac{y_{21}^d}{y_{11}^d} = -\frac{y_{12}^d}{y_{22}^d}$$

$$= 1 + y_{11}^d (1 - \alpha_d)$$

The last result above is obtained by recognizing that y_{11} and y_{22} have the same frequency variation, and that $g_{22} \ll g_{11}$, so that we may neglect the effect of y_{22}. Also, for a typical transistor having $r_b' = 100$ ohms and $C_{TC} =$ 5 mmfd., the $r_b' C_{TC}$ product represents a time constant of 5×10^{-4} microseconds or a frequency of about 300 megacycles. This time constant can be neglected compared to the much larger time constants present in $y_{11}^d(1 - \alpha)$. |See Eq. 2-76|.

Declassified in Part - Sanitized Copy Approved for Release @ 50-Yr 2013/09/03 : CIA-RDP81-01043R002500170003-9

Declassified in Part - Sanitized Copy Approved for Release @ 50-Yr 2013/09/03 : CIA-RDP81-01043R002500170003-9

is obtained from it.

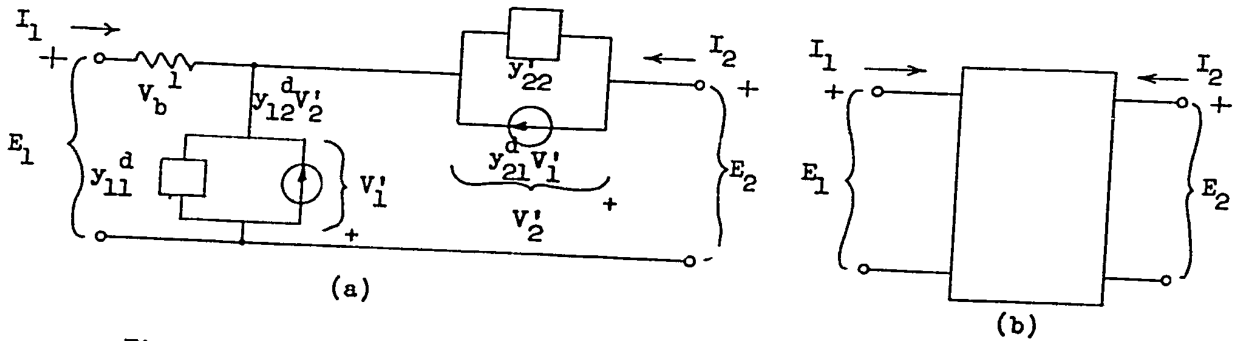

Fig. 2-5. The y's in this figure are those for the grounded-base connection.

In the grounded-emitter connection, the extrinsic base spreading resistance r_b' appears effectively in series with the source driving the transistor. From a consideration of the definition of the y-system parameters, it is seen that each of the y's in the grounded-emitter connection will involve r_b' and the y's for the grounded-base connection. The work of obtaining the former can be shortened by deriving only some of the y's for the grounded-emitter connection, and some of the h's, or hybrid parameters, from Figure 2-5. Since conversions between the two systems are available (as listed in Figure 2-6), the complete y or h representation is easily obtained.

Figure 2-6. h-and y-system equations and conversion tables. The reference directions are the same as those shown in Figure 2-5(b)

y - System	h - System
$I_1 = y_{11e}E_1 + y_{12e}E_2$ $I_2 = y_{21e}E_1 + y_{22e}E_2$	$E_1 = h_{11e}I_1 + h_{12e}E_2$ $I_2 = h_{21e}I_1 + h_{22e}E_2$
$y_{11e} = \frac{1}{h_{11e}}$ $y_{12e} = -\frac{h_{12e}}{h_{11e}}$ $y_{21e} = \frac{h_{21e}}{h_{11e}}$ $y_{22e} = \frac{\Delta_{he}}{h_{11e}}$	$h_{11e} = \frac{1}{y_{11e}} + h_{12e}E_2$ $h_{12e} = -\frac{y_{12e}}{y_{11e}}$ $h_{21e} = \frac{y_{21e}}{y_{11e}}$ $h_{22e} = \frac{\Delta_{ye}}{y_{11e}}$

Declassified in Part - Sanitized Copy Approved for Release @ 50-Yr 2013/09/03 : CIA-RDP81-01043R002500170003-9

Declassified in Part - Sanitized Copy Approved for Release @ 50-Yr 2013/09/03 : CIA-RDP81-01043R002500170003-9

2-4. Transistor Parameters in the Grounded-Emitter Connection

The discussion in the two preceeding sections has dealt with the y-parameters of the transistor in the grounded-base connections. For use as a video amplifier, as well as a considerable number of their applications, the grounded-emitter connection is more advantageous, primarily because it offers the possibility of a reasonably high low-frequency input resistance coupled with very considerable voltage gains. (These points are discussed in detail in Chapter 4.

Figure 2-3 shows the transistor in the grounded-emitter connection, together with reference directions for the small-signal voltages and currents. We may define a set of y-parameters[6] for the grounded-emitter connection, and, to distinguish these from their grounded-base counterparts, denote them by y_{11e}, etc. This is shown in Figure 2-4, which represents the equations.

$$I_1 = y_{11e}E_1 + y_{12e}E_2 \qquad I_2 = y_{21e}E_1 + y_{22e}E_2 \qquad (2\text{-}32)$$

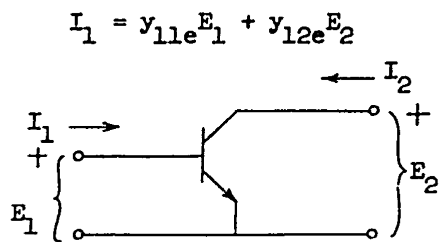

Fig. 2-3. Transistor in Grounded-Emitter Connection.

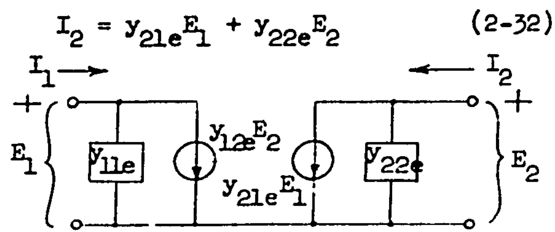

Fig. 2-4. y-parameter representation of (2-3), small-signal basis.

The y's in Figure 2-4 can be expressed in terms of those for the grounded-base connection, either by considering the relations among currents and voltages in each connection, and solving for the desired quantity using the defining equations for each case, or by re-drawing Figure 2-2(b) as is shown in Figure 2-5 and computing the grounded-emitter parameters from it. The latter procedure will be used here, as a better overall picture of the circuit performance

[6] Here taken to include both r_b' and C_{TC}.

Declassified in Part - Sanitized Copy Approved for Release @ 50-Yr 2013/09/03 : CIA-RDP81-01043R002500170003-9

Declassified in Part - Sanitized Copy Approved for Release @ 50-Yr 2013/09/03 : CIA-RDP81-01043R002500170003-9

The characteristic feature of the h-system is that measurements on the input side of the network are made with the output end short-circuited, while those on the output side are made with the input open-circuited. For the transistor, with its high output and low input impedances (in both grounded- base and grounded-emitter connections), these parameters are a logical choice. It is to be emphasized, however, that at high frequencies parasitic capacitances and other loading considerations make the achievement of a true open-circuit at the input terminals difficult to realize, in which case the y-system, with its short circuit terminations on both input and output, becomes the most practical choice.

We note that $h_{21e} = I_2/I_1 \big|_{E_2 = 0} = b$ is the short circuit current gain for the grounded emitter connection, analogous to α for the grounded base connection. Since the grounded emitter stage is approximately terminated in a short circuit and fed from a high impedance source in a simple cascade GE or GB amplifier h_{21e} is of considerable practical value in determining the behavior of cascaded transistor amplifiers. Similarly, h_{11e} (or y_{11e}) is a useful design parameter.

In the preceeding paragraph, we have assumed that the input impedance of the driven transistor is small compared to that of the resistances used to provide DC biases for the stages. This requirement is not difficult to meet for practical circuits; however, if we investigate the question of the effect of these resistances on the voltage-gain bandwidth product of the GE stage, we find that wide bandwidths require low values of resistance, and vice versa. In other words, a low value of resistance reduces the low-frequency voltage gain, but increases the bandwidth. The important conclusion to be drawn from this situation is that, to achieve wide bandwidths, the transistor is driven not from a high, but a very low impedance source; hence the y-parameters are more representative of the circuit conditions than are the h-parameters. Since wide-band amplifiers are the subject of interest here, the emphasis will be

Declassified in Part - Sanitized Copy Approved for Release @ 50-Yr 2013/09/03 : CIA-RDP81-01043R002500170003-9

Declassified in Part - Sanitized Copy Approved for Release @ 50-Yr 2013/09/03 : CIA-RDP81-01043R002500170003-9

placed on the former, although the latter will also be included.

Returning to the problem of obtaining the common-emitter circuit parameters from the configuration of Figure 2-5, the y-parameters which are most easily obtained are y_{11e} and y_{22e}, while h_{12e} and h_{21e} are also obtained without undue difficulty. The expressions for these in terms of r_b' and the grounded base y's of the diffusion transistor are:

$$y_{11e} = \frac{1}{r_b' + \frac{1}{\sum y_d + sC_{TC}}} \tag{2-32}$$

$$h_{12e} = \frac{y_{12}{}^d + y_{22}{}^d + sC_{TC}}{\sum y_d + sC_{TC}} \tag{2-33}$$

$$h_{21e} = \frac{-\left(y_{21}{}^d + y_{22}{}^d + sC_{TC}\right)}{\sum y_d + sC_{Tc}} \tag{2-34}$$

$$y_{22e} = y_{22} = \frac{y_{22}{}^d + sC_{TC}}{1 + r_b' \sum y_d + sC_{TC}} \tag{2-35}$$

where

$$\begin{aligned} \sum y_d &= \text{sum of the y-parameters of the diffusion transistor} \\ &= y_{11}{}^d + y_{12}{}^d + y_{21}{}^d + y_{22}{}^d \\ &= y_{11}{}^d (1 - \alpha_d) \end{aligned} \tag{2-36}$$

the latter expression being obtained from the development in Eq. 2-31. Using the table in Figure 2-6, we fill in the additional parameters in each system:

$$h_{11e} = \frac{1}{y_{11e}} = r_b' + \frac{1}{\sum y_d + sC_{TC}} \tag{2-37}$$

Declassified in Part - Sanitized Copy Approved for Release @ 50-Yr 2013/09/03 : CIA-RDP81-01043R002500170003-9

Declassified in Part - Sanitized Copy Approved for Release @ 50-Yr 2013/09/03 : CIA-RDP81-01043R002500170003-9

$$y_{12e} = -\frac{h_{12e}}{h_{11e}} = \frac{\dfrac{y_{12}^{d} + y_{22}^{d} + sC_{TC}}{\sum y_d + sC_{TC}}}{-\left(r_b' + \dfrac{1}{\sum y_d + sC_{TC}}\right)} \qquad (2\text{-}38)$$

$$= -\frac{y_{12}^{d} + y_{22}^{d} + sC_{TC}}{1 + r_b' \left(\sum y_d + sC_{TC}\right)}$$

$$y_{21e} = \frac{h_{21e}}{h_{11e}} = \frac{\dfrac{-\ y_{21}^{d} + y_{22}^{d} - sC_{TC}}{\sum y_d + sC_{TC}}}{r_b' + \dfrac{1}{\sum y_d + sC_{TC}}} \qquad (2\text{-}39)$$

$$= \frac{+(y_{21}^{d} + y_{22}^{d} + sC_{TC})}{1 + r_b' \left(\sum y_d + sC_{TC}\right)}$$

$$h_{22e} = \frac{\Delta_{ye}}{y_{11e}} = \frac{y_{11e}\, y_{22e} - y_{12e}\, y_{21e}}{y_{11e}} = y_{22e} - \frac{y_{21e}}{y_{11e}}\, y_{12e} \qquad (2\text{-}40)$$

In the case of h_{22e}, the result has been left in terms of the other GE parameters, as it is simpler to interpret after we have discussed the behavior of the y-parameters. However, an equivalent circuit involving hyperbolic functions is so cumbersome as to be worthless for design purposes, so that the next section considers the problem of approximating the hyperbolic functions, the accuracy to be expected of different types of representations, and the types of laboratory measurement which will yield the greatest amount of design information.

Declassified in Part - Sanitized Copy Approved for Release @ 50-Yr 2013/09/03 : CIA-RDP81-01043R002500170003-9

Declassified in Part - Sanitized Copy Approved for Release @ 50-Yr 2013/09/03 : CIA-RDP81-01043R002500170003-9

2-5. Approximating the Parameters as Functions of Frequency

A. One method of representing sinh x and cosh x for small values of x is to take their power series expansions and use only the first few terms, depending on how much accuracy is desired. These expansions are, for sinh x and cosh x:

$$\sinh x = x + \frac{x^3}{3!} + \frac{x^5}{5!} + - - + \frac{x^n}{n!} \qquad n \text{ odd} \qquad (2\text{-}41)$$

$$\cosh x = 1 + \frac{x^2}{2!} + \frac{x^4}{4!} + - - - + \frac{x^n}{n!} \qquad n \text{ even} \qquad (2\text{-}42)$$

and for tanh x we use sinh x/cosh x,

$$\tanh x = \frac{x + x^3/3! + x^5/5! + --}{1 + \frac{x^2}{2!} + \frac{x^4}{4!} - - -} \qquad (2\text{-}43)$$

Using these expressions, we could proceed to approximate any of the parameters which were derived in the previous section. However, it turns out that the low-frequency values of certain parameters are very simply expressed in terms of τ_p, w_o, and L, these being physical quantities which were defined in connection with Eqs. (2-1) through (2-4).

B. Low frequency value of short-circuit current gain in GB connection.

The short circuit GB current gain for the diffusion transistor is approximated as follows:

$$\alpha_o{}^d = - \frac{g_{21}{}^d}{g_{11}{}^d} = \frac{1}{\cosh \frac{w_o}{L}} = \frac{1}{1 + \frac{1}{2!} (\frac{w_o}{L})^2} \qquad (2\text{-}44)$$

Since α_o, the current gain for the actual transistor considering r_b', is nearly equal to $\alpha_o{}^d$, the above expression can be used for α_o as well.

C. Low frequency value of short-circuit current gain in GE connection

This is the low frequency value of $h_{21e} = b$ (see Eq. 2-34), and will be denoted by b_o. Referring to Eq. 2-34, we have

Declassified in Part - Sanitized Copy Approved for Release @ 50-Yr 2013/09/03 : CIA-RDP81-01043R002500170003-9

Declassified in Part - Sanitized Copy Approved for Release @ 50-Yr 2013/09/03 : CIA-RDP81-01043R002500170003-9

$$b_o = \frac{-(g_{21}{}^d + g_{22}{}^d)}{\sum g_d} = \frac{-g_{12}{}^d}{g_{11}{}^d\ (1 - \alpha_o{}^d)} = \frac{\alpha_o{}^d}{1 - \alpha_o{}^d} \qquad (2\text{-}45)$$

and, substituting for $\alpha_o{}^d$ from the preceeding equation 2-44.

$$b_o = \frac{2}{(\frac{w_o}{L})^2} \qquad \frac{w_o}{L} \ll 1 \qquad (2\text{-}46)$$

which shows that, for L constant, b_o varies as the square of the base width w_o. Also, since $[w_o/L]^2$ is much less than 1, b_o is quite large, on the order of 20 to 100 for commercially available transistors, so that the GE connection offers a high current gain, in contrast to the nearly unity current gain of the GB connection.

D. Cutoff frequencies for α_d and b.

It can be seen from Eqs. (2-26) and 2-34) that both α_d and b are frequency dependent. If we set $s = j\omega$ to examine the steady-state behavior, the cutoff frequencies f_α and f_b are defined as those frequencies at which the magnitudes of α and b, respectively are 70.7% of their low frequency values, or 3 db down. This definition for the cutoff frequencies is a holdover from vacuum tube amplifiers, where response functions of the form

$$K(j\omega) = \frac{k_o}{1 + j\frac{f}{f_1}}$$

are frequently encountered, and is logical inasmuch as it corresponds to a simply computed value of $K(j\omega)$. In the case of the transistor, we are usually concerned with functions which cannot be represented in this simple form, so that the analytical determination of the cutoff frequencies is a much more complex task than would be the case if a new definition had been adopted.

Starting with Eq. (2-26) for α_d, we have

Declassified in Part - Sanitized Copy Approved for Release @ 50-Yr 2013/09/03 : CIA-RDP81-01043R002500170003-9

Declassified in Part - Sanitized Copy Approved for Release @ 50-Yr 2013/09/03 : CIA-RDP81-01043R002500170003-9

$$|\alpha_d(j\omega_\alpha)| = \left|\frac{1}{\cosh k\sqrt{1 + j\omega_\alpha\tau_p}}\right| = \frac{1}{\sqrt{2}}, \qquad (2\text{-}47)^*$$

since $k = \frac{w_c}{L}$. Also, $\omega_\alpha\tau_p \gg 1$, so that 2-47 simplifies

$$\left|\cosh k\sqrt{j\omega_\alpha\tau_p}\right|^2 = \left|\cosh k\sqrt{\frac{\omega_\alpha\tau_p}{2}}(1 + j)\right|^2 = 2 \qquad (2\text{-}48)$$

The use of the identity for $\cosh z = \cosh (x + jy)$

$$|\cosh (x + jy)|^2 = \sinh^2 y \qquad (2\text{-}49)$$

leads to the expression

$$\sinh^2 k\sqrt{\frac{\omega_\alpha\tau_p}{2}} + \cos^2 k\sqrt{\frac{\omega_\alpha\tau_p}{2}} = 2 \qquad (2\text{-}50)$$

This can be further reduced, through the use of the exponential forms for sinh x and cos x, to obtain a transcedental equation

$$\sinh 2k\sqrt{\frac{\omega_\alpha\tau_p}{2}} + \cos 2k\sqrt{\frac{\omega_\alpha\tau_p}{2}} = 4 \qquad (2\text{-}51)$$

A cut-and-try solution of this yields $k\sqrt{\frac{\omega_\alpha\tau_p}{2}} = 1.12$, and finally

$$\omega_\alpha = \left(\frac{2}{k^2}\right)\frac{1.25}{\tau_p} \qquad (2\text{-}52)$$

The factor $2/k^2$ is brought out separately, since we showed previously that this is the same as b_c.

$$\omega_\alpha = \frac{1.25\, b_c}{\tau_p} \qquad (2\text{-}53)$$

The only approximation made in this derivation, that $\omega_\alpha\tau_p \gg 1$, is seen to be a very good one, as b_o is on the order of 20 to 100, so that (2-53) may be considered as virtually an exact relationship.

---

*Results similar to those obtained here have been obtained by R. L. Pritchard "Frequency Variations of Current-Amplification Factor for Junction Transistor", Proc. I. R. E., 40, p. 1476, Nov. 1952.

Declassified in Part - Sanitized Copy Approved for Release @ 50-Yr 2013/09/03 : CIA-RDP81-01043R002500170003-9

Declassified in Part - Sanitized Copy Approved for Release @ 50-Yr 2013/09/03 : CIA-RDP81-01043R002500170003-9

We proceed in an analogous manner to find the b-cutoff frequency by substituting from Eq. (2-26) into Eq. (2-34, to obtain

$$b(s) = h_{21e} = \frac{-(y_{21}{}^{d} + y_{22}{}^{d} + sC_{TC})}{\sum y_d + sC_{TC}} \qquad (2\text{-}54)$$

$$\simeq \frac{\alpha_d + \dfrac{sC_{TC}}{y_{11}{}^{d}}}{1 - \alpha_d + \dfrac{sC_{TC}}{y_{11}{}^{d}}} \quad \text{since } y_{22}{}^{d} \ll y_{21}{}^{d}$$

The effect of the term $j\omega C_{TC}/y_{11}{}^{d}$ in determining the b-cutoff frequency is negligible here, the major contributing factor being $1 - \alpha_d$. The result for the angular b-cutoff frequency ω_b is, to a very good approximation[7],

$$\omega_b = \frac{1}{\tau_p} \qquad (2\text{-}55)$$

Substituting this result back into Eq. (2-53), we have the relation

$$\omega_\alpha = 1.25\ b_o\ \omega_b \text{ or } f_\alpha = 1.25\ b_o\ f_b \qquad (2\text{-}56)$$

which is in the nature of a (current) gain-bandwidth product dependent only on the cutoff frequency of the transistor. This relation is of considerable value in the design of wide-band transistor amplifiers.

E. In deriving the ab-ve results, we have used series approximations only to simplify the low-frequency values, and have used what amounts to the exact analytical expressions in determining the cutoff frequencies. This is an important point, as the process of first taking the series approximation <u>as a function of frequency</u>, and then determining the cutoff frequencies from the approximation, is of dubious value <u>unless</u> the results are checked against the exact values.

---

[7] This assumes that both the emitter efficiency γ and the transport factor β are very close to unity (see reference of Footnote 1).

Declassified in Part - Sanitized Copy Approved for Release @ 50-Yr 2013/09/03 : CIA-RDP81-01043R002500170003-9

Declassified in Part - Sanitized Copy Approved for Release @ 50-Yr 2013/09/03 : CIA-RDP81-01043R002500170003-9

In addition to the power series approximation which has been given, an alternate method exists of expanding the functions of $ku_p = k\sqrt{1 + s\tau_p}$ which are present in the expressions for the transistor parameters. This is to express the function as the product of an infinite number of terms[8] of the form $(1 - sT_n,)$ i.e.,

$$F(ku_p) = A(1 - sT_o)(1 - sT_1) - - - - (1 - sT_n) \qquad (2\text{-}57)$$

where A is a constant. We see by setting $s = 0$ (which corresponds to the low-frequency value of F) that A is real and equal to F(k). An expansion of the form of (2-57) has considerable practical utility in network analysis, as the quantities T_1, T_2, etc. enter directly into the response of the network to an arbitrary excitation as determined through the use of the Laplace transformation.

As it turns out, it is not difficult to obtain such expansions for the most important parameters. For example, to find the T_n's for α, we set $\cosh ku_p = 0$, and solve for the resulting values of s. These are

$$s_n = \frac{1}{\tau}\left[-1 - (n + \tfrac{1}{2})^2 \frac{\pi^2}{k^2}\right] \cong -\frac{1}{\tau}(n + \tfrac{1}{2})^2 \frac{\pi^2}{k^2} \qquad (2\text{-}58)$$

$$n = 0, 1, 2, 3 - - -$$

The steps in this process are as follows: first, since s may be a complex number, we set $ku_p = k\sqrt{1 + s\tau_p} = z$, where z is the complex variable $x + jy$. Setting $\cosh z = 0$ requires that both the real and imaginary parts be simultaneously zero, giving

$$\cosh x \cos y = 0 \qquad \sinh x \sin y = 0 \qquad (2\text{-}59)$$

which have the solutions

8. For a discussion of infinite products, see E. T. Copson, "An Introduction to the Theory of Functions of a Complex Variable" Oxford University Press (1935) pp. 102-106.

Declassified in Part - Sanitized Copy Approved for Release @ 50-Yr 2013/09/03 : CIA-RDP81-01043R002500170003-9

Declassified in Part - Sanitized Copy Approved for Release @ 50-Yr 2013/09/03 : CIA-RDP81-01043R002500170003-9

$$Z_n = x + jy = 0 + j\left(n + \frac{1}{2}\right)\pi \quad n = 0, 1, 2, \text{ etc.} \qquad (2\text{-}60)$$

The values of s_n in (2-58) follow directly from this. Using the relations $b_o = 2/k^2$ and $\omega_b = \frac{1}{\tau_p}$, (2-58) can be written

$$s_n = \frac{-\omega_b\, b_o}{2}\left(n + \frac{1}{2}\right)^2\pi^2 \qquad (2\text{-}61)$$

Thus,

$$\cosh ku_p = (s - s_o)(s - s_1) - - - - (s - s_n) \quad n = 0,1,2,3 - -$$

$$= \frac{1}{s_1\, s_2 - - s_n}\left(1 + \frac{s}{s_1}\right)\left(1 + \frac{s}{s_2}\right) - - - \left(1 + \frac{s}{s_n}\right) \qquad (2\text{-}62)$$

If we compare the latter form of (2-62) with (2-57), we see that $T_n = 1/s_n$ and that A is the product of all the T_n's. Our product expansion for $\alpha(s)$ becomes

$$\alpha(s) = \frac{1}{\cosh k \quad (1 + sT_o)(1 + sT_1) - - - - (1 + sT_n)}$$

$$= \frac{\alpha_o}{\left[1 + \frac{s}{\frac{\pi^2}{8}\omega_b\, b_o}\right]\left[1 + \frac{s}{\frac{9\pi^2}{8}\omega_b\, b_o}\right] - - \text{ etc.}} \qquad (2\text{-}63)$$

If we set $s = j\omega$ in Eq. (2-63) to determine the steady-state behavior of α, the α cutoff frequency as predicted from using the first term only is seen to be $\omega_\alpha = \frac{\pi^2}{8} b_o\, \omega_b = 1.23\, \omega_b\, b_o$. which is almost exactly equal to ω_α as determined from an exact solution.[9] The reason for this can be seen from (2-63) where the second factor involving T_1 has a cutoff frequency by itself of $9\omega_\alpha$. Thus, the second factor contributes almost no amplitude error, but does contribute an appreciable phase error at $\omega = \omega_\alpha$, since the phase lag due to the first

9. Due to the fact that this is, for all practical purposes, the exact α-cutoff frequency, we will consider it as interchangeable with the ω_α of Eq. (2-56).

Declassified in Part - Sanitized Copy Approved for Release @ 50-Yr 2013/09/03 : CIA-RDP81-01043R002500170003-9

Declassified in Part - Sanitized Copy Approved for Release @ 50-Yr 2013/09/03 : CIA-RDP81-01043R002500170003-9

factor is 45°, and that due to the second is $\tan^{-1} 1/9$ or 6.30^o- - - - an error of about 12% . Due to the fact that the values of T_n go as $1/n^2$, the product approximation converges rapidly, although an estimate of the number of terms required for a given amplitude (or phase) error in a specified frequency range is still difficult. As can be seen from the example above, the major source of error is the next higher order term in the expansion.

It is interesting to compare this first order approximation with that obtained by using the power series expansion for cosh ku_p. If this is done, we have

$$\alpha (j\omega) = \frac{\alpha_o}{1 + j \frac{\omega}{b_o \omega_b}} \tag{2-64}$$

and the 3 db α-cutoff frequency as predicted from this is simply $b_o\omega_b$, which only 80% of the value as predicted from the exact analysis. The reason for this discrepancy is that higher order terms in the power series expansion cannot be neglected at ω_α, so that (2-64) leads to erroneous results even at frequencies less than ω_α. From this it can be seen that an approximation using the first order term in (2-63) is to be preferred.

F. Approximations for b.

To find the product series expansion for b, we form

$$b(s) \cong \frac{\alpha(s)}{1 - \alpha(s)} = \frac{\frac{1}{\cosh ku_p}}{1 - \frac{1}{\cosh ku_p}} = \frac{1}{\cosh ku_p - 1} \tag{2-65}$$

Setting $\cosh ku_p - 1 = 0$ leads to

$$\begin{aligned} \cosh x \cos y - 1 &= 0 \\ \sinh x \sin y &= 0 \end{aligned} \qquad Z = ku_p = x + jy \tag{2-66}$$

Declassified in Part - Sanitized Copy Approved for Release @ 50-Yr 2013/09/03 : CIA-RDP81-01043R002500170003-9

Declassified in Part - Sanitized Copy Approved for Release @ 50-Yr 2013/09/03 : CIA-RDP81-01043R002500170003-9

The solutions of (2-66) are:

$$s_n = -\frac{1}{\tau_p} - \frac{1}{\tau_p}\left(\frac{4n\pi}{k}\right)^2 = -\omega_b\left[1 + 8\pi^2 n^2 b_o\right] \qquad (2\text{-}67)$$

The interesting part of this result is that the f[illegible]st factor in the product expansion, i.e., n = 0, has a cutoff frequency of precisely ω_b, which is the same as the exact result (2-55). This would seem to indicate that contributions from the remaining terms in (2-67) are negligible, and this is borne out by examining the term for n = 1. This, by itself has a cutoff frequency of $8\pi^2 b_o \omega_b$, which is 64 times the alpha-cutoff frequency. Hence, for b(s) we have the extremely good approximation,

$$b(s) \cong \frac{b_o}{1 + \frac{s}{\omega_b}}, \quad \omega_b = \frac{1}{\tau_p} \qquad (2\text{-}68)$$

If we substitute $\alpha_d(j\omega)$ from (2-64) above into $b = \frac{\alpha_d}{1 - \alpha_d}$, the b-cutoff frequency obtained is again ω_b, making the approximation that $\alpha_o{}^d$ is very close to unity. On the other hand, if we take $\alpha_d(j\omega) = \frac{\alpha_o{}^d}{1 + j\frac{\omega}{\omega_\alpha}}$, where this is the first-order approximation from the product expansion with $\omega_\alpha = 1.23\,\alpha_b b_o$, and substitute it into $b \cong \frac{\alpha_d}{1 - \alpha_d}$, the 3 db cutoff frequency for this expression is $1.23\,\omega_b$, which is considerably different from the correct value of ω_b.

The results of the various approximations for α_d and b are compared in Figure 2-6.

	Form of $\alpha_d(j\omega)$	Form of $b(j\omega)$	Predicted 3 db α_d-cutoff freq.	Predicted 3 db b-cutoff freq.
Exact case	Eq. 2-28	Eq. 2-54	$\omega_\alpha = 1.25\,\omega_b b_o$	ω_b
1st term of product exp.	$\frac{\alpha_o{}^d}{1 + j\,\omega/1.23\,\omega_b b_o}$	$\frac{b_o}{1 + j\frac{\omega}{\omega_b}}$	$1.23\,\omega_b b_o$	ω_b
1st term of power series	$\frac{\alpha_o{}^d}{1 + j\,\omega/\omega_b b_o}$	$\frac{b_o}{1 + j\frac{\omega}{\omega_b}}$	$\omega_b b_o$	ω_b

Figure 2-6. Results for α_d and b. Here, b_o and $\alpha_o{}^d$ are the low-frequency values of $b(j\omega)$ and $\alpha_d(j\omega)$ as determined from the power series expansions.

Declassified in Part - Sanitized Copy Approved for Release @ 50-Yr 2013/09/03 : CIA-RDP81-01043R002500170003-9

Declassified in Part - Sanitized Copy Approved for Release @ 50-Yr 2013/09/03 : CIA-RDP81-01043R002500170003-9

It is apparent that using the first term of the product expansions for α_d and b gives cutoff frequencies which are remarkably close to the exact values. This does not indicate that these should be used without careful attention to the frequency range covered, as has been previously mentioned.

G. Product Expansions for the Transistor Parameters

The process of finding these is essentially the same as that employed for α and b, except that the factor $u_p = \sqrt{1 + s\tau_p}$ which appears in the numerator of certain parameters causes difficulty if the expansion is attempted in terms of s. As an example of this, we take

$$y_{11}{}^d = g_{11}{}^d \frac{u_p \tanh k}{\tanh ku_p} = g_{11}{}^d \frac{\sqrt{1 + s\tau_p}\ \dfrac{\sinh k}{\cosh k}}{\dfrac{\sinh k\sqrt{1 + s\tau_p}}{\cosh k\sqrt{1 + s\tau_p}}} \qquad (2\text{-}69)$$

$$= g_{11}{}^d \ \frac{\cosh k\sqrt{1 + s\tau_p} \quad \sinh k}{\cosh k} \cdot \frac{\sqrt{1 + s\tau_p}}{\sinh k\sqrt{1 + s\tau_p}}$$

where the problem results from the factor $\sqrt{1 + s\tau_p}$ in the numerator. Although the value $s = -1/\tau_p$ causes this to become zero, it is a non-analytic (due to the radical being double-valued) and hence does not have an infinite product expansion. This can be solved by setting $z = k\sqrt{1 + s\tau_p}$, so that the last fraction in (2-69) becomes $1/k \frac{z}{\sinh z}$. The values of z which cause sinh z to vanish can be found without difficulty, these being $z_n = 0 + jn\pi$, $n = 0, \pm 1, \pm 2$, etc. Then sinh z can be expressed as

$$\sinh z = \prod_{n=-\infty}^{n=+\infty} (Z - jn\pi) \qquad (2\text{-}70)$$

where the symbol $\prod$ indicates the multiplication of all terms for the values

Declassified in Part - Sanitized Copy Approved for Release @ 50-Yr 2013/09/03 : CIA-RDP81-01043R002500170003-9

Declassified in Part - Sanitized Copy Approved for Release @ 50-Yr 2013/09/03 : CIA-RDP81-01043R002500170003-9

of n[10]. We see that for $n = 0$, the term is just z, so that (2-70) can be rewritten

$$= \left\{ \prod_{n=-\infty}^{n=-1} (Z - jn\pi) \right\} Z \left\{ \prod_{n=1}^{n=+\infty} (Z - jn\pi) \right\} \tag{2-71}$$

$$= Z \prod_{n=1}^{n=+\infty} (Z - jn\pi)(Z + jn\pi) = Z \prod_{n=1}^{n=+\infty} (Z^2 + n^2\pi^2)$$

With this last result, we have

$$\frac{z}{\sinh z} = \frac{1}{\prod_{n=1}^{\infty} (Z^2 + n^2\pi^2)} \cdot \tag{2-72}$$

$$= \frac{1}{\prod_{n=1}^{\infty} \left[k^2 (1+s\tau_p) + n^2\pi^2\right]} = \frac{1}{\left[\prod_{n=1}^{\infty} k^2 \left(1 + \left[\frac{n\pi}{k}\right]^2\right)\right]\left[\prod_{n=1}^{\infty} \left\{\frac{s\tau}{1 + \left(\frac{n\pi}{k}\right)^2} + 1\right\}\right]}$$

In the second infinite product, setting $s = 0$ gives us the value of the first one as $\frac{\sinh k}{k}$, so we get

$$\frac{z}{\sinh z} = \frac{k}{\sinh k} \cdot \frac{1}{\prod_{n=1}^{\infty} (1 + sT_n)} \qquad T_n = \frac{\tau}{1 + \left(\frac{n\pi}{k}\right)^2} \cong \frac{T_\alpha}{4n^2}$$

$$= \frac{k}{\sinh k} \frac{1}{\left(1 + s\frac{T_\alpha}{4}\right)\left(1 + s\frac{T_\alpha}{16}\right) \cdots} \tag{2-73}$$

---

10 That is, $\prod_{n=1}^{n=N} a_n = a_1 a_2 a_3 \cdots a_n$, just as $\sum_{n=1}^{n=N} a_n = a_1 + a_2 + a_3 + \cdots + a_n$

Declassified in Part - Sanitized Copy Approved for Release @ 50-Yr 2013/09/03 : CIA-RDP81-01043R002500170003-9

Declassified in Part - Sanitized Copy Approved for Release @ 50-Yr 2013/09/03 : CIA-RDP81-01043R002500170003-9

The infinite product expansion of $y_{11}{}^d$ becomes

$$y_{11}{}^d = g_{11}{}^d \frac{\left[1 + s\,T_\alpha\right]\left[1 + s\,\frac{T_\alpha}{9}\right] - - -}{\left[1 + s\,\frac{T_\alpha}{4}\right]\left[1 + s\,\frac{T_\alpha}{16}\right] - - -} \qquad (2\text{-}74)$$

where the product expansion in the numerator is identical with that derived for $\alpha_d(s)$. It is worthwhile noting that the time constants in the numerator interlace those in the denominator; this fact, coupled with all roots of the numerator and denominator being real and negative, allows $y_{11}{}^d$ to be realized as an RL network.

An expansion for the quantity $(1 - \alpha_d)$ can be obtained as

$$1 - \alpha_d = \frac{\alpha}{b} = \frac{\alpha_o}{b_o} \frac{(1 + sT_b)}{\left[1 + s\,\frac{T_\alpha}{4}\right]\left[1 + s\,\frac{T_\alpha}{16}\right] - - -} \qquad (2\text{-}75)$$

and combining this with Eq. (2-74) gives us the expansion for a quantity which appears in many of the transistor parameters where the effect of r_b' is included:

$$y_{11}{}^d\,(1 - \alpha_d) = \frac{g_{11}{}^d\,\alpha_o}{b_o} \frac{(1 + sT_b)(1 + sT_\alpha)}{\left[1 + s\,\frac{T_\alpha}{4}\right]^2 - - -} \qquad (2\text{-}76)$$

An examination of (2-76) shows that, due to the fact that T_b is a much larger time constant than any present in the denominator, $y_{11}{}^d(1 - \alpha_d)$ can be represented with good accuracy out to the α_d-cutoff frequency by a parallel RC circuit as is shown in Figure 2-7 below.

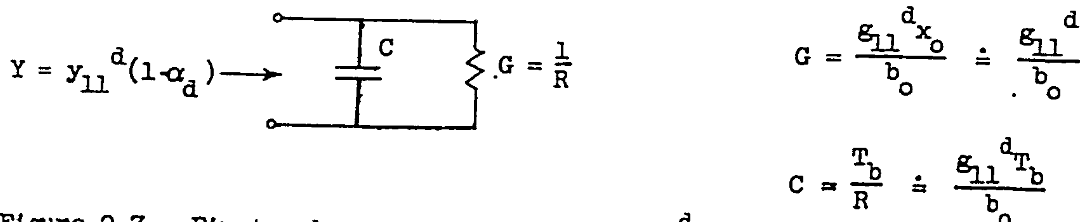

Figure 2-7. First order approximation for $y_{11}{}^d(1-\alpha_d)$. The admittance of the circuit, with the values shown, has the form $G(1 + sT_b)$ and approximates Eq. 2-76 out to the α_d-cutoff frequency.

Declassified in Part - Sanitized Copy Approved for Release @ 50-Yr 2013/09/03 : CIA-RDP81-01043R002500170003-9

Declassified in Part - Sanitized Copy Approved for Release @ 50-Yr 2013/09/03 : CIA-RDP81-01043R002500170003-9

An accurate circuit for this expression becomes very complicated, due to the second-order pole. The amplitude error for the approximate expression is about 10% at the α-cutoff frequency, while the phase error is considerably greater, the approximation giving a phase shift of 90° leading, while the actual value is close to 75° leading. In many cases where this is used in the expressions for the y-parameters, it is therefore necessary to use the expression in Eq. (2-76) rather that the simplified form of Figure 2-7.

By expanding the numerator and denominator of (2-76) we have

$$y_{11}^{d}(1-\alpha_d) = \frac{g_{11}^{d}\,\alpha_o}{b_o} \cdot \frac{1 + s(T_\alpha + T_b) + s^2 T_\alpha T_b}{1 + s\frac{T_\alpha}{2} + s^2\left[\frac{T_\alpha}{4}\right]^2} \qquad (2\text{-}77)$$

and neglecting the terms in s^2 gives a better approximation for $y_{11}^{d}(1-\alpha_d)$

$$y_{11}^{d}(1-\alpha_d) \cong \frac{g_{11}^{d}}{b_o} \cdot \frac{1 + sT_b}{1 + s\frac{T_\alpha}{2}} \qquad \alpha_o \cong 1 \quad T_b \gg T_\alpha \quad (2\text{-}77a)$$

which is valid out to about $2\omega_\alpha$ and which is realized by the circuit shown in Figure 2-8.

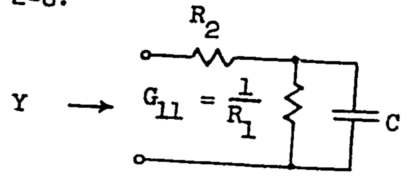

$$Y = \frac{1}{R_2 + R_1} \cdot \frac{1 + SCR_1}{1 + SCR_1\frac{R_2}{R_1 + R_2}}$$

$$= \frac{g_{11}^{d}}{b_o} \cdot \frac{1 + ST_b}{1 + ST\alpha/2}$$

Figure 2-8. Second order approximation for $y_{11}^{d}(1-\alpha)$. When the parameters satisfy the design equations at the right, the representation is good out to $2\omega_\alpha$.

If we solve the three equations resulting from Figure 2-8 for R_2,

$$\frac{1}{R_2+R_1} = \frac{g_{11}^{d}}{b_o}, \quad CR_1 = T_b, \quad CR_1\frac{R_2}{R_1+R_2} = \frac{T_\alpha}{2} \qquad (2\text{-}77b)$$

Declassified in Part - Sanitized Copy Approved for Release @ 50-Yr 2013/09/03 : CIA-RDP81-01043R002500170003-9

Declassified in Part - Sanitized Copy Approved for Release @ 50-Yr 2013/09/03 : CIA-RDP81-01043R002500170003-9

we obtain $R_2 = \frac{b_o T_\alpha}{2 g_{11}^d T_b}$. The use of the relations $\omega_\alpha = \frac{5}{4} b_o \omega_b$, $T_\alpha = \frac{4}{5b_o} T_b$ reduces this to $R_2 = \frac{2}{5 g_{11}^d}$. This is of interest in connection with the high-frequency value of y_{11e}, which is an important design parameter in grounded-emitter video amplifiers.

The derivation of the infinite product expansion for the other y's for the diffusion transistor presents no new problems, so that the results for the complete set are summarized below.

$$y_{11}^d = g_{11}^d \frac{(1 + sT_\alpha)(1 + s\frac{T_\alpha}{9}) - -}{(1 + s\frac{T_\alpha}{4})(1 + s\frac{T_\alpha}{16}) - -}$$

$$y_{12}^d = - g_{12}^d \frac{1}{(1 + s\frac{T_\alpha}{4}) \quad (1 + s\frac{T_\alpha}{16}) \quad - -}$$

$$y_{21}^d = - g_{21}^d \frac{1}{(1 + s\frac{T_\alpha}{4}) \quad (1 + s\frac{T_\alpha}{16}) \quad - - -} \tag{2-78}$$

$$y_{22}^d = g_{22}^d \frac{(1 + sT_\alpha)(1 + s\frac{T_\alpha}{9}) \quad - - -}{(1 + s\frac{T_\alpha}{4})(1 + s\frac{T_\alpha}{16}) - - -}$$

where

$$T_\alpha = \frac{1}{\omega_\alpha} = \frac{4}{5b_o\omega_b} = \frac{2k^2\tau_p}{5} \tag{2-79}$$

Using these, together with the expansion for $y_{11}^d (1 - \alpha_d)$, an approximation can be obtained for y_{11e}, etc. Referring to Eq. (2.32), the circuit configuration obtained for y_{11e} is that shown in Figure (2-9), where it is to be emphasized that this is valid in the range $0 < \omega \leq 2\omega_\alpha$

Declassified in Part - Sanitized Copy Approved for Release @ 50-Yr 2013/09/03 : CIA-RDP81-01043R002500170003-9

Declassified in Part - Sanitized Copy Approved for Release @ 50-Yr 2013/09/03 : CIA-RDP81-01043R002500170003-9

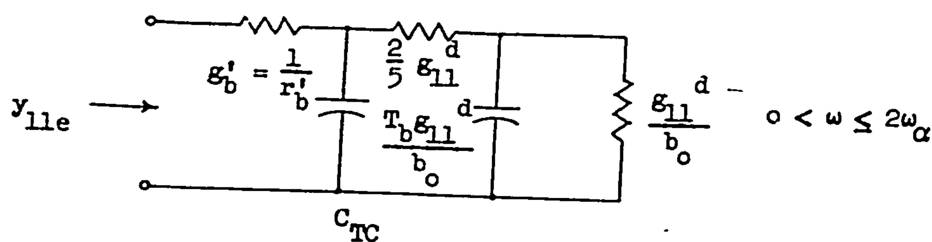

Figure 2-9 . Circuit representation for y_{11e} which is valid out to $z\omega_\alpha$. The capacitor C_{TC} has been included, but can usually be neglected as is explained in the text.

That this circuit does correspond to y_{11e} can be seen by inverting Eq. (2-32)

$$\frac{1}{y_{11e}} = r_b' + \frac{1}{\sum y^d + sC_{TC}} \cong r_b' + \frac{1}{y_{11}{}^d(1 - \alpha_d) + sC_{TC}} \qquad (2\text{-}80)$$

Over the frequency range specified above the effect of C_{TC} can usually be neglected. To demonstrate this, consider a typical high-frequency triode transistor with

$$b_o = 40$$

$$T_b = 10^{-6} \text{ second,}$$

and $g_{11e} = \frac{qI_e}{kT} = .04$ mho at room temperature and I_e of 1 milliampere. Then

$$\frac{T_b g_{11}{}^d}{b_o} = \frac{(10^{-6})(.04)}{40} = 1000 \quad \mu\mu\text{fd} \qquad (2\text{-}81)$$

so that, with C_{TC} on the order of 5 μμfd and r_b' in the range of 50 to 100 ohms, the reactance of C_{TC} is very high compared to that of the series combination of R_2 (which is $2/5g_{11}{}^d$ or 10 ohms) and the 1000 μμfd capacitor. The important

Declassified in Part - Sanitized Copy Approved for Release @ 50-Yr 2013/09/03 : CIA-RDP81-01043R002500170003-9

Declassified in Part - Sanitized Copy Approved for Release @ 50-Yr 2013/09/03 : CIA-RDP81-01043R002500170003-9

aspect of this discussion is that the high-frequency input impedance is <u>not</u> just r_b', but has an added component of $2/5g_{11}{}^d$, although the latter adds only 20% even for a transistor with the unusually low value of 50 ohms for r_b'.

In the derivations that follow, time constants of the form $r_b'C_{TC}$, $C_{TC}/g_{11}{}^d$, and $C_{TC}/g_{21}{}^d$ are removed in the approximating process, as these are so extremely small that their effect is negligible until frequencies on the order of $10\omega_\alpha$. On the other hand, those of the form $C_{TC}/g_{12}{}^d$ and $C_{TC}/g_{22}{}^d$ must be retained, due to the low values of $g_{12}{}^d$ and $g_{22}{}^d$. Also, the quantity $r_b'\, g_{11}{}^d$, which frequently appears in the expressions, will be denoted by x, for brevity.

For the case of y_{12e}, we have, referring to Eq. 2-38.

$$y_{12e} = -\frac{y_{12}{}^d + y_{22}{}^d + sC_{TC}}{1 + r_b'\left[\sum y_d + sC_{TC}\right]}$$

$$= -\frac{y_{22}{}^d\left(1 + \dfrac{y_{12}{}^d}{y_{22}{}^d}\right) + sC_{TC}}{1 + r_b'\left[\sum y_d + sC_{TC}\right]} \qquad (2\text{-}82)$$

$$\cong -\frac{\dfrac{\alpha_o}{b_o}\, g_{22}{}^d\left[\dfrac{(1 + sT_b)(1 + sT_\alpha)}{\left(1 + s\frac{T_\alpha}{4}\right)^2}\right] + sC_{TC}}{1 + r_b'\,\dfrac{g_{11}{}^d\alpha_o}{b_o}\cdot\dfrac{(1 + sT_b)(1 + sT_\alpha)}{\left[1 + s\frac{T_\alpha}{4}\right]^2}}$$

$$\cong -\frac{\dfrac{g_{22}{}^d}{b_o}\left[(1 + sT_b)(1 + sT_\alpha)\right] + sC_{TC}}{1 + \dfrac{x}{b_o} + s\left[\dfrac{T_\alpha}{2} + \dfrac{xT_b}{b_o}\right]}$$

Declassified in Part - Sanitized Copy Approved for Release @ 50-Yr 2013/09/03 : CIA-RDP81-01043R002500170003-9

Declassified in Part - Sanitized Copy Approved for Release @ 50-Yr 2013/09/03 : CIA-RDP81-01043R002500170003-9

$$\cong - \frac{g_{22}^{\ d}}{b_o} \frac{(1 + s\,T_b)(1 + sT_\alpha) + \dfrac{sb_oC_{TC}}{g_{22}^{\ d}}}{1 + \dfrac{x}{b_o} + s\left[\dfrac{T_\alpha}{2} + \dfrac{xT_b}{b_o}\right]} \qquad (2\text{-}82)$$

Thus y_{12e} has a low frequency value of $g_{22}^{\ d}/b_o$, which represents a very high resistance. For frequencies which are much less than the α-cutoff frequency, the numerator term of importance is $j\omega b_oC_{TC}/g_{22}^{\ d}$, the time constant representing a frequency on the order of a few kilocycles. As the frequency is increased, y_{12e} increases at the rate of 6 db. per octave until a frequency on the order of 20% of the α-cutoff frequency (corresponding to the time constant in the denominator).

In the expression for y_{21e}, the terms $y_{22}^{\ d}$ and sC_{TC} can be neglected in the numerator:

$$y_{21e} = -\frac{y_{21}^{\ d} + y_{22}^{\ d} + sC_{TC}}{1 + r_b'\left[\sum y_d + sC_{TC}\right]} \cong -\frac{y_{21}^{\ d}}{1 + r_b'\left[\sum y_d + sC_{TC}\right]}$$

$$\cong -\frac{g_{21}^{\ d}}{1 + \dfrac{x}{b_o} + s\left[\dfrac{T_\alpha}{2} + \dfrac{xT_b}{b_o}\right]} \qquad (2\text{-}83)$$

Here the numerator is independent of frequency over the range in which we are interested, while denominator is the same as that for y_{12e}.

The exact expression for y_{22e} from Eq. (2-24) is

$$y_{22e} = y_{22} = \frac{y_{22}^{\ d} + sC_{TC} + r_b'\,\Delta y_d}{1 + r_b'\left[\sum y_d + sC_{TC}\right]} \qquad (2\text{-}84)$$

Declassified in Part - Sanitized Copy Approved for Release @ 50-Yr 2013/09/03 : CIA-RDP81-01043R002500170003-9

Declassified in Part - Sanitized Copy Approved for Release @ 50-Yr 2013/09/03 : CIA-RDP81-01043R002500170003-9

where the quantity $r_b' \Delta y_d$ has been included, as its frequency variation is of interest in this case. Referring to Eq. (2-28), we have

$$\Delta y_d = y_{11}{}^d \left(-y_{12}{}^d\right) \left[\frac{(1 - \alpha_d)(1 + \alpha_d)}{\alpha_d}\right] + s y_{11}{}^d C_{TC}$$

$$\cong y_{11}{}^d \left(-y_{12}{}^d\right) \frac{1}{b\alpha_d} \qquad \text{since } b = \frac{\alpha_d}{1 - \alpha_d} \tag{2-85}$$

Using the infinite product expansions for the quantities involved and retaining terms out to $4\omega_\alpha$,

$$\Delta y_d \cong g_{11}{}^d \frac{1 + sT_\alpha}{1 + s\frac{T_\alpha}{4}} \; g_{12}{}^d \frac{1}{1 + s\frac{T_\alpha}{4}} \left[\frac{1 + sT_b}{b_o}\left(1 + \frac{\alpha_o}{1 + sT_\alpha}\right)\right]$$

$$= \frac{2g_{11}{}^d g_{12}{}^d}{b_o} \frac{(1 + sT_b)(1 + sT\alpha/2)}{\left(1 + \frac{sT\alpha}{4}\right)^2} \tag{2-86}$$

The denominator of Eq. (2-86), when expanded, has the form $1 + \frac{sT_\alpha}{2} + \frac{s^2 T_\alpha{}^2}{16}$ so that this cancels the term $1 + s\frac{T_\alpha}{2}$ in the numerator for frequencies out to $2\omega_\alpha$. This, coupled with the fact that $g_{12}{}^d \cong g_{22}{}^d$, simplifies (2-86) to

$$r_b' \Delta y^d \cong \frac{2 \times g_{22}{}^d}{b_o} (1 + sT_b) \tag{2-87}$$

Declassified in Part - Sanitized Copy Approved for Release @ 50-Yr 2013/09/03 : CIA-RDP81-01043R002500170003-9

Declassified in Part - Sanitized Copy Approved for Release @ 50-Yr 2013/09/03 : CIA-RDP81-01043R002500170003-9

$$y_{22e} \cong \frac{g_{22}^{d} \frac{1 + sT_{\alpha}}{1 + sT_{\alpha/4}} + sC_{TC} + \frac{2\,x\,g_{22}^{d}}{b_o}(1 + sT_b)}{1 + \frac{x}{b_o} \frac{(1 + sT_b)(1 + sT_{\alpha})}{\left[1 + s\frac{T_{\alpha}}{4}\right]^2}}$$

$$\cong \frac{g_{22}^{d}(1 + sT_{\alpha})(1 + s\frac{T_{\alpha}}{4}) + s\,C_{TC}\,(1 + s\frac{T_{\alpha}}{4})^2 + \frac{2\,x\,g_{22}^{d}}{b_o}(1 + sT_b)(1 + s\frac{T_{\alpha}}{2})}{1 + s\frac{T_{\alpha}}{2} + \frac{x}{b_o}(1 + sT_b)}$$

$$\cong g_{22}^{d} \frac{1 + \frac{2x}{b_o} + s\frac{C_{TC}}{g_{22}^{d}} + s^2\frac{T_{\alpha}\,C_{TC}}{2g_{22}^{d}}}{1 + \frac{x}{b_o} + s\left[\frac{T_{\alpha}}{2} + \frac{xT_b}{b_o}\right]}$$

In simplifying this expression, we have retained only the first order terms in the expansion of $(1 + sT_{\alpha/4})^2 \cong 1 + s\frac{T_{\alpha}}{2}$, as was done in the case of y_{11e}. We see that the low frequency value of y_{22e} is very nearly g_{22}^{d}, since for a typical transistor with $x = 4$ and $b_o = 50$, it is only 7 % larger than g_{22}^{d}. At high frequencies the predominant term is a capacitance having the value $C_1 = \frac{C_{TC}}{1 + \frac{5x}{2}}$, the latter form being obtained with the aid of the relation $T_{\alpha} = \frac{4}{5b_o}T_b$.

$$y_{22e} = G_1 \frac{1 + s(T_1 + T) + s^2 T_1 T_2}{1 + sT_2}$$

$T_2 = R_2 C_2$

$T_1 = R_1 C_1$

$T = (R_1 + R_2)\,C_2$

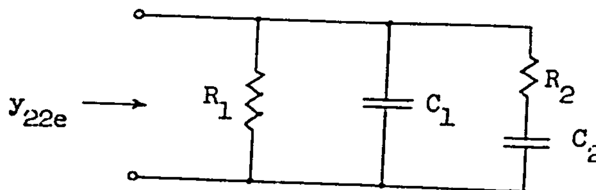

Figure 2-10. A circuit which represents y_{22e} when R_1, T, T_1, T_2 have the values given by Eqs. 2-38.

Declassified in Part - Sanitized Copy Approved for Release @ 50-Yr 2013/09/03 : CIA-RDP81-01043R002500170003-9

Declassified in Part - Sanitized Copy Approved for Release @ 50-Yr 2013/09/03 : CIA-RDP81-01043R002500170003-9

The circuit of Figure 2-10 represents y_{22e} when the parameters are properly chosen. The conditions are

$$G_1 = g_{22}{}^d \frac{1 + \frac{2x}{b_o}}{1 + \frac{x}{b_o}} \cong g_{22}{}^d$$

$$T_1 T_2 = \frac{T_\alpha C_{TC}}{2 g_{22}{}^d (1 + \frac{2x}{b_o})} \qquad (2\text{-}88)$$

$$T_1 + T = \frac{C_{TC}}{g_{22}{}^d (1 + \frac{2x}{b_o})}$$

$$T_2 = \frac{\frac{T_\alpha}{2} + \frac{x T_b}{b_o}}{1 + \frac{x}{b_o}} = \frac{\frac{T_\alpha}{2} (1 + \frac{5x}{2})}{1 + \frac{x}{b_o}}$$

The value of T_2 is given directly by the third equation above; the others are easily determined as follows:

$$T_1 = \frac{\frac{\frac{T_\alpha}{2} C_{TC}}{(1 + \frac{2x}{b_o})\, g_{22}{}^d}}{\frac{\frac{T_\alpha}{2} (1 + \frac{5x}{2})}{1 + \frac{x}{b_o}}} \cong \frac{C_{TC}}{g_{22}{}^d (1 + \frac{5x}{2})} \qquad (2\text{-}89)$$

$$T = \frac{C_{TC}}{g_{22}{}^d (1 + \frac{2x}{b_o})} - T_1 \cong \frac{\frac{5x}{2} C_{TC}}{g_{22}{}^d (1 + \frac{2x}{b_o})}$$

Declassified in Part - Sanitized Copy Approved for Release @ 50-Yr 2013/09/03 : CIA-RDP81-01043R002500170003-9

Declassified in Part - Sanitized Copy Approved for Release @ 50-Yr 2013/09/03 : CIA-RDP81-01043R002500170003-9

These values can be used to obtain the values of R_1, R_2, etc., but this is unwieldy due to the complicated forms for T, T_1, and T_2. The important feature of Eqs. (2-89) is that the value of x has a considerable effect on the time constants appearing in y_{22e}. Leakage across the collector-base junction is present in the actual transistor, the major effect of which is to increase the observed value of g_{22}^{d}. An increase of 10 to 1 is not uncommon in commercial units. Further discrepancies result as the termination of this leakage conductance may be "tapped down" on r_b'.

Declassified in Part - Sanitized Copy Approved for Release @ 50-Yr 2013/09/03 : CIA-RDP81-01043R002500170003-9

Declassified in Part - Sanitized Copy Approved for Release @ 50-Yr 2013/09/03 : CIA-RDP81-01043R002500170003-9

2-6. Summary

In the preceeding sections we have considered a theoretical model for the alloy - or fused-junction transistor, and derived expressions for the y-parameters as functions of frequency in the grounded-base connection. The addition of the collector junction capacitance C_{TC} and the extrinsic base spreading resistance r_b' approximated conditions in the physical transistor. The y-parameters for this model in the grounded-emitter connection were obtained, and the problem of approximating the hyperbolic functions occuring in both cases discussed in detail.

From the standpoint of error, as well as ease of application in network analysis, the product expansion is superior to the power series expansion in approximating many important quantities. It was also noted that appreciable phase error may be present even when the amplitude error is negligible.

In connection with the important problem of approximating complicated functions of frequency by expressions of the form $(1 + sT)$ or $\frac{1}{1 + sT}$, the best possible approximation is not given by simply taking the corresponding term of the infinite product expansion for that function. The value of T to be used depends on the frequency range over which the approximation is used, whether it is on a phase or amplitude basis, etc. It is possible to set up various error criteria analytically which indirectly determine the value of T; however, these expressions frequently are so complicated as to make the solution impractical. The infinite product expansion provides an approximation which is easily obtained, and is of a form commonly used in network analysis, irrespective of how many terms are used.

Declassified in Part - Sanitized Copy Approved for Release @ 50-Yr 2013/09/03 : CIA-RDP81-01043R002500170003-9

Declassified in Part - Sanitized Copy Approved for Release @ 50-Yr 2013/09/03 : CIA-RDP81-01043R002500170003-9

CHAPTER 3

Measurement of Transistor Parameters

3-1 Measurement Techniques

Before the measurements of small signal parameters of amplifying devices can be undertaken a number of fundamental principles must be understood Among these, the most important are:

(1) The type of circuit in which the device is to be used.

(2) The parameters most significant in the light of (1).

(3) The number of independent measurements required to determine the desired parameters.

(4) The specific technique of measurement to be used for each parameter.

At first glance item (1) may appear to be an unnecessary consideration since from four terminal network theory a set of four complex frequency parameters which may be chosen in a large number of ways suffice to specify the transistor completely and can therefore be used to calculate the bahavior of any linear network in which the device is immersed. However, as a practical matter, it can often happen that the accuracy requirement on the measurement is very severe for good accuracy of the circuit performance if the parameters are not selected judiciously. A very simple example of this is the use of the measured common base parameters for the representation of the common emitter circuit. Here the common emitter short circuit current amplification h_{21e} is given approximately by

$$h_{21e} \doteq - \frac{\alpha}{1-\alpha}$$

The fractional error in finding h_{21e} due to a fractional error $\frac{\Delta\alpha}{\alpha}$ in measurement of α is

Declassified in Part - Sanitized Copy Approved for Release @ 50-Yr 2013/09/03 : CIA-RDP81-01043R002500170003-9

Declassified in Part - Sanitized Copy Approved for Release @ 50-Yr 2013/09/03 : CIA-RDP81-01043R002500170003-9

$$\frac{\Delta h_{21e}}{h_{21e}} = h_{21e} \frac{\Delta\alpha}{\alpha}$$

Since h_{21e} is a number much larger than unity, α must be measured very accurately for moderate accuracy in h_{21e}. Since the common emitter connection is the configuration most often used in the wide band amplifier work studied in this report, parameter measurements were made using this connection.

Besides the choice of the configuration, a decision is also necessary on the parameters to be measured. This depends on the termination conditions which the transistor meets in the circuit. Since the wide band equalization process is essentially one of obtaining increased bandwidth at the expense of gain, it is expected that in most cases the total load impedance will be small compared to the transistor output impedance. Thus the output termination, at least for an internal transistor in a cascade arrangement, can be considered more nearly a short circuit than an open circuit. From this it follows that y_{11e} or its reciprocal h_{11e} is the most reasonable input driving point parameter and y_{21e} or h_{21e} is the most logical forward transfer parameter. The considerations leading to choice of the other two parameters are somewhat more complicated due to the fact that the input circuit is often terminated in an impedance which cannot be considered high or low compared to the transistor input impedance. Accordingly both y_{22} and $h_{22} = \frac{1}{z_{22}}$ are discussed. The feedback parameter h_{12} was also measured but it was found that it could often be neglected in actual design work with great saving in labor and with little error.

The common emitter h parameters having been chosen with h_{11e} and h_{21e} being considered most important, the next problem is the specific technique of measurement. Here two philosphies were employed. One was the use of a high quality bridge (a Wayne Kerr bridge type B 601 was used) as a standard and as a means of making non-routine measurements. Results of measurement of actual transistor

Declassified in Part - Sanitized Copy Approved for Release @ 50-Yr 2013/09/03 : CIA-RDP81-01043R002500170003-9

Declassified in Part - Sanitized Copy Approved for Release @ 50-Yr 2013/09/03 : CIA-RDP81-01043R002500170003-9

parameters on this bridge and comparison of these measured results with theory are reported later in this Chapter. The second approach was to develop a simpler (but not quite as accurate) tester which could give rapid results with a maximum of convenience. A schematic diagram of the circuit used is shown in Fig. 3-1 and a photograph of the completed model is shown in Fig. 3-2. It was designed to measure h_{11e} and h_{21e} over the frequency range of 100 Cps. to 6 M Cps. to an accuracy within 10%. The circuit was tested by measuring an impedance which simulates h_{11e} on the tester and comparing the results with the theoretical response. The results of this are shown in Fig. 3-3. A number of precautions in construction were necessary before the tester gave the above mentioned performance. First, since a 100 ohm termination was used and the driving source impedance was 100,000 ohms, the desired parameters are given by

$$h_{21e} = \frac{E_2}{E_1} \times 10^3$$

$$h_{11e} = 100 \frac{E_1'}{E_1} \text{ kilohms}$$

To prevent over loading of the transistor E_1 was limited to .1 volt so that for typical values E_1' and E_2 were in the millivolt range (E_1' was especially small at high frequencies). Because of the low level involved special provision was made to construct the output terminals so that a direct fit could be made to the terminals of the output vacuum tube voltmeter. This completely eliminated the hum problem in spite of the low signal level.

Another important consideration is the effect of distributed capacitance across the input 100K resistor. This was overcome by passing the resistor through a hole in a shield which was tied to ground. This reduced the capacitance across the resistor to a low value at the expense of increasing the capacitance of each end of the resistor to ground. The latter effect was not serious

Declassified in Part - Sanitized Copy Approved for Release @ 50-Yr 2013/09/03 : CIA-RDP81-01043R002500170003-9

Declassified in Part - Sanitized Copy Approved for Release @ 50-Yr 2013/09/03 : CIA-RDP81-01043R002500170003-9

Figure 3-2. Simple Parameter Tester for Measurement of h_{11e}, h_{12e}, and h_{21e}.

Declassified in Part - Sanitized Copy Approved for Release @ 50-Yr 2013/09/03 : CIA-RDP81-01043R002500170003-9

Declassified in Part - Sanitized Copy Approved for Release @ 50-Yr 2013/09/03 : CIA-RDP81-01043R002500170003-9

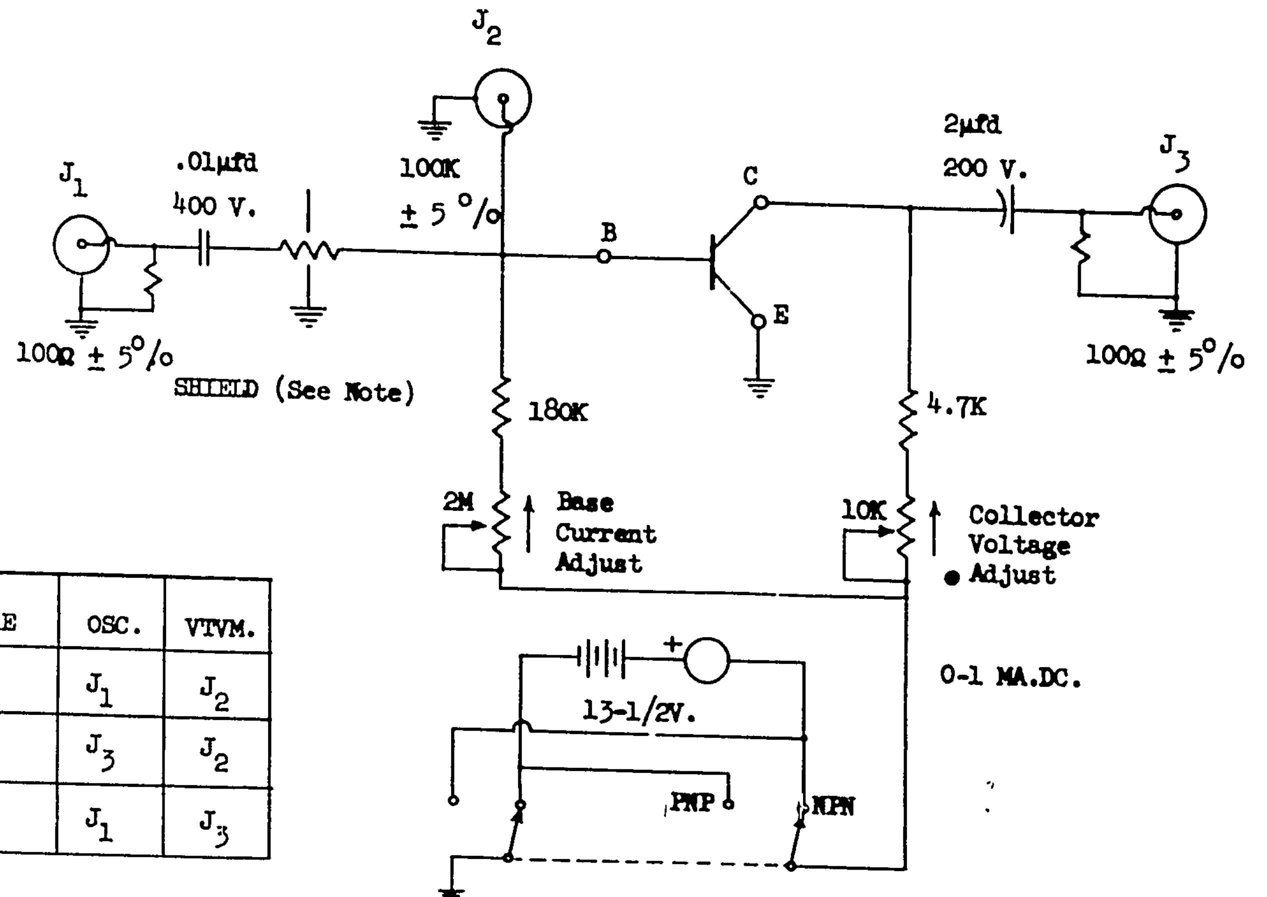

TO MEASURE	OSC.	VTVM.
h_{11e}	J_1	J_2
h_{12e}	J_3	J_2
h_{21e}	J_1	J_3

Figure 3-1. Circuit Diagram for the simple parameter tester. A screwdriver adjust potentiometer in the collecter circuit permits setting the DC collector voltage for a given DC collector current (usually 5 volts at 1 milliampere). The shield around the 100K constant-current resistor reduces feed-through at high frequencies due to the capacitance across the resistor terminals.

Declassified in Part - Sanitized Copy Approved for Release @ 50-Yr 2013/09/03 : CIA-RDP81-01043R002500170003-9

Declassified in Part - Sanitized Copy Approved for Release @ 50-Yr 2013/09/03 : CIA-RDP81-01043R002500170003-9

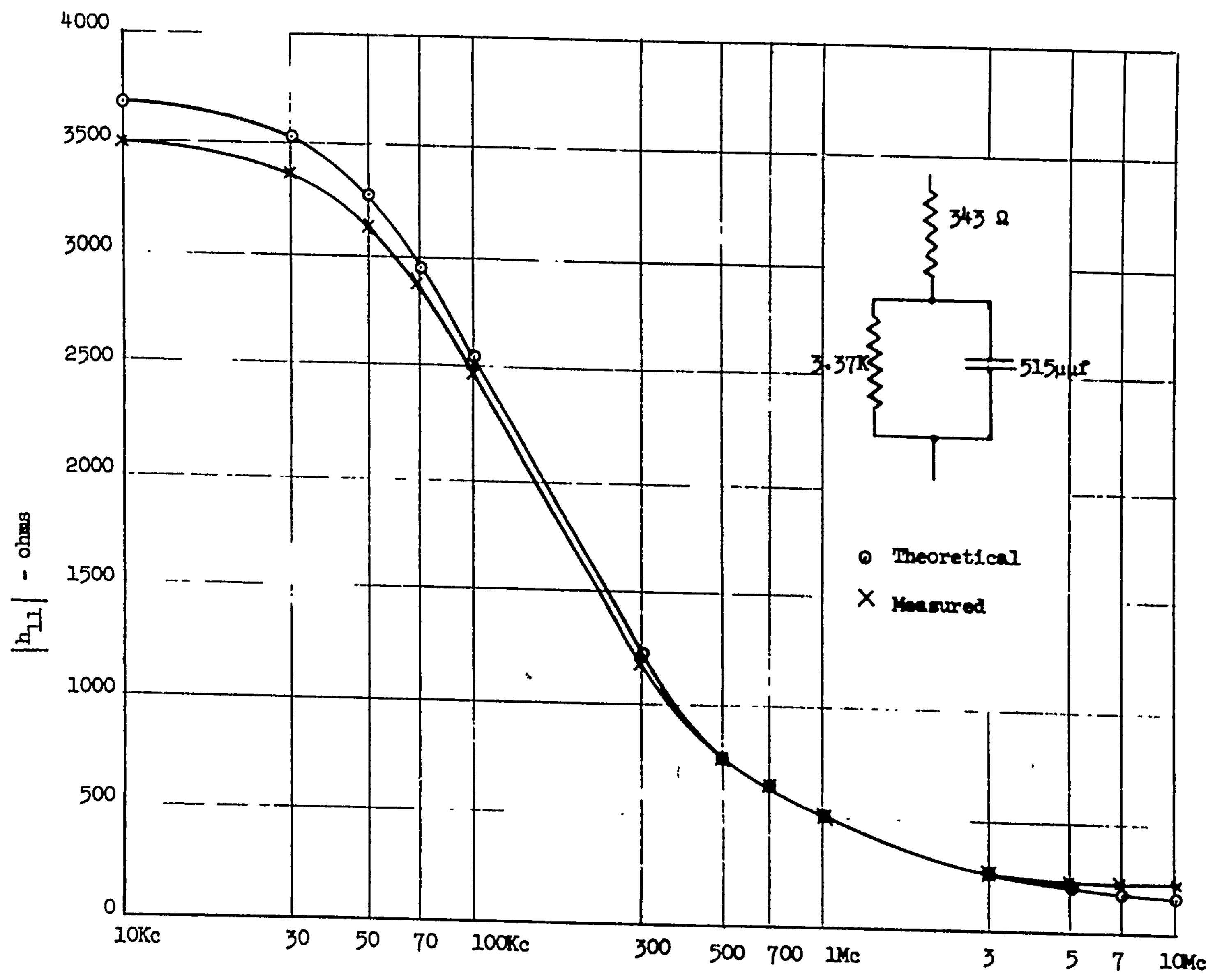

Fig. 3-3 Calibration Test for h_{11e} on Small Tester

Declassified in Part - Sanitized Copy Approved for Release @ 50-Yr 2013/09/03 : CIA-RDP81-01043R002500170003-9

Declassified in Part - Sanitized Copy Approved for Release @ 50-Yr 2013/09/03 : CIA-RDP81-01043R002500170003-9

for the impedance level normally met. The tester can be built in a single day and was found especially useful for routine checking of units.

Declassified in Part - Sanitized Copy Approved for Release @ 50-Yr 2013/09/03 : CIA-RDP81-01043R002500170003-9

Declassified in Part - Sanitized Copy Approved for Release @ 50-Yr 2013/09/03 : CIA-RDP81-01043R002500170003-9

3-2. Measurement of Transistor Parameters using Bridge Techniques

The accurate measurement of the small signal parameters which were discussed in Chapter 2 is complicated by two important considerations. The first is that the required DC bias voltages and currents must be supplied during the measurement; the second is the extremely wide range of impedance values which are encountered in the different transistor connections. As an example of the latter we have y_{11} with a typical value of .03 mhos, compared with y_{22} which may be on the order of 2 <u>micromhos</u>. For the former, the problem of minimizing the error due to the bias supply impedance (which is effectively in parallel with y_{11}) is relatively simple; in the latter case, it is extremely difficult.

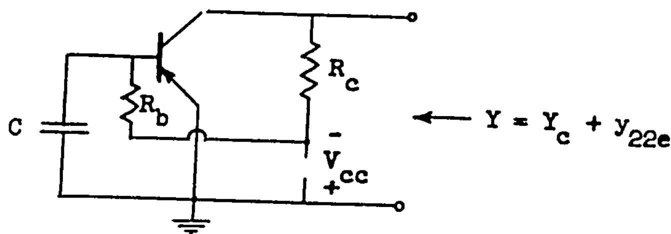

Fig. 3-4. The power-supply resistance R_c is included in the measurement of Y.

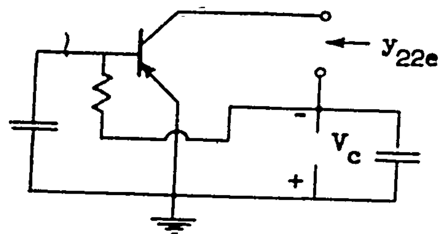

Fig. 3-5. The error with this type of circuit is dependent on the bypass capacitor across V_c.

Figure 3-4 illustrates the situation which is encountered when the power-supply resistance R_c is in parallel with the terminals across which the measurement is made. Since y_{22e} is a relatively small percentage of Y_c, an accuracy of $1^o/c$ in the measurement of the sum and of Y_c may result in large errors in the computed value of y_{22e}. On the other hand, the accuracy obtained with the circuit of Figure 3-5 is dependent only on making the impedance due to the capacitor across V_c negligible compared to $1/y_{22e}$, a condition which is much easier to satisfy than that of making Y_c negligible compared to y_{22e} in Fig. 3-4.

Declassified in Part - Sanitized Copy Approved for Release @ 50-Yr 2013/09/03 : CIA-RDP81-01043R002500170003-9

Declassified in Part - Sanitized Copy Approved for Release @ 50-Yr 2013/09/03 : CIA-RDP81-01043R002500170003-9

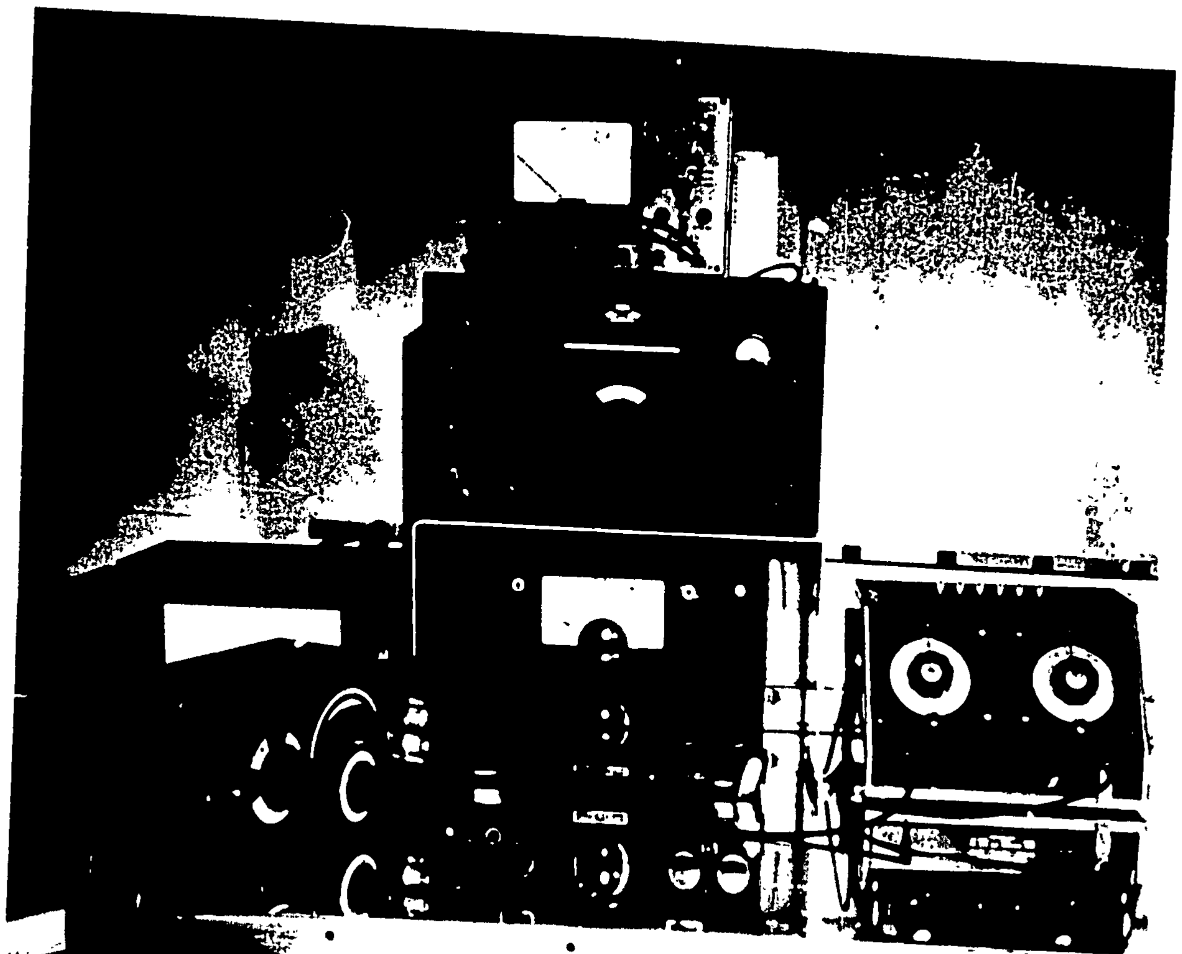

Figure 3-6. Wayne-Kerr Type B-601 RF Bridge with associated equipment. Two receivers are used as detectors, the lower one covering the range of 15-500 kc, and the upper one from 500 kc. to 5 mc., the latter being the upper limit of the bridge.

Declassified in Part - Sanitized Copy Approved for Release @ 50-Yr 2013/09/03 : CIA-RDP81-01043R002500170003-9

Declassified in Part - Sanitized Copy Approved for Release @ 50-Yr 2013/09/03 : CIA-RDP81-01043R002500170003-9

An instrument which permits the use of the type of circuit in Figure 3-5 for the measurement of two-terminal driving-point impedances (such as y_{11e} and y_{22e}) on devices such as transistors and vacuum tubes is the Wayne-Kerr B-601 RF Bridge[1], which is shown in Figure 3-6. This instrument is designed for measurements over a frequency range from 15 kilocycles to 5 megacycles, with an accuracy of 1°/o over the major part of the ranges. The range of values for R, L, and C are as follows: R, 10 ohms to 10 megohms: L, 0.5 microhenry to 50 millihenrys; C, 0.01 mmfd. to 0.02 mfd. The circuit used in the bridge permits the accurate measurement of the impedance between any two terminals in a 3-terminal network, and also the transfer admittances, although the latter presents some problems with bias supplies for active elements such as transistors and vacuum tubes.

Figure 3-7 shows the basic circuit used in the bridge. The source voltage E_s feeds the primary of T_1, the secondary of which is center-tapped at N. The coupling between the two halves of the secondary is very tight, so that N is a true center-tap even with unbalanced loads on the secondary. The unknown impedance Z_u and a standard impedance Z_s are connected in series across the entire secondary, while the detector is connected between N and the junction of the two impedances.

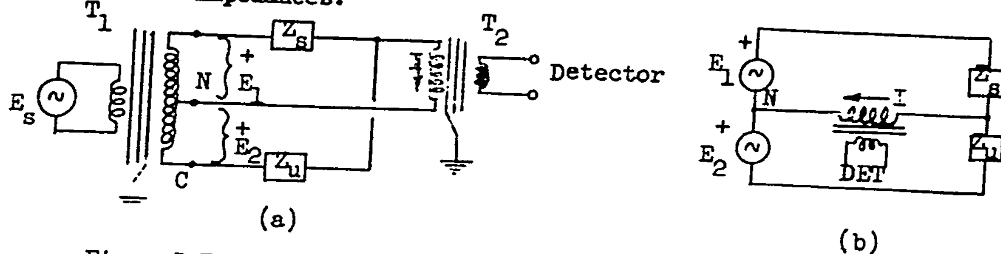

Fig. 3-7. Basic Circuit of the Wayne-Kerr B-601 RF Bridge.

[1] Manufactured by the Wayne-Kerr Laboratories, New Malden, Surrey, England. A unit having the same basic circuit, the Type B-801, is available for the frequency range from 1 to 100 megacycles.

Declassified in Part - Sanitized Copy Approved for Release @ 50-Yr 2013/09/03 : CIA-RDP81-01043R002500170003-9

Declassified in Part - Sanitized Copy Approved for Release @ 50-Yr 2013/09/03 : CIA-RDP81-01043R002500170003-9

From Figure 3-7(b) the configuration of the bridge becomes evident. At balance, the potential of the junction of the impedances is the same as that of point N, so that the current I must be zero. With $E_2 = E_1$ (due to the very tightly coupled halves of the secondary of T_1), this gives $Z_u = Z_s$. In the actual bridge, a wider range of measurements is obtained by changing the ratio E_2/E_1, as well as changing the effective Z_u through the use of transformers.

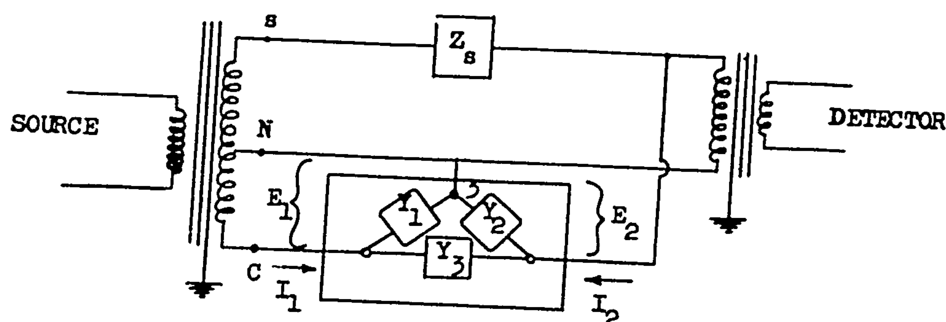

Fig. 3-7(c). The admittances Y_1 and Y_2 do not affect the measurement of Y_3, so the y-system parameters of a network may be determined by direct measurement.

Figure 3-7(c) shows a property of the circuit which is extremely useful in connection with the measurement of network properties. If a three terminal network is represented by a delta connection of the admittances Y_1, Y_2, and Y_3, these may be measured directly with only the three terminals available for external connections. In the example shown, Y_1 has no effect since, due to the very tight coupling between the halves of the secondary of T_1, it essentially becomes merely an added load for the source generator; Y_2 has no effect as it is connected across the detector where the voltage is zero at balance. The procedure for obtaining Y_1 and Y_2 follows directly from Figure 3-7(c). The y-system equations for the network are

$$I_1 = y_{11} E_1 + y_{12} E_2$$

$$I_2 = y_{21} E_1 + y_{22} E_2$$

Declassified in Part - Sanitized Copy Approved for Release @ 50-Yr 2013/09/03 : CIA-RDP81-01043R002500170003-9

Declassified in Part - Sanitized Copy Approved for Release @ 50-Yr 2013/09/03 : CIA-RDP81-01043R002500170003-9

and the y's are related to Y_1, Y_2, and Y_3 as follows:

$$y_{11} = Y_1 + Y_3 \quad , \quad y_{12} = y_{21} = -Y_3 \quad , \quad y_{22} = Y_2 + Y_3$$

This constitutes what is essentially an indirect method of evaluating the y-system parameters of a 3-terminal network, since they are not read directly on the bridge. Since the transistor is an active network, it has four independent y-parameters, and these cannot be obtained by the preceding method, as only three measurements are made. However, the bridge can be used to measure both two-terminal admittances and transfer admittances directly. For the former in the case of a passive network the procedure is straightforward, but for an active network, where biases must be applied, the basic circuit of Figure 3-5 may be used.

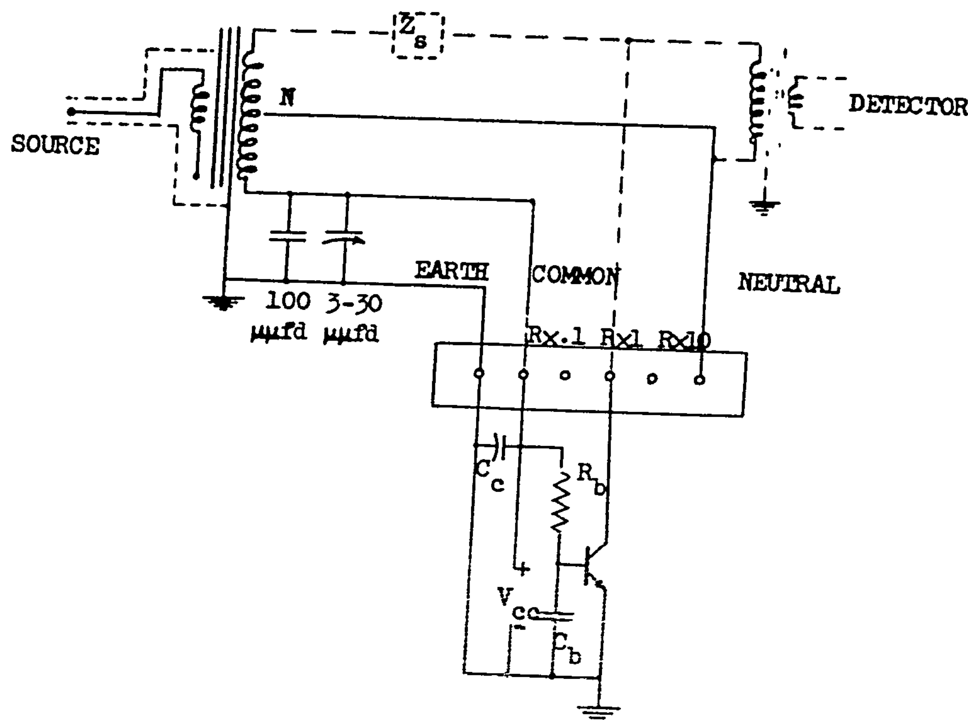

Fig. 3-8. Connections for the measurement of y_{22e} on the Wayne-Kerr B-601 Bridge. The circuit wiring in dashed lines shows the path through the bridge for the DC collector current.

Declassified in Part - Sanitized Copy Approved for Release @ 50-Yr 2013/09/03 : CIA-RDP81-01043R002500170003-9

Declassified in Part - Sanitized Copy Approved for Release @ 50-Yr 2013/09/03 : CIA-RDP81-01043R002500170003-9

The method of connecting the bridge for the measurement of y_{22e} is shown in Figure 3-8. (An NPN transistor is sketched here; for PNP transistors it is only necessary to reverse the polarity of V_{cc}.) The path of the DC collector current is through the lower half of the secondary of T_1 and the primary of T_2, to the R x 1 terminal. The bypass capacitor C_c is mounted directly on the bridge terminals and consists of two 0.1 mfd. ceramic capacitors in parallel. The reactance presented by C_c is sufficiently low for frequencies covered by the bridge that negligible error results in the measurement of the y-parameters in the grounded-emitter connection. These units were used in preference to paper or electrolytic types because of their excellent high frequency characteristics. The same combination would be suitable at C_b, although a paper capacitor was used in the actual system due to space limitations.

A mounting jig which simplifies the problem of making the necessary connections and of disconnecting the transistor from the bridge for initial balance is shown in Figures 3-9(a) and (b). The unit automatically connects the collector of the transistor under test to the "R x 1" terminal on the bridge for the measurement of y_{22e} (or h_{22e} when C_b is removed), or the base to the "R x 0.1" terminal for measurement of y_{11e}. The system pivots on a stud which is supported by the "Earth" terminal on the bridge, so that, as in Figure 3-9(a), the complete assembly may be turned for initial balance of the bridge, and then re-positioned (Figure 3-9(b)) for the actual measurement. The advantages of this system are that there is no mechanical motion of the transistors leads relative to its case, so the possibility of broken leads is eliminated. Also, short, low-inductance connections are easily obtained with this arrangement.

The components for this jig are taken from the DuMont K-100 Breadboard Chassis Kit. The terminals in this kit are arranged so that a permanent soldered connection or temporary connections with bus bar may be made, allowing the quick conversion from y_{11e} to y_{22e} measurement without unsoldering

Declassified in Part - Sanitized Copy Approved for Release @ 50-Yr 2013/09/03 : CIA-RDP81-01043R002500170003-9

Declassified in Part - Sanitized Copy Approved for Release @ 50-Yr 2013/09/03 : CIA-RDP81-01043R002500170003-9

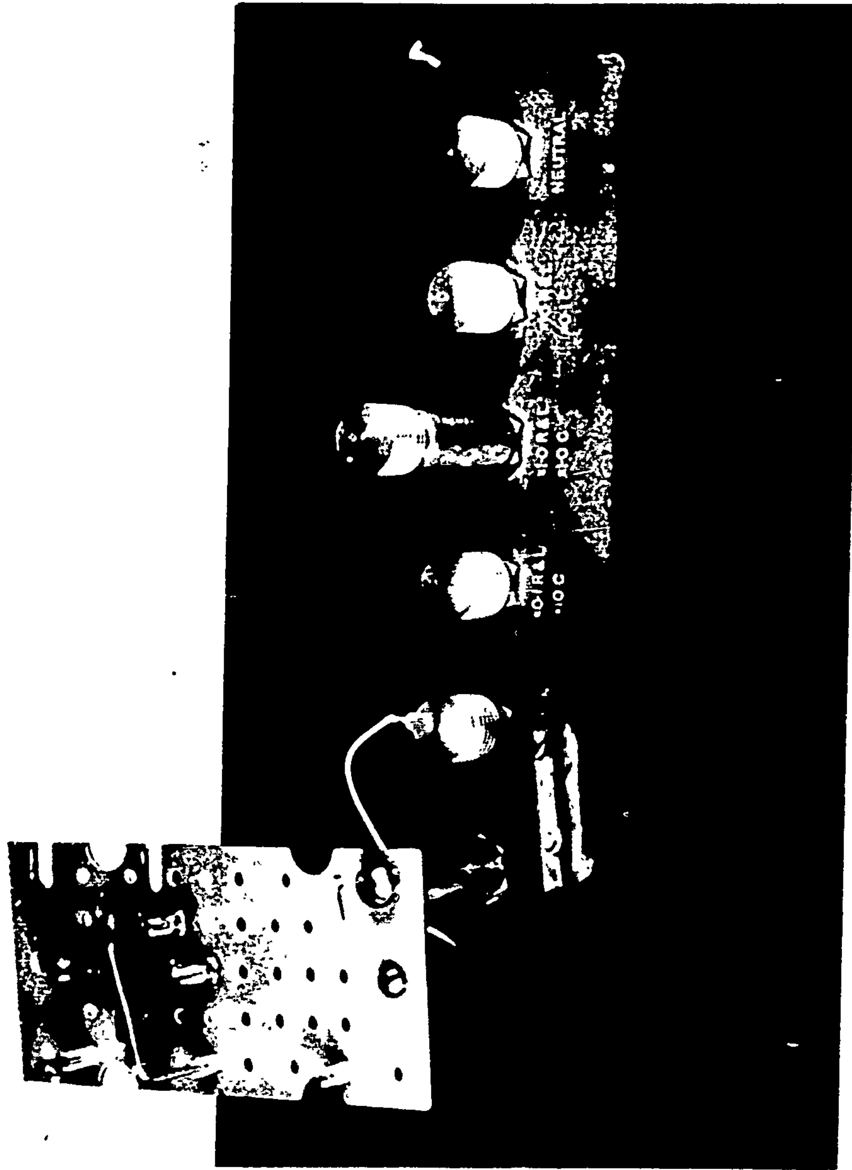

Figure 3-9(a). Test Jig in Position for Initial Balance of Bridge.

Declassified in Part - Sanitized Copy Approved for Release @ 50-Yr 2013/09/03 : CIA-RDP81-01043R002500170003-9

Declassified in Part - Sanitized Copy Approved for Release @ 50-Yr 2013/09/03 : CIA-RDP81-01043R002500170003-9

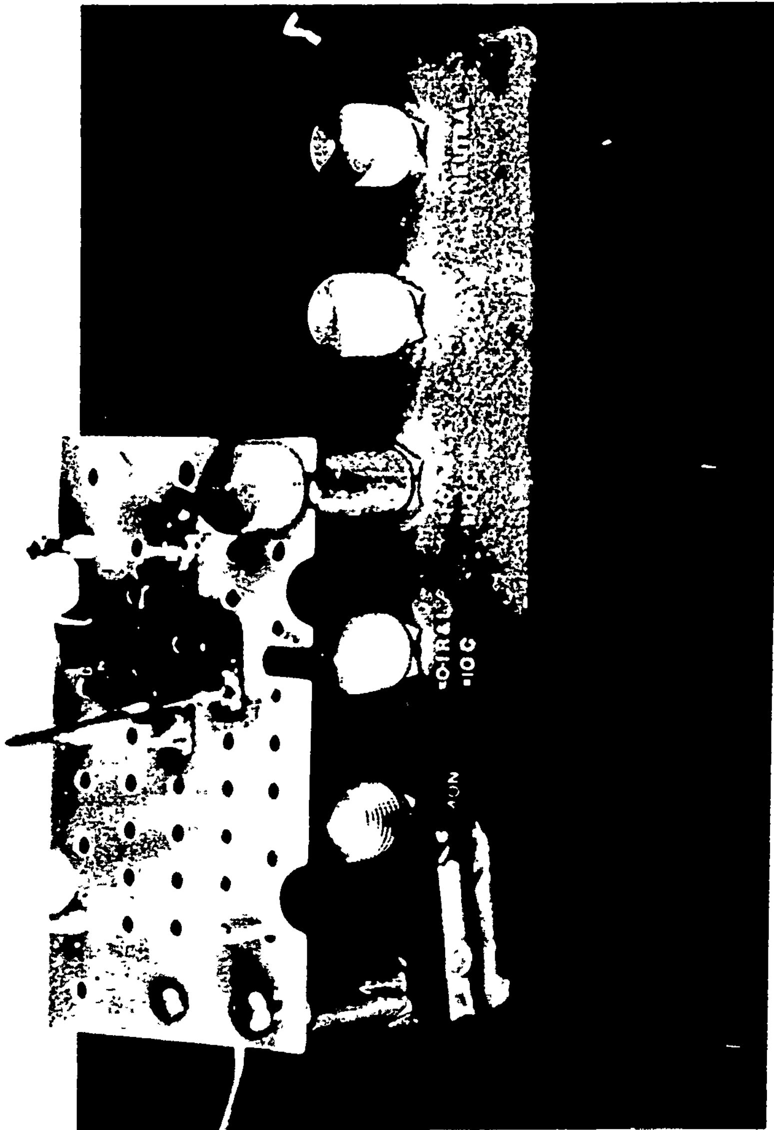

Figure 3-9(b). Test Jig in Position for Measurement of y_{22e}.

Declassified in Part - Sanitized Copy Approved for Release @ 50-Yr 2013/09/03 : CIA-RDP81-01043R002500170003-9

Declassified in Part - Sanitized Copy Approved for Release @ 50-Yr 2013/09/03 : CIA-RDP81-01043R002500170003-9

connections. Extension posts of 1/2" aluminum rod 1" long are used to hold the chassis above the surface of the bridge and provide clearance. The arrangement of Fahenstock clips used here to make the connections to the transistor is the same as that used in the video amplifiers described in Chapter 5. This provides a positive electrical contact with the transistor lead, but insertion of the transistor is somewhat difficult, so that future units will employ different terminals.

The disadvantage of this type of mount is that a small but measurable error is introduced in the results, due to the capacitance between the "hot" terminal and the "Earth" terminal caused by the mount. Since the bridge results are in the form of the values of R and C in a parallel RC circuit, this correction is easily taken into account. The capacitance to be subtracted from the C reading can be accurately determined, and is 0.9 mmfd. for the "R x 1" terminal; 0.95 mmfd. for the "R x 0.1" terminal. In many measurements, it is adequate to take the error as 0.9 mmfd. in either case.

The transfer admittances for a three-terminal network may also be measured using this bridge.[2] For the network of Figure 3-10 the y-system equations are

$$I_1 = y_{11} E_1 + y_{12} E_2$$

$$I_2 = y_{21} E_1 + y_{22} E_2$$

so that the transfer y's are defined as $y_{12} = I_1/E_2\big|_{E_1=0}$, $y_{21} = I_2/E_1\big|_{E_2=0}$. If the network is connected in the bridge as in Figure 3-11, the voltage E_1 is

[2] This is described in "A Junction-Transistor High Frequency Equivalent Circuit," by R. D. Middlebrook (Technical Report No. 83, Electronics Research Laboratory, Stanford University). Transistor measurements in this case were in the grounded-base connection.

Declassified in Part - Sanitized Copy Approved for Release @ 50-Yr 2013/09/03 : CIA-RDP81-01043R002500170003-9

Declassified in Part - Sanitized Copy Approved for Release @ 50-Yr 2013/09/03 : CIA-RDP81-01043R002500170003-9

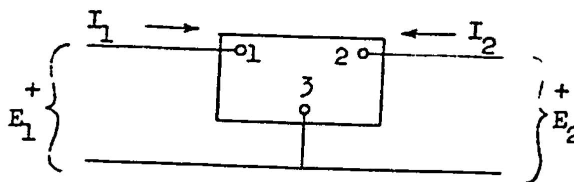

Fig. 3-10. A three-terminal network with reference directions.

zero at balance, and the current through the standard impedance Z_s is equal to I_2, and we have

$$Z_s = \left.\frac{E_1}{I_2}\right|_{E_2=0} = \frac{1}{y_{21}}$$

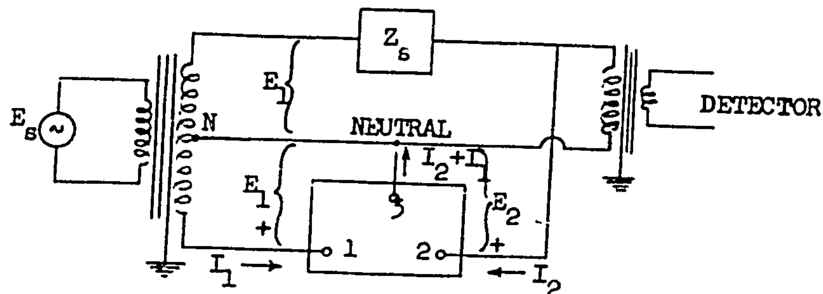

Fig. 3-11. The network connected for the measurement of y_{21}. At balance, $y_{21} = 1/Z_s$.

The fact that the transfer admittances can be measured on this bridge is of great importance, as the measurement of these at high frequencies is a very difficult problem.

A mounting jig for transfer parameter measurement similar to the type shown in Figure 3-9 has not yet been designed and built, since the test unit described in Section 3-1 was available for the measurement of h_{12e} and h_{21e}. However, accuracy considerations at higher frequencies make the use of bridge measurements essential, so that this is scheduled for completion in the very near future.

The bias problem which is present when measuring transfer parameters of active elements such as transistors or vacuum tubes arises because different potentials relative to the neutral lead are needed on the input and output

Declassified in Part - Sanitized Copy Approved for Release @ 50-Yr 2013/09/03 : CIA-RDP81-01043R002500170003-9

Declassified in Part - Sanitized Copy Approved for Release @ 50-Yr 2013/09/03 : CIA-RDP81-01043R002500170003-9

sides of the network. In general, the basic circuit of Figure 3-5 may be used on one side, while a direct connection may be made on the other. It appears that a possible solution for low voltages is a battery power supply of sufficiently small physical size so that it may be placed on the transistor mount on the bridge without introducing error due to parasitic coupling between it and the bridge terminals.

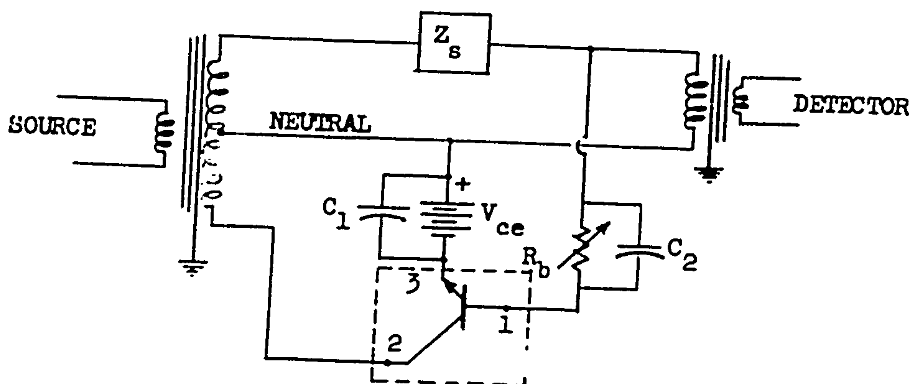

Fig. 3-12. A possible method of connecting the transistor and bias supplies for the measurement of y_{12e}. A discussion of the values required for C_1 and C_2 is given in the text.

A circuit for this purpose is shown in Figure 3-12, where a battery furnishing the desired collector-to-emitter voltage V_{ce} is placed in series with the emitter and the Neutral terminal of the bridge. An examination of the connections involved shows that the impedance due to the bypass capacitor C_1 should be negligible compared to $1/y_{11b}$, and, as the latter quantity is on the order of 35 ohms at low frequencies, C_1 is a fairly large capacitor. For example, if the reactance of C_1 is to be 10°/o of $1/y_{11e}$ or 3.5 ohms at 15 kc., C_1 is found to be 3 mfd. An electrolytic of this value, in parallel with a ceramic capacitor, to insure good high-frequency bypassing, could be used. In the case of C_2, its impedance should be negligible compared to $1/y_{11e}$, and a value of 0.1 mfd. is adequate.

Declassified in Part - Sanitized Copy Approved for Release @ 50-Yr 2013/09/03 : CIA-RDP81-01043R002500170003-9

Declassified in Part - Sanitized Copy Approved for Release @ 50-Yr 2013/09/03 : CIA-RDP81-01043R002500170003-9

An alternate possibility exists as in Figure 3-13. Here the battery furnishing V_{ce} is placed in series with the collector lead. The requirements for C_2 are unchanged, but the value of C_1 required is much smaller, since the criterion to be met is that its reactance be negligible compared to $1/y_{22e}$, a condition which is easily satisfied by making C_1 = 0.1 mfd. On the basis of eliminating measurement errors due to the odd behavior of electrolytic capacitors with frequency, this circuit is to be preferred.

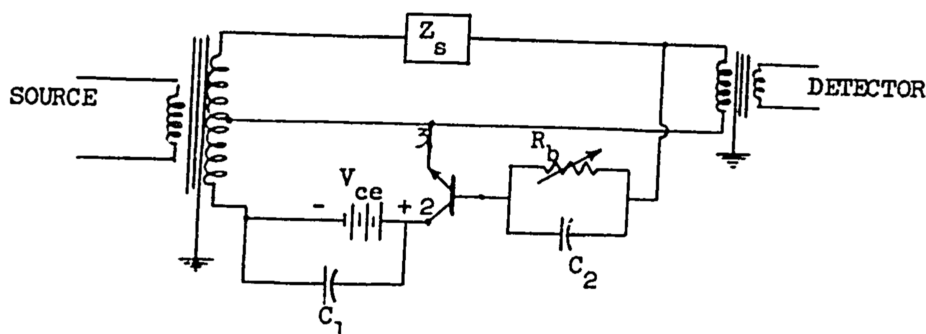

Fig. 3-13. An alternate method of providing bias for the measurement of y_{12e}. The values for C_1 and C_2 are small enough to permit the use of either ceramic or paper tubular capacitors having good high-frequency characteristics.

For the measurement of y_{21e} it is only necessary to interchange the base and collector leads (with their associated bias components) relative to the bridge terminals. Since the bridge readings are in terms of the values of R and C for the equivalent parallel RC circuit at the frequency of measurement, the form in which the results may be presented with a minimum amount of calculation is a polar plot of the form Y = G + jB. For certain parameters, notably y_{22e}, a great deal of information may be obtained from such a plot, even when relatively few experimental points are available. In other cases, such as y_{11e}, a polar plot of $h_{11e} = 1/y_{11e}$ is much more easily compared with the pre-

Declassified in Part - Sanitized Copy Approved for Release @ 50-Yr 2013/09/03 : CIA-RDP81-01043R002500170003-9

Declassified in Part - Sanitized Copy Approved for Release @ 50-Yr 2013/09/03 : CIA-RDP81-01043R002500170003-9

dicted theoretical form. In either the admittance or impedance case both the theoretical and measured polar plots are sections of circles over at least part of the frequency range of interest, so that useful information may be obtained from either type of representation.

3-3. Results for a Fused-Junction Transistor

The measurements of y_{11e} and y_{22e} were made using the Wayne-Kerr B-601 RF Bridge, while those of h_{12e} and h_{21e} were made using the unit described in Section 3-1. All measurements were made at a collector-to-emitter voltage V_{ce} of 5 volts and a collector current I_c of 1 milliampere, as the data furnished by many manufacturers specifies either this operating point or ones very close to it.

A. Complex Plot of y_{11e}

Figure 3-14 shows both measured and calculated frequency characteristics of y_{11e} for a fused-junction transistor, Raytheon type 2N113-2. (The last number is used for purposes of identification in the laboratory and is not part of the manufacturer's type number.) The measured value of b_o for this unit is 44, and the b-cutoff frequency, f_b, is 200 kilocycles. As theory predicts a definite correlation between the frequency dependence of y_{11e} and f_b, data for y_{11e} was taken at frequencies which are integral multiples and sub-multiples of f_b.

It is seen that the portion of the measured characteristic for frequencies up to $f/f_b = 10$ is virtually a perfect section of the circular locus as predicted by theory. The theoretical locus shown here was obtained by selecting the radius so as to provide the best match with the measured characteristic in this region. For this case, the intercept on the G-axis is $G_1 = 750$ µmhos at $\omega = 0$, $G_2 = 8760$ µmhos at $\omega = \infty$, and the frequency of 45° phase shift is approximately $1.2 f_b$.

The analytical expression for this locus is

Declassified in Part - Sanitized Copy Approved for Release @ 50-Yr 2013/09/03 : CIA-RDP81-01043R002500170003-9

Declassified in Part - Sanitized Copy Approved for Release @ 50-Yr 2013/09/03 : CIA-RDP81-01043R002500170003-9

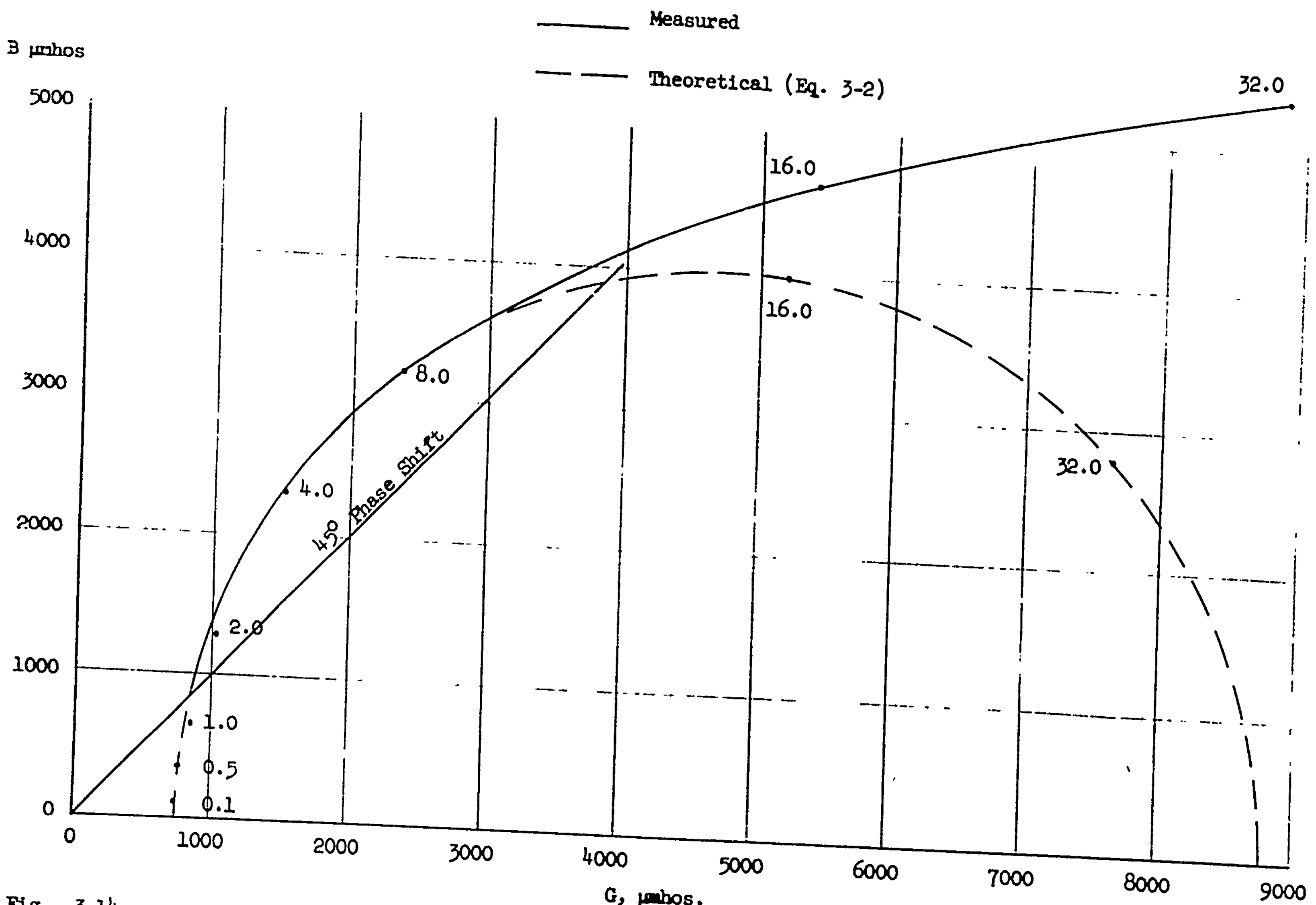

Fig. 3-14. $y_{11e} = G + jB$ for Raytheon 2N113-2 fused-junction transistor, measured with the Wayne-Kerr B-601 RF Bridge at $V_{ce} = -5$ volts, $I_c = -1$ ma. Figures represent f/f_b values for the corresponding points. For this transistor, $b_o = 44$ and $f_b = 200$ kc.

Declassified in Part - Sanitized Copy Approved for Release @ 50-Yr 2013/09/03 : CIA-RDP81-01043R002500170003-9

Declassified in Part - Sanitized Copy Approved for Release @ 50-Yr 2013/09/03 : CIA-RDP81-01043R002500170003-9

$$y_{11e} = G_1 \frac{1 + j\omega T}{1 + j\omega \gamma T}$$

where

$$\gamma = \frac{G_1}{G_2} = \frac{750 \times 10^{-6}}{8760 \times 10^{-6}} = .085 \quad (3\text{-}1)$$

and the value of T, according to theorem should be $T_b = 1/2\pi f_b$. If we take the values of G_1 and G_2 given above and substitute them in Eq. (3-1), the value of ωT which represents 45^0 phase shift is approximately 1.19. This is in good agreement with the value obtained from the measured characteristics, so that, in the frequency range up to $f/f_b \cong 10$, we have

$$y_{11e} = (750 \times 10^{-6}) \frac{1 + j\, f/f_b}{1 + .085\, j\, f/f_b} \quad \frac{f}{f_b} \leqq 10 \quad (3\text{-}2)$$

The agreement between this expression and the measured points for other values of f/f_b in this range is quite good.

The corresponding plot of $h_{11e} = 1/y_{11e}$ is shown in Figure 3-15. On this plot, the difference between the measured and theoretical characteristics is less pronounced, as it occurs in a range where the plotted values are small. In connection with the point for $f/f_b = 32$, it should be noted that, as f_b for this transistor is 200 kilocycles, this is a frequency of 6.4 megacycles, which is outside the 5 megacycle upper limit for the bridge accuracy specification.

A number of other fused-junction units showed a deviation from theory similar to that in Figures 3-14 and 3-15 as was mentioned above, some error is contributed due to the bridge at $f/f_b = 32$. It is planned to use a Wayne-Kerr B-801 Bridge, presently on order, to make measurements up to at least 10 megacycles so that the behavior of y_{11e} in this frequency range may be accurately determined. For this reason, we will discuss some of the possible causes of this difference, but will make no effort at this time to correlate any of these causes with the observed phenomena.

Declassified in Part - Sanitized Copy Approved for Release @ 50-Yr 2013/09/03 : CIA-RDP81-01043R002500170003-9

Declassified in Part - Sanitized Copy Approved for Release @ 50-Yr 2013/09/03 : CIA-RDP81-01043R002500170003-9

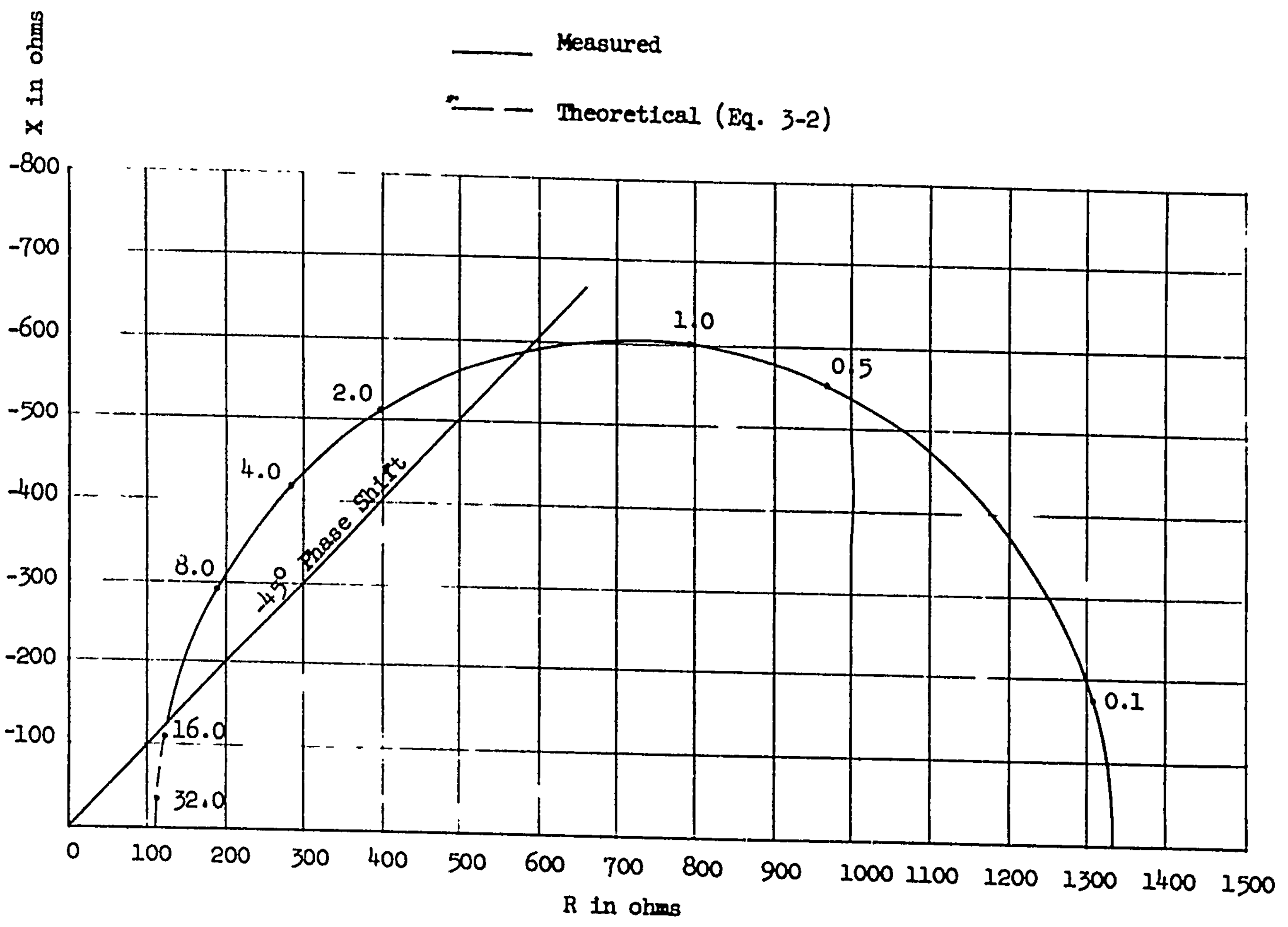

Fig. 3-15. $h_{11e} = 1/y_{11e} = R + jX$ for Raytheon 2N113-2 fused-junction transistor, measured with the Wayne-Kerr B-601 RF Bridge at V_{ce} = -5 volts, I_c = -1ma. Figures represent f/f_b values for the corresponding points. For this transistor, b_o = 44 and f_b = 200 kilocycles.

Declassified in Part - Sanitized Copy Approved for Release @ 50-Yr 2013/09/03 : CIA-RDP81-01043R002500170003-9

Declassified in Part - Sanitized Copy Approved for Release @ 50-Yr 2013/09/03 : CIA-RDP81-01043R002500170003-9

One source of error is that the physical structure of the transistor, rather than being of the idealized type discussed in Chapter 2, is more of the form shown in Figure 3-16. If this form is, in turn, approximated by the geometry of Figure 3-17 which is discussed in the paper[1] by Early previously mentioned, the simple r_b model must be replaced by the more complex circuit of Figure 3-18. Here, as in the case of the simpler model, we have neglected the effect of feedback due to base width modulation.

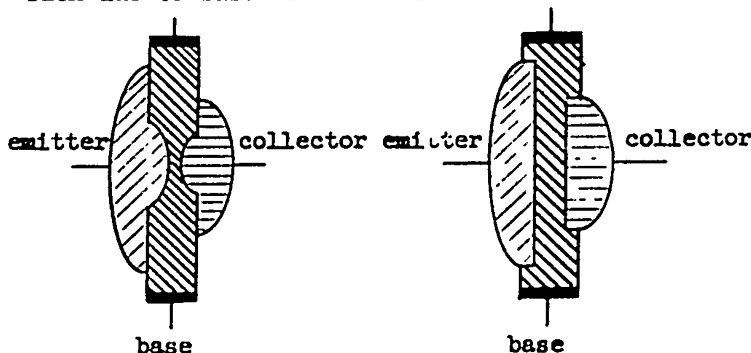

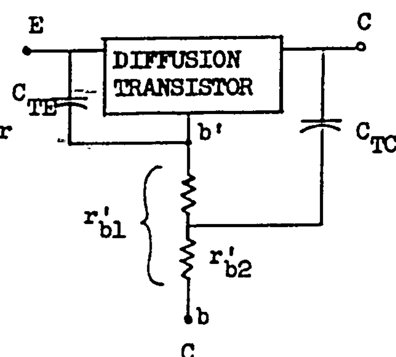

Fig. 3-16. Cross-section of typical fused-junction transistor. The base is in the form of a disc, with the contact made by a metal ring around the periphery of the disc. The transistor elements are symmetrical about the axis of the disc.

Fig. 3-17 Idealized cross-section for the geometry of Fig. 3-13.

Fig. 3-18. Approximate circuit representation for the geometry of Fig. 3-14.

For the measurement of h_{11e} (or y_{11e}) in the grounded emitter connection, the collector terminal is a-c short-circuited to the emitter terminal, so that the behavior of h_{11e} for the circuit of Figure 3-18 is not difficult to predict. At high frequencies, i.e., many times the b-cutoff frequency, h_{11e} approaches r'_{b1} as it did for the simpler model. For a typical transistor, r'_{b2} may be on the order of 1/2 of r'_{b1}, so that the effect of C_{TC} would not enter in until the reactance of C_{TC} was comparable to $r'_{b2}/2$. This represents an extremely high frequency for commonly encountered values of C_{TC} and r'_{b2}, so that it does not

Declassified in Part - Sanitized Copy Approved for Release @ 50-Yr 2013/09/03 : CIA-RDP81-01043R002500170003-9

Declassified in Part - Sanitized Copy Approved for Release @ 50-Yr 2013/09/03 : CIA-RDP81-01043R002500170003-9

serve to explain the experimental results. It should be emphasized that the fact that C_{TC} is "tapped down" on the base spreading resistance may have a significant effect on the performance of the transistor when operated as a grounded-emitter amplifier, due to the fact that the collector and emitter terminals are not a-c short circuited. This is because there is a multiplication of the actual value of C_{TC} as far as the input circuit is concerned, this being similar to the Miller effect in vacuum-tube amplifiers.

B. Complex Plot of y_{22e}

This is shown in Figure 3-19, for the same transistor, Raytheon 2N113-2. As in the case of y_{11e}, the initial part of the locus is circular, which permits us to draw a semicircular locus shown by the dashed lines. This locus goes from a low value of conductance at zero frequency to a higher value at infinite frequency, and has a positive phase angle in between. This may be represented by an admittance Y which consists of a resistance in parallel with a series RC circuit. The form of y_{22e} as predicted from theory has this form of circuit, with an added capacitance in parallel, as shown in Figure 3-20.

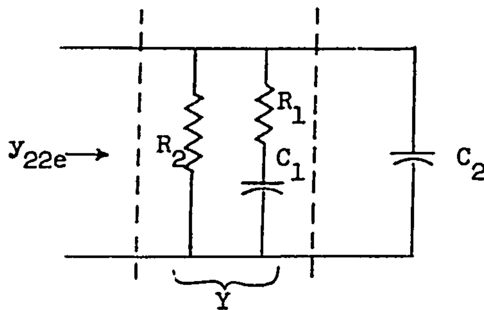

Fig. 3-20. $y_{22e} = Y + j\omega C_2$

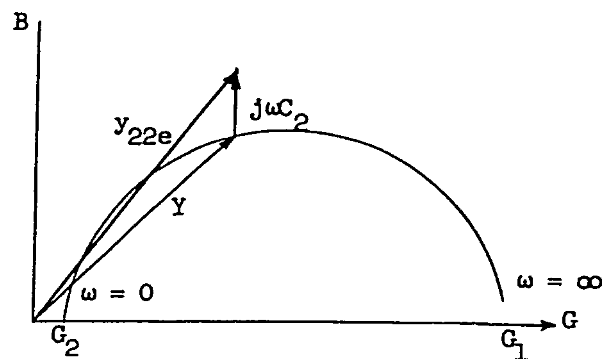

Fig. 3-21. Plot of the admittance $y_{22e} = G + jB$ of Fig. 3-20.

Declassified in Part - Sanitized Copy Approved for Release @ 50-Yr 2013/09/03 : CIA-RDP81-01043R002500170003-9

Declassified in Part - Sanitized Copy Approved for Release @ 50-Yr 2013/09/03 : CIA-RDP81-01043R002500170003-9

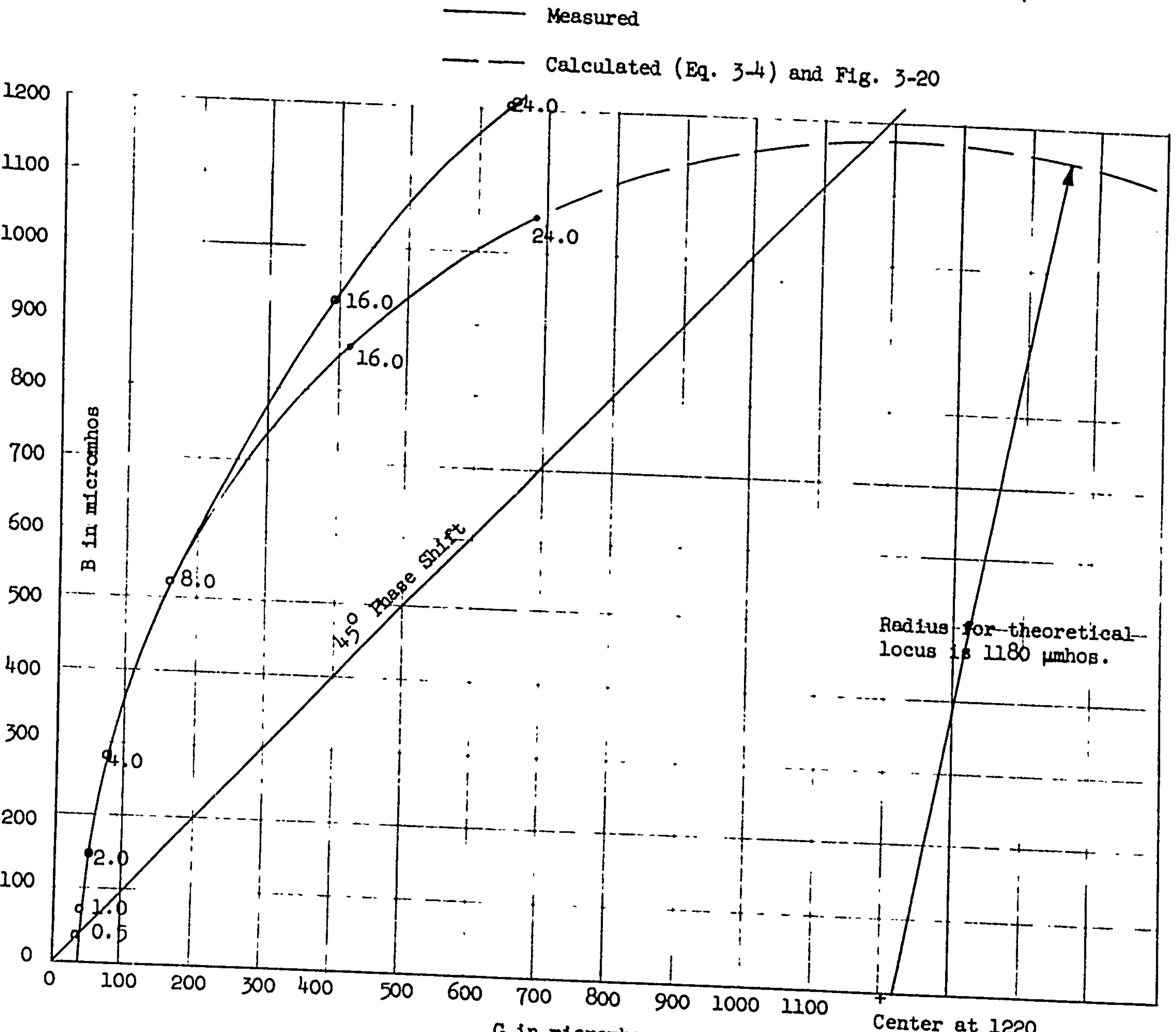

Fig. 3-19. $y_{22e} = G + jB$ for Raytheon 2N113-2 transistor with $V_{ce} = -5$ volts, $I_c = -1$ ma. For this transistor, $b_o = 44$ and $f_b = 200$ kilocycles.

Declassified in Part - Sanitized Copy Approved for Release @ 50-Yr 2013/09/03 : CIA-RDP81-01043R002500170003-9

Declassified in Part - Sanitized Copy Approved for Release @ 50-Yr 2013/09/03 : CIA-RDP81-01043R002500170003-9

The problem at hand is to determine whether the measured characteristic of Figure 3-19 is accurately represented by the $Y + j\omega C_2$ predicted by theory. This may be solved by noting that, if this is true, the real components of the measured curve and those of Y should be equal, since the $j\omega C_2$ term affects only the imaginary component of y_{22e}. Also, the difference in the imaginary components of the measured curve and Y should be proportional to frequency. These properties are diagramed in Figure 3-21, and a reference to Figure 3-19 shows that the first requirement is met. As for the second, if ΔB is the difference in the imaginary components of the measured and Y characteristics, we have

$$\Delta B \cong 90 \text{ micromhos} \quad \text{at } f/f_b = 16 \text{ or } 3.2 \text{ megacycles;}$$
$$\Delta B \cong 180 \text{ micromhos} \quad \text{at } f/f_b = 24 \text{ or } 4.8 \text{ megacycles;} \qquad (3\text{-}3)$$

and calculation gives a value of $C_2 = 2$ mmfd. for $f/f_b = 16$ and $C_2 = 1.7$ mmfd. for $f/f_b = 24$. While the agreement is by no means exact, it should be kept in mind that this method for determining C_2 is very sensitive to small changes in the locus of Y, as well as to small percentage errors in the measurement of B for y_{22e}. Better accuracy could be obtained, of course, by making measurements at higher frequencies, so that ΔB is an appreciable fraction of B for y_{22e}. This in turn indicates the use of a bridge covering the range above 5 megacycles, such as the Wayne-Kerr B-801 RF Bridge, which is not presently available. Thus, using the data from Figure 3-19, we will use the representation of Figure 3-20 for y_{22e} and take $C_2 = 2$ mmfd., while determining the other circuit constants from the locus of Y in Figure 3-19. The latter procedure is not difficult, as the intercepts on the G-axis determine G_1 and G_2, while the first frequency of 45° phase shift may be used to determine the R_2C_1 product, as it is only a small percentage of the second. The circuit constants for Figure 3-20 are found to be:

$$R_2 = 25{,}000 \text{ ohms;} \quad R_1 = 397 \text{ ohms;}$$
$$C_2 = 2 \text{ mmfd.;} \quad C_1 = 64 \text{ mmfd.} \qquad (3\text{-}4)$$

Declassified in Part - Sanitized Copy Approved for Release @ 50-Yr 2013/09/03 : CIA-RDP81-01043R002500170003-9

Declassified in Part - Sanitized Copy Approved for Release @ 50-Yr 2013/09/03 : CIA-RDP81-01043R002500170003-9

The large value of C_1 and very low value of R_1 impose severe limitations on the gain-bandwidth relationship of the transistor when used as a grounded-emitter video amplifier. The effects of these elements are considered in detail in Chapter 5.

C. Frequency Dependence of h_{12e} and h_{21e}

These were measured using the parameter tester described in Section 3-1, and, as this unit provides amplitude information only, the results are shown in decibels relative to the low frequency value, versus frequency normalized to the b-cutoff frequency of the transistor.

The behavior of $|h_{12e}|$ for the Raytheon 2N113-2 is shown in Figure 3-22. It begins to increase at .01 f_b, or 2 kc., and approaches a slope of 6 db per octave, tending to level off somewhat as f_b is approached. At $f = 10\ f_b$, or 2 megacycles, it is only 6 db above its value at $f = f_b$. The estimated constant value which the curve approaches is on the order of 38 db above its low frequency value.

It should be noted that the accuracy to be expected using this method of measuring h_{12e} is quite good. As $h_{12e} = E_1/E_2$ with $I_1 = 0$, a requirement for good results is that the external meter used to measure E_1 have an input impedance which is very high compared to the effective source impedance looking into the base and emitter terminals. Since the collector is fed from a very low impedance source, the impedance in question is essentially h_{11e}, which at high frequencies approaches r_b. As r_b' is on the order of 100 ohms, capacitive loading by the vacuum-tube voltmeter used to measure E_1 is not a serious problem. For example, an input capacitance of 25 mmfd. has a reactance of 20 r_b' (for the typical case of $r_b' = 100$ ohms) at a frequency of 3 megacycles.

It is seen from Figure 3-23 that $h_{21e} = b$ follows the predicted form of frequency dependence very closely. The theoretical characteristic shown here represents the function

Declassified in Part - Sanitized Copy Approved for Release @ 50-Yr 2013/09/03 : CIA-RDP81-01043R002500170003-9

Declassified in Part - Sanitized Copy Approved for Release @ 50-Yr 2013/09/03 : CIA-RDP81-01043R002500170003-9

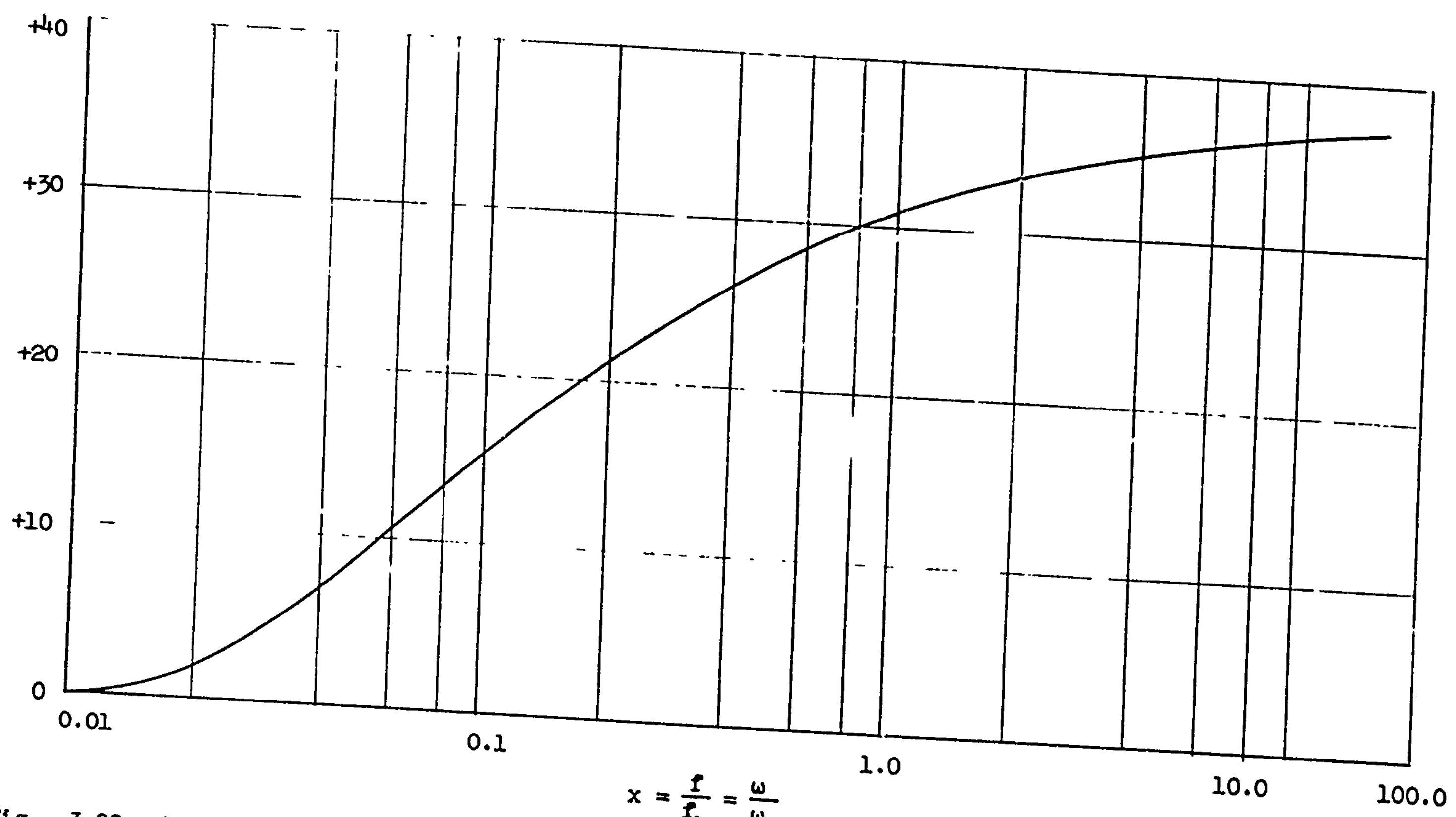

Fig. 3-22. h_{12e} vs. $x = f/f_b$ for Raytheon 2N113-2 transistor, biased at $V_{ce} = -5$ volts, $I_c = 1$ ma. For this transistor, $b_o = 44$ and $f_b = 200$ kilocycles. h_{12e} at zero db. reference level is 0.5×10^{-3}.

Declassified in Part - Sanitized Copy Approved for Release @ 50-Yr 2013/09/03 : CIA-RDP81-01043R002500170003-9

Declassified in Part - Sanitized Copy Approved for Release @ 50-Yr 2013/09/03 : CIA-RDP81-01043R002500170003-9

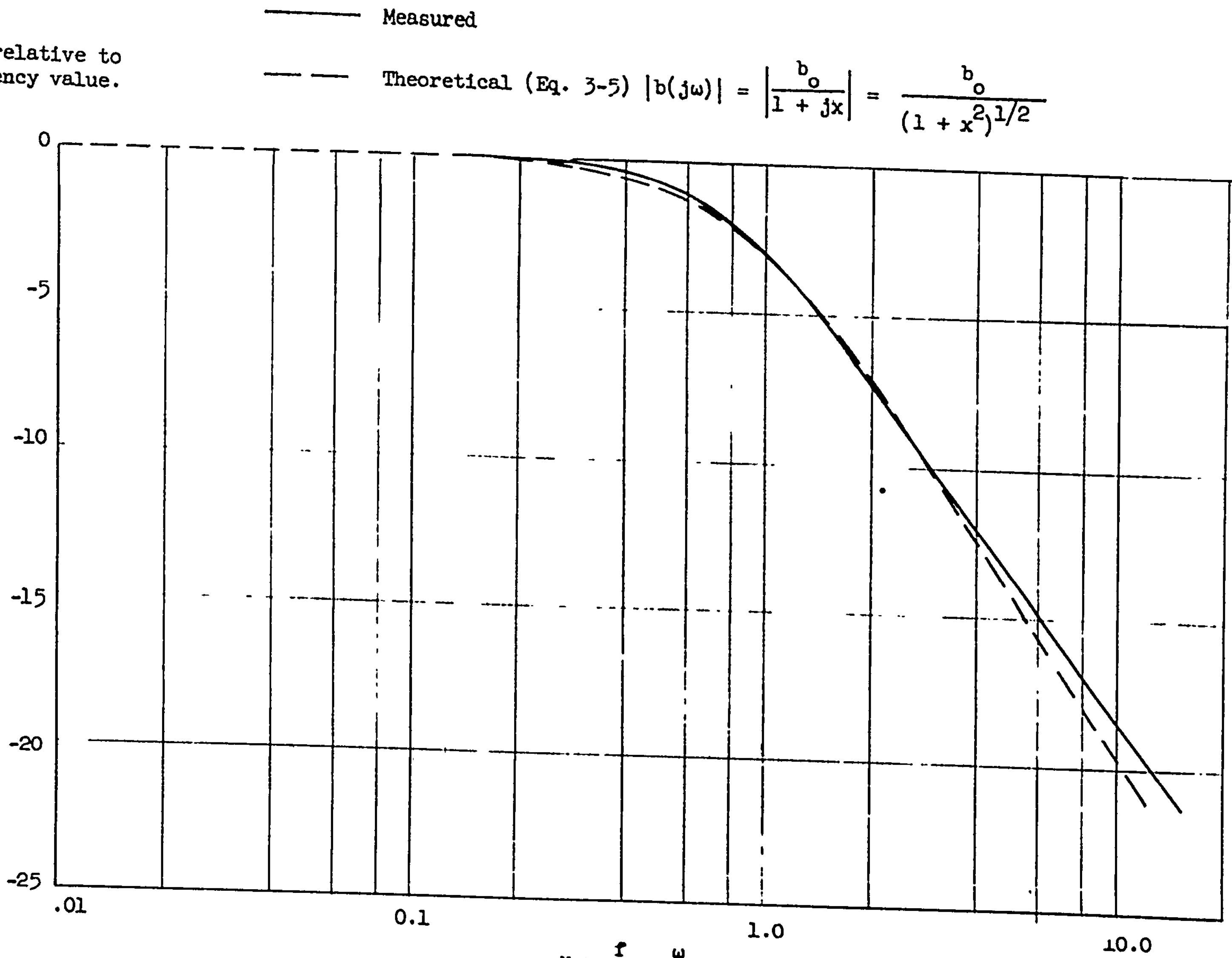

Fig. 3-23. $|b(j\omega)| = |h_{21e}(j\omega)|$ vs. $x = f/f_b$ for Raytheon 2N113-2, biased at $V_{ce} = -5$ volts, $I_c = 1$ ma. For this transistor, $b_o = 44$ and $f_b = 200$ kilocycles.

Declassified in Part - Sanitized Copy Approved for Release @ 50-Yr 2013/09/03 : CIA-RDP81-01043R002500170003-9

Declassified in Part - Sanitized Copy Approved for Release @ 50-Yr 2013/09/03 : CIA-RDP81-01043R002500170003-9

$$\left|h_{21e}(j\omega)\right| = \left|b(j\omega)\right| = \left|\frac{b_o}{1 + j\omega T_b}\right| = \left|\frac{b_o}{1 + j\, f/f_b}\right| = \frac{b_o}{\left[1 + (\frac{f}{f_b})^2\right]^{1/2}} \qquad (3\text{-}5)$$

where the frequency f_b was determined experimentally as that at which the magnitude of b was 70.7°/o of the low-frequency value b_o. This means, of course, that the points for $f/f_b = 1$ are made to coincide, and that agreement elsewhere depends upon the validity of the theoretical form. The major difference evident in Figure 3-23 is that the measured characteristic does not approach a slope of -6 db per octave at high frequencies, the actual slope being on the order of $-4^1/2$ db per octave. It is possible to approximate this slope through the use of a more complicated network function, but the considerable labor involved would not justify this step where an expression useful for design purposes is needed.

D. Comparison with Theory

For y_{11e}, the agreement with the theory as regards the frequency dependence is reasonably good, as in the case of y_{22e}. For the latter, however, the parameter values in the circuit representation are in poor agreement with those predicted by theory, especially as concerns the low-frequency value of y_{22e}. This is generally caused by leakage effects across the collector-base junction which completely mask the much smaller value of conductance due to transistor action.

In the case of y_{12e}, we use the relation $y_{12e} = -\, h_{12e}/h_{11e}$. The curve for h_{12e} in Figure 3-22 may be approximated by the analytical expression

$$h_{12e} = \mu_e \frac{1 + \lambda_1\, j \frac{\omega}{\omega_b}}{1 + \lambda_2\, j \frac{\omega}{\omega_b}} \qquad (3\text{-}6)$$

where μ_e is the low-frequency value of h_{12e} and the constants λ_1 and λ_2 are determined from the frequencies at which the curve is 3 db above its low-frequency value and 3 db below its high frequency value, respectively. (This method of approximation is discussed in detail in connection with the grown-junction transistor later in this section.)

Declassified in Part - Sanitized Copy Approved for Release @ 50-Yr 2013/09/03 : CIA-RDP81-01043R002500170003-9

Declassified in Part - Sanitized Copy Approved for Release @ 50-Yr 2013/09/03 :
CIA-RDP81-01043R002500170003-9

For the curve of Figure 3-22, $\mu_e = 0.5 \times 10^{-3}$, $\lambda_1 = 40$, $\lambda_2 = 0.4$, so that

$$h_{12e} = 0.5 \times 10^{-3} \frac{1 + j\,40 \frac{\omega}{\omega_b}}{1 + j\,0.4 \frac{\omega}{\omega_b}} \tag{3-7}$$

Combining this with the expression for h_{11e} previously derived,

$$h_{11e} = R \frac{1 + j\,\gamma \frac{\omega}{\omega_b}}{1 + j \frac{\omega}{\omega_b}} = 1330 \frac{1 + j\,.085 \frac{\omega}{\omega_b}}{1 + j \frac{\omega}{\omega_b}} \tag{3-8}$$

we obtain the form for y_{12e} which approximates the measured characteristics,

$$y_{12e} = -\frac{h_{12e}}{h_{11e}} \doteq \frac{0.5 \times 10^{-3}}{1330} \cdot \frac{(1 + j\,40 \frac{\omega}{\omega_b})\,(1 + j \frac{\omega}{\omega_b})}{(1 + j\,0.4 \frac{\omega}{\omega_b})\,(1 + j\,.085 \frac{\omega}{\omega_b})} \tag{3-9}$$

which is quite complicated as it stands, but may be simplified considerably for design purposes. At present, however, this is to be compared with the theoretical expression for y_{12e}, Eq. (2-82), Chapter 2:

$$y_{12e} \doteq -\frac{g_{22}^d}{b_o + x} \; \frac{(1 + j \frac{\omega}{\omega_b})\,(1 + j \frac{\omega}{\omega_\alpha}) + j\omega \frac{b_o\, C_{TC}}{g_{22}^d}}{1 + j \frac{\omega}{\omega_b} \; \frac{x + 0.4}{b_o + x}} \tag{3-10}$$

where the relation $T_\alpha = \frac{4}{5b_o} T_b$ has been used to obtain $\frac{T_\alpha}{2} + \frac{xT_b}{b_o} = \frac{1}{b_o \omega_b}\,(x + 0.4)$. Here, x is $r_b'\, g_{11}^d$, which for the transistor discussed here is $113(0.04) = 4.5$ at room temperature. In this case, x is comparable to b_o, so that it must be included in the analysis.

Comparing this with the expression representing the measured characteristic, we see that the numerators are of the same power in ω, but that the denominators are not. Disregarding this for the present, we may determine g_{22}^d by equating the low-frequency values,

Declassified in Part - Sanitized Copy Approved for Release @ 50-Yr 2013/09/03 :
CIA-RDP81-01043R002500170003-9

Declassified in Part - Sanitized Copy Approved for Release @ 50-Yr 2013/09/03 : CIA-RDP81-01043R002500170003-9

$$g_{22}^{d} = (b_o + x)\,\frac{\mu_e}{R} = (44 + 4.5)\,\frac{0.5 \times 10^{-3}}{1330} = 18.2\ \mu\text{mhos} \qquad (3\text{-}11)$$

This corresponds to a resistance of about 55,000 ohms, which is much larger than the value of y_{22} at low frequencies, the latter being about 25,000 ohms.

Similarly, equating coefficients of $j\omega$ for the numerator of each expression enables us to find C_{TC},

$$j\omega\left[\frac{1}{\omega_b} + \frac{1}{\omega_\alpha} + \frac{b_o\ C_{TC}}{g_{22}^{d}}\right] = j(\lambda_1 + 1)\,\frac{\omega}{\omega_b}$$

$$\frac{b_o\ C_{TC}}{g_{22}^{d}} \cong \frac{\lambda_1}{\omega_b} \qquad\qquad \omega_\alpha >> \omega_b$$

$$C_{TC} \doteq \frac{g_{22}^{d}\ \lambda_1}{b_o\ \omega_b} = \frac{18.2}{44} \times \frac{40}{2\pi \times 0.2} \times 10^{-12}$$

$$= 13.2\ \mu\mu f \qquad (3\text{-}12)$$

This value of C_{TC} does not agree with that predicted from the measurement of y_{22}, the latter value being on the order of 2 μμf. The error in this case is undoubtedly in the measurement of h_{12e}, and it is planned to resolve this problem by direct bridge measurement of y_{12e} in order to obtain better correlation with the theoretical model. It should be noted that, as a matter of practical interest, the effect of h_{12e} (or y_{12e}) on the performance of the unit as a wide-band amplifier is sufficiently small that excellent results may be obtained from a design theory which does not include it.

For the case of y_{21e}, we obtain y_{21e} as

$$y_{21e} = y_{11e}\ h_{21e} = G\,\frac{1 + j\,\frac{\omega}{\omega_b}}{1 + rj\,\frac{\omega}{\omega_b}} \cdot b_o\,\frac{1}{1 + j\,\frac{\omega}{\omega_b}} = \frac{b_o\ G}{1 + \gamma j\,\frac{\omega}{\omega_b}} \qquad (3\text{-}13)$$

where $\gamma = r_b'\,G$ and G is the low-frequency value of y_{11e}. The form for y_{21e} as predicted from the theory developed in Chapter 2 is Eq. (2-83):

Declassified in Part - Sanitized Copy Approved for Release @ 50-Yr 2013/09/03 : CIA-RDP81-01043R002500170003-9

Declassified in Part - Sanitized Copy Approved for Release @ 50-Yr 2013/09/03 : CIA-RDP81-01043R002500170003-9

$$y_{21e} = \frac{g_{21}^{d}}{1 + \frac{x}{b_o} + j\,\frac{\omega}{\omega_b}\frac{1}{b_o}(x + 0.4)} = \frac{g_{21}^{d}}{1 + \frac{x}{b_o}} \quad \frac{1}{1 + j\,\frac{\omega}{\omega_b}\frac{x + 0.4}{b_o + x}} \qquad (3\text{-}14)$$

A comparison of Eqs. (3-13) and (3-14) shows that we should have

$$g_{21}^{d} = (1 + \frac{x}{b_o})\, b_o\, G \qquad \gamma = \frac{x + 0.4}{b_o + x} \qquad (3\text{-}15)$$

The second relation of (3-15) may be checked immediately for the 2N113-2. The value of γ for this transistor, from Eq. (3-1), is .085; and the value of x is 4.5. When this is substituted in the right hand-side of (3-15), the value obtained is 0.1, which is comparable with the measured value of .085. Thus we have good agreement between the theoretical and measured frequency dependence of y_{21e}, which is a useful parameter in the design of wide band transistor amplifiers, using the grounded-emitter connection. As will be shown later, a reduction of the driving source impedance results in a greater bandwidth, so that the transistor is frequently driven from a low-impedance source, a condition approximating that under which the y-parameters are defined.

3-4 Results for the Grown-Junction Transistor

A set of theoretical results for circuit parameters of the grown junction transistor as complete as those available for the fused junction type has not yet been published, although much work has been done from a primarily experimental point of view. In particular, Pritchard[2] has shown that one of the major differences between the equivalent circuit representations for the grown-and fused-junction transistor is that the former must be considered to have a complex base spreading resistance z_b' instead of the r_b' which provides reasonably good agreement between experiment and theory for the case of fused-junction transistors. In addition, the frequency dependence of z_b' is

[2] R. L. Pritchard and W. N. Coffey, "Small-Signal Parameters of Grown-Junction Transistors at High Frequencies", Convention Record of the Institute of Radio Engineers, Part 3, 90-98, 1954.

Declassified in Part - Sanitized Copy Approved for Release @ 50-Yr 2013/09/03 : CIA-RDP81-01043R002500170003-9

Declassified in Part - Sanitized Copy Approved for Release @ 50-Yr 2013/09/03 : CIA-RDP81-01043R002500170003-9

such that it cannot be exactly represented by physically realizable, lumped-parameter networks. A further point of importance is that, for the fused-junction transistor r_b' may be on the order of 5 % of the low-frequency value of h_{11e}, whereas the ratio $\frac{\text{low frequency value of } z_b'}{\text{low frequency value of } h_{11e}}$ may be on the order of 50 % for the grown junction unit, so that the non-physically-realizable nature of z_b' is markedly present in h_{11e}. These effects make the development of a satisfactory design theory for video amplifiers using the grown-junction transistor very difficult, due to the necessity of approximating h_{11e} by a complicated network function.

A plot of $|h_{11e}|$ vs. f/f_b for a grown junction transistor is shown in Figure 3-24. It will be noted that a slope of -3 db. per octave is approached after $f/f_b = 5$, rather than the 6 db. per octave characteristic of h_{11e} for the fused- or grown-junction transistor. However, the characteristic does not flatten out at high frequencies as is the case for the latter type of transistor.

As h_{11e} is an important quantity in the design of transistor wide-band amplifiers, it is necessary to obtain an approximation to h_{11e} in terms of a physically realizable network. Although an exact representation would be extremely difficult, the quantities $\omega_1, \omega_2, \omega_3, \ldots$ for the form

$$h_{11e}(j\omega) = R \frac{\left(1 + j\frac{\omega}{\omega_1}\right)\left(1 + j\frac{\omega}{\omega_3}\right)\cdots}{\left(1 + j\frac{\omega}{\omega_2}\right)\cdots} \qquad (3\text{-}16)$$

may be approximated by a graphical construction from the characteristic of Figure 3-24. The procedure for this is shown in Figure 3-25.

Declassified in Part - Sanitized Copy Approved for Release @ 50-Yr 2013/09/03 : CIA-RDP81-01043R002500170003-9

Declassified in Part - Sanitized Copy Approved for Release @ 50-Yr 2013/09/03 : CIA-RDP81-01043R002500170003-9

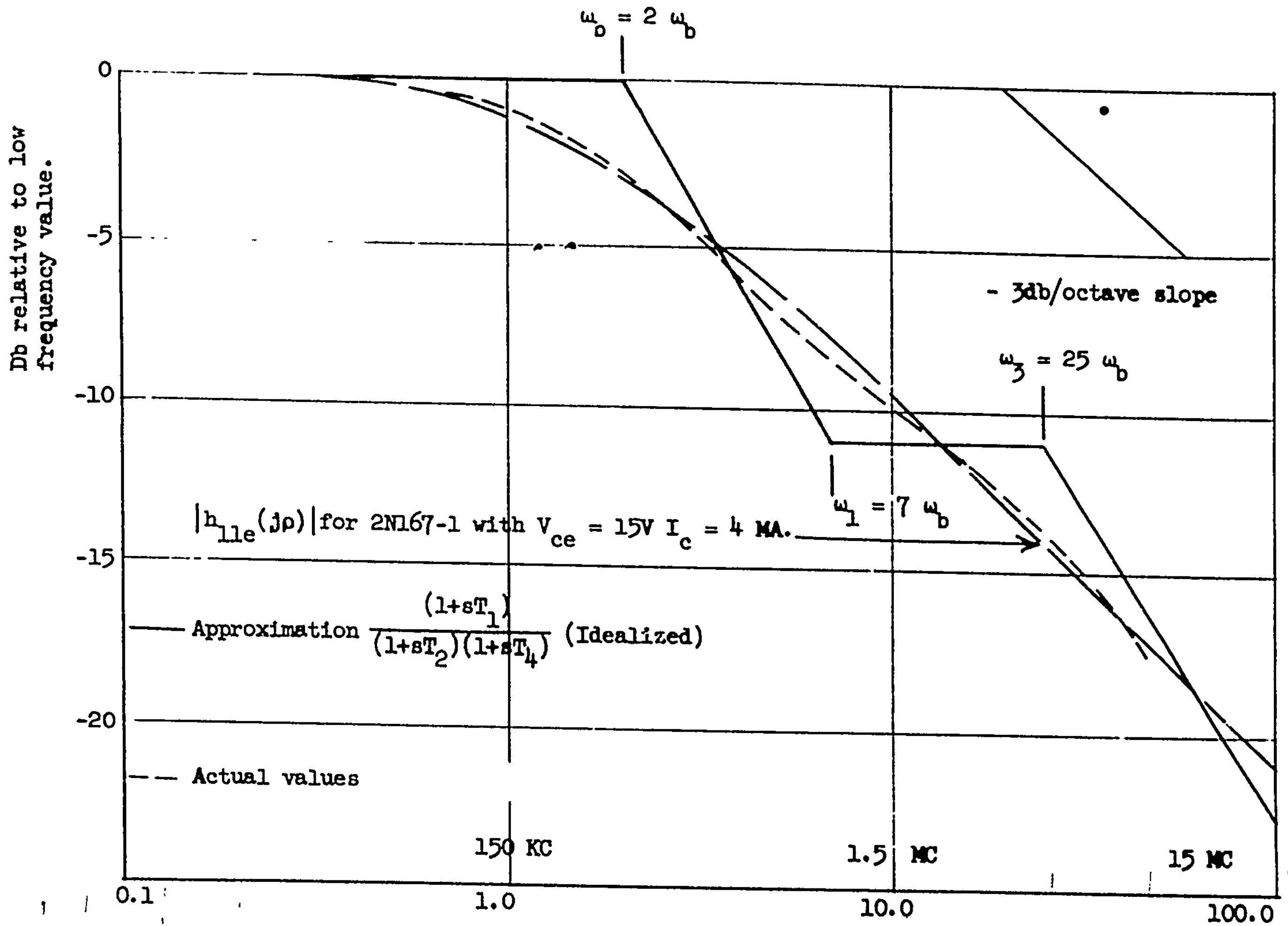

Figure 3-24.

Declassified in Part - Sanitized Copy Approved for Release @ 50-Yr 2013/09/03 : CIA-RDP81-01043R002500170003-9

Declassified in Part - Sanitized Copy Approved for Release @ 50-Yr 2013/09/03 : CIA-RDP81-01043R002500170003-9

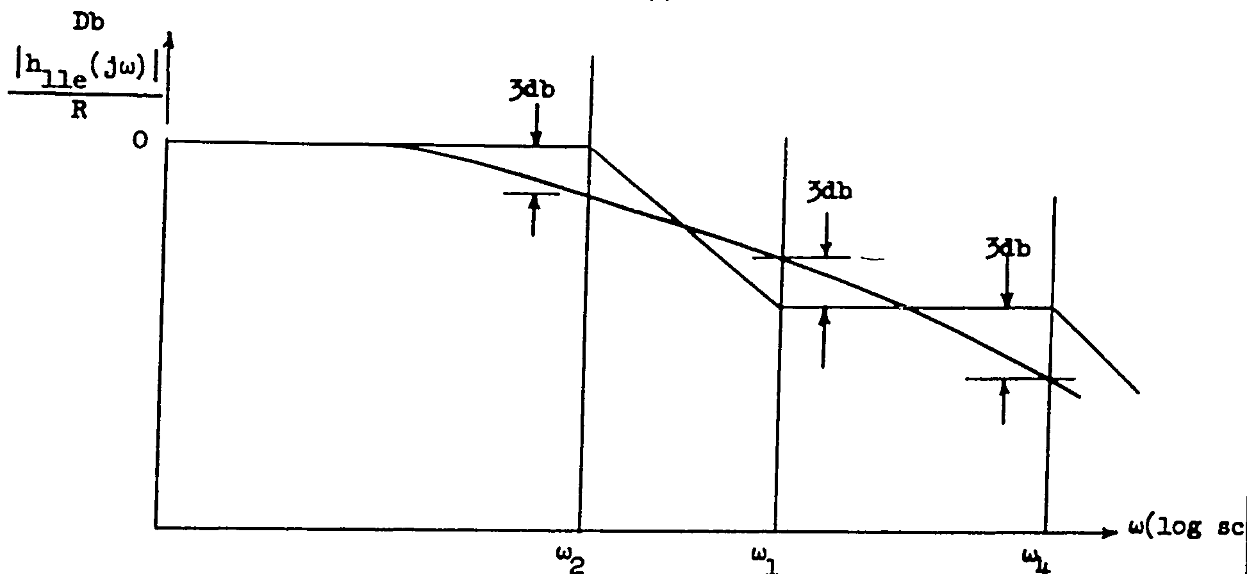

Fig. 3-25. Method of Approximating a Network to Represent $h_{11e}(j\omega)$. The Significance of the Frequencies ω_1, ω_2 and ω_4 is explained in the text.

A line having a slope of 0 db per octave is drawn from the low-frequency value out to the frequency where the characteristic is 3 db down. At thi ~oint, the slope of the line is abruptly changed to -6 db. per octave, and the frequency is that corresponding to ω_2 above. The line is extended at this slope until that frequency where its value is 3 db. below that of the characteristic. This frequency corresponds to ω_1, and the slope is again changed to 0 db. per octave. The process is continued as far as necessary until the characteristic has been approximated over the frequency range of interest.

The frequencies ω_1, ω_2, ω_3 are called the "break points" of Eq. 3-16, and it is to be emphasized that the foregoing method of determining these from a measured characteristic is valid only when these frequencies are well separated from each other. This may be seen from the fact that

Declassified in Part - Sanitized Copy Approved for Release @ 50-Yr 2013/09/03 : CIA-RDP81-01043R002500170003-9

Declassified in Part - Sanitized Copy Approved for Release @ 50-Yr 2013/09/03 : CIA-RDP81-01043R002500170003-9

$$\left|\frac{h_{11e}}{h_{11eo}}\right| = \left\{\frac{\left[1+\left(\frac{\omega}{\omega_1}\right)^2\right]\left[1+\left(\frac{\omega}{\omega_3}\right)^2\right] - - -}{\left[1+\left(\frac{\omega}{\omega_2}\right)^2\right] \quad - - -}\right\}^{\frac{1}{2}} \tag{3-17}$$

and if we have the condition $\omega_2 << \omega_1 << \omega_4$, etc., then at $\omega = \omega_2$, for example, we have

$$\left|\frac{h_{11e}}{h_{11eo}}\right|_{\omega = \omega_2} \doteq \left\{\frac{1}{1+\left(\frac{\omega}{\omega_2}\right)^2}\right\}^{\frac{1}{2}}_{\omega = \omega_2} = \frac{1}{\sqrt{2}} \tag{3-18}$$

which shows that Eq. 3-17 is 3.db. below its low frequency value at $\omega = \omega_2$. Similarly, at $\omega = \omega_1$,

$$\left|\frac{h_{11e}}{h_{11eo}}\right|_{\omega = \omega_1} \doteq \left\{\frac{1+\left(\frac{\omega}{\omega_1}\right)^2}{1+\left(\frac{\omega}{\omega_2}\right)^2}\right\}^{\frac{1}{2}}_{\omega=\omega_1} \doteq \frac{\sqrt{2}}{\frac{\omega_1}{\omega_2}} \tag{3-19}$$

which shows that $|h_{11e}|$ is approximately 3 db above its value at the horizontal line through the break point at ω_1. From Eq. 3-17 we see that, if $\omega_1/\omega_2 = 3.16$, the value of the quantity $\sqrt{1+\left(\frac{\omega_2}{\omega_1}\right)^2}$ is only 1.05, so that the approximations involved in Eq. 3-18 and 3-19 are quite good even for this relatively small ratio of break point frequencies.

This method applied to the characteristic of Figure 3-24 results in an expression of the form

Declassified in Part - Sanitized Copy Approved for Release @ 50-Yr 2013/09/03 : CIA-RDP81-01043R002500170003-9

Declassified in Part - Sanitized Copy Approved for Release @ 50-Yr 2013/09/03 : CIA-RDP81-01043R002500170003-9

$$\frac{h_{11e}}{h_{11eo}} = \frac{\left(1 + j\frac{\omega}{7\omega_b}\right)\left(1 + j\frac{\omega}{25\omega_b}\right)}{\left(1 + j\frac{\omega}{2\omega_b}\right)} \qquad (3\text{-}20)$$

The exact curve as calculated from Eq. 3-20 is also shown in Figure 3-24. It is seen that this provides a remarkable good approximation for $\omega \leqq 60\ \omega_b$, which for this transistor corresponds to a frequency of 9 megacycles. A point of major importance is that the network function of Eq. 3-20 may be realized with z_b' as a parallel RC circuit. This adds one additional element to the simplified equivalent circuit, which materially complicates the design of wide-band amplifiers using grown junction transistors.

Due to the form of the h-system parameters, z_b' will appear only in h_{11e} and not in any of the other h-parameters.

Measurements on the transistor of Figure 3-24 verify this experimentally. On the other hand, z_b' will affect the value of y_{22e}. This problem will be considered in Chapter 5, in connection with the effect of z_b' on the performance of a wide-band amplifier.

Declassified in Part - Sanitized Copy Approved for Release @ 50-Yr 2013/09/03 : CIA-RDP81-01043R002500170003-9

Declassified in Part - Sanitized Copy Approved for Release @ 50-Yr 2013/09/03 : CIA-RDP81-01043R002500170003-9

CHAPTER 4

Compensation Using R-C Networks

In this chapter the problem of transistor wide band equalization is attacked in a somewhat limited sense in that circuits using only resistance and capacitance will be considered. The question naturally arises as to what are the fundamental restrictions on what can be done with this special class of network. For a passive R-C network the restrictions on a realizable transfer function can be stated as

1. All the poles must be simple and lie on the negative real axis.
2. All the zeros must occur in conjugate pairs.

A special class of transfer function, the minimum phase function, is sometimes of interest since it can be realized in the familiar ladder structure, in fact any ladder network has a transfer function which is minimum phase. A minimum phase transfer function of the R-C type will satisfy conditions 1 and 2 stated above with the added restriction that it have its zeros in the left half plane.

In transistor networks based on the simplified equivalent circuit discussed previously for the common emitter configuration, (where h_{12e} is considered as zero) the use of passive interstage R-C networks will not alter the restrictions on the pole zero configuration of the transfer function over that obtainable from some equivalent R-C passive network. This is true because the transistor simply contributes a real axis pole due to h_{21e} and networks due to h_{11e} and h_{22e} which are composed of only R-C elements.

A different situation can be encountered, however, when R-C networks are placed in the feedback path of a transistor or other amplifier circuit. In this case the poles of the resultant transfer function may leave the real axis (although they must of course remain in the left half plane). Thus it is possible to obtain transfer functions using R-C networks in the feedback path of an amplifier which could be obtained with passive elements only by using inductances. This is one reason why a feedback configuration is of interest.

Declassified in Part - Sanitized Copy Approved for Release @ 50-Yr 2013/09/03 : CIA-RDP81-01043R002500170003-9

Declassified in Part - Sanitized Copy Approved for Release @ 50-Yr 2013/09/03 :
CIA-RDP81-01043R002500170003-9

Before entering into the details of the cases to be considered it is well t recall the discussion of Chapter 1 which emphasized that the ultimate limitatio on gain bandwidth product is due to the properties of the transistors used and that the results for even the simpliest type of amplifier can give a good idea of what can be expected with more complicated methods. We begin therefore by considering the simpliest configuration shown in Fig. 4-1a. The circuit is fed by a current generator having a resistive impedance R_g (or admittance G_g). Th transfer functions of interest are the ratios of output current/input short circuit current and output voltage to input open circuit voltage. The transist equivalent circuit used is shown in Fig. 4-1b. The transistor is represented b h_{11e}, h_{21e} and y_{22e} with h_{12e} neglected. Under the termination conditions considered here this is often a usable assumption. The current transfer function defined above assuming

$$R_L << \frac{1}{g_{22}}$$

$$\omega << \frac{1}{R_L C_c}$$

is given by

$$\frac{I_o}{I_g} = \frac{-b_o \gamma_1 \left(1 + \frac{ST_b}{\gamma_o}\right)}{\left(1 + \frac{ST_b}{\gamma_2}\right)\left[1 + \frac{ST_b}{\gamma_o} \quad (1 + b_o \omega_b C_c R_L)\right]} \qquad (4\text{-}1)$$

where

$$\gamma_o = 1 + \frac{R_d}{r_b'} \;\; ; \;\; \gamma_1 = \frac{R_g}{R_g + r_b' + R_d} \;\; ; \;\; \gamma_2 = 1 + \frac{R_d}{R_g + r_b'}$$

For small load resistances which satisfy

$$R_L << \frac{1}{b_o \omega_b C_c}$$

Declassified in Part - Sanitized Copy Approved for Release @ 50-Yr 2013/09/03 :
CIA-RDP81-01043R002500170003-9

Declassified in Part - Sanitized Copy Approved for Release @ 50-Yr 2013/09/03 : CIA-RDP81-01043R002500170003-9

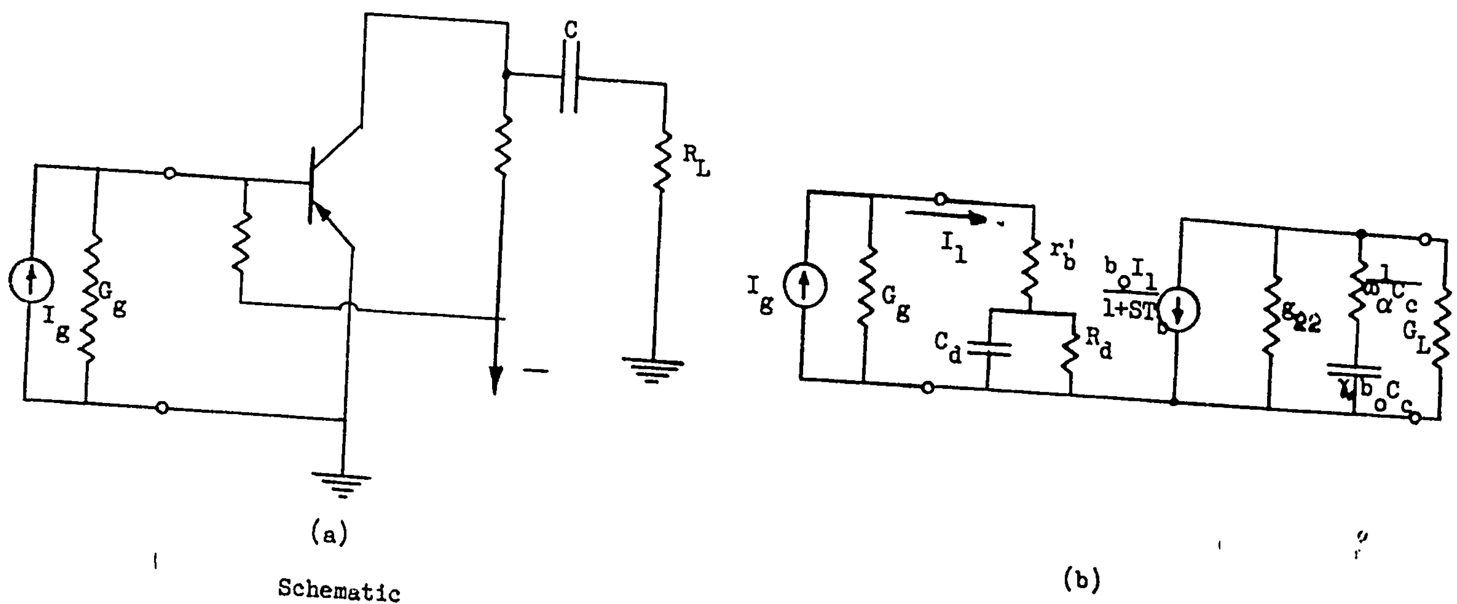

(a)

Schematic

(b)

Approximate Equivalent Circuit for $\omega \ll \omega_\alpha$

Fig. 4-1 Single Transistor Amplifier

Declassified in Part - Sanitized Copy Approved for Release @ 50-Yr 2013/09/03 : CIA-RDP81-01043R002500170003-9

Declassified in Part - Sanitized Copy Approved for Release @ 50-Yr 2013/09/03 : CIA-RDP81-01043R002500170003-9

The zero in the transfer function is cancelled by one of the poles. The response then becomes of the single time constant type and the 3db bandwidth f_o is seen to be

$$f_o = \frac{\gamma_2}{2\pi T_b} = \gamma_2 f_b = \left(1 + \frac{R_d}{R_g + r_b'}\right) f_b \qquad (4\text{-}2)$$

The midband gain is given by

$$|K_{1o}| = b_o \gamma_1 = \frac{b_o R_g}{R_g + r_b' + R_d} \qquad (4\text{-}3)$$

Equations (4-2) and (4-3) may be rearranged into the form of two design equations to meet a specified bandwidth requirement f_o. These are

$$R_g = R_d \left[\frac{f_b}{f_o - f_b} - \frac{r_b'}{R_d}\right] \qquad (4\text{-}4a)$$

$$|K_{1o}| = \frac{b_o f_b}{f_o}\left[1 - \frac{r_b'}{R_d}\left(\frac{f_o}{f_b} - 1\right)\right] \qquad (4\text{-}4b)$$

The gain bandwidth product can be found directly from Eq. 4-4b and is seen to depend upon $b_o f_b$ (.8 times the alpha cut-off frequency of the transistor), the ratio of extrinsic base resistance to diffusion input resistance $\left(\frac{r_b'}{R_d}\right)$ and $\frac{f_o}{f_b}$.

Example

Given a transistor having the following constants

Declassified in Part - Sanitized Copy Approved for Release @ 50-Yr 2013/09/03 : CIA-RDP81-01043R002500170003-9

Declassified in Part - Sanitized Copy Approved for Release @ 50-Yr 2013/09/03 : CIA-RDP81-01043R002500170003-9

$$f_b = 100 \text{ kc}$$

$$b_o = 50$$

$$G_d = 500\mu \text{ mho}$$

$$C_c = 5 \ \mu\mu f$$

$$r_b' = 80 \ \Omega$$

If the load resistance is restricted to

$$R_L \ll \frac{10^6}{2\pi \times 25} = 6380 \ \Omega$$

the single time constant response is controlling. Thus for large R_g, the gain is 50 the bandwidth 100 kc. If the bandwidth must be extended to f_o = 1MC, from Eq. (4-4)

$$R_g = R_d \frac{\left[1 - r_b' \, G_d (\frac{f_o}{f_b} - 1)\right]}{\frac{f_o}{f_b} - 1} = 142 \ \Omega$$

The gain is found to be (from Eq. 4-4b)

$$\left| K_{1o} \right| = 3.2$$

The form of response is not altered if voltage gain rather than current gain (as defined previously) is considered provided the load resistance is kept low enough compared to $\frac{1}{\omega_\alpha C_c}$. Although by breaking this restriction much larger mid-band voltage gains are possible than the maximum of b_o for the current ratio, the increased gain results in a more rapid deterioration of the bandwidth due principally to the effect of the collector shunt capacitance It is instructive to carry the above analysis one step further and consider the case of two transistors in cascade, fed by a generator having

Declassified in Part - Sanitized Copy Approved for Release @ 50-Yr 2013/09/03 : CIA-RDP81-01043R002500170003-9

Declassified in Part - Sanitized Copy Approved for Release @ 50-Yr 2013/09/03 : CIA-RDP81-01043R002500170003-9

a fixed resistance R_g and working into some specified load admittance Y_L. The network is shown in Fig. 4-2 and is seen to contain a shunt admittance Y_s in the interstage which is to be adjusted to obtain wide-band response.

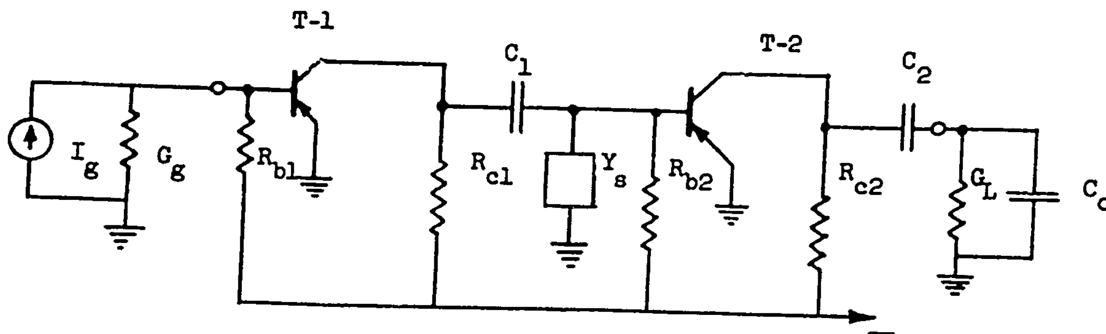

Fig. 4-2 Two Transistor Amplifier With Shunt Interstage

The voltage transfer function as defined previously may be found using the approximate transistor equivalent circuit of Fig. 4-1b.*

$$\frac{E_o}{E_g} = b_1 b_2 \frac{Y_{11}}{Y_{11} + G_g} \quad \frac{Y_{12}}{Y_{12} + Y_{O1} + Y_s} \quad \frac{Y_L}{Y_L + Y_{O2}} \quad \frac{G_g}{Y_L} \qquad (4\text{-}5)$$

where

$$h_{21e} = b = \frac{b_o}{1 + ST_{b1}}$$

*Since the high frequency performance is of primary interest in Eq. (4-5), the bias resistors R_{b1}, R_{b2}, R_{c1}, R_{c2} are assumed to be large enough so that they can be neglected. The same is true for C_1 and C_2. The low frequency response is however strongly dependent on the time constants R_{c1} C_1 and $R_{c2}C_2$.

Declassified in Part - Sanitized Copy Approved for Release @ 50-Yr 2013/09/03 : CIA-RDP81-01043R002500170003-9

Declassified in Part - Sanitized Copy Approved for Release @ 50-Yr 2013/09/03 : CIA-RDP81-01043R002500170003-9

$$\frac{1}{h_{11e}} = Y_i = G_i \quad \frac{1 + ST_b}{1 + ST_b \, r_b' \, G_i}$$

$$h_{22e} = Y_o \doteq \frac{S \, C_c \, b_o}{1 + ST_b}$$

$$Y_L = G_L + SC_o$$

Eq. (4-5) is written so as to point out clearly the factors which degrade the response. These are seen to be:

1. The current fall-off due to frequency variation of b. This is due to diffusion effects within the transistor.

2. The current division between the generator internal admittance and the transistor input admittance Y_{i1}. The latter quantity is a function of diffusion effects (in G_i and T_b) and r_b' the majority carrier (extrinsic) base resistance.

3. The division of current in the output circuit of the first transistor where some control may be exerted by choice of the interstage admittance Y_s. The other quantities in this factor are the input admittance to the second stage and the output admittance of the first stage (Y_{O1}). This latter quantity is determined by the alpha cut-off frequency of the transistor, the collector capacitances C_c and the low frequency common emitter short circuit current gain b_o.

4. Finally there is a division of current between the load admittance Y_L and the output admittance Y_{O2}.

5. The quantity $\frac{G_g}{Y_L}$ represents the ratio of load to generator impedance to obtain a voltage gain expression.

Declassified in Part - Sanitized Copy Approved for Release @ 50-Yr 2013/09/03 : CIA-RDP81-01043R002500170003-9

Declassified in Part - Sanitized Copy Approved for Release @ 50-Yr 2013/09/03 : CIA-RDP81-01043R002500170003-9

Although the separate factors appearing in Eq. (4-5) were discussed above, one interesting feature of the behavior of this equation are the cancellation of the poles of b_1 and b_2 by the zeros of Y_{11} and Y_{12}. The remaining expression contains time constants involving T_{b1} and T_{b2} but these appear modified by other circuit parameters. One simplifying assumption which can sometimes be made without drastically affecting the result is to neglect Y_{02} and Y_{01} in comparison to the admittances which appear in parallel with them. This assumption is least valid for an output stage especially if the load impedance is as high as $\frac{1}{\omega_\alpha C_C}$. However, in an interstage where the minimum loading is the following transistor, the approximation is better although it will affect the response to some extent even in this case. Neglecting the Y_0's Eq. (4-5) becomes

$$\frac{E_o}{E_g} = b_1 b_2 \quad \frac{Y_{11}}{Y_{11} + G_g} \quad \frac{Y_{12}}{Y_{12} + Y_s} \quad \frac{G_g}{Y_L} \qquad (4\text{-}6)$$

A specific example of Y_s being a series L-R circuit will be considered in the next chapter.

Declassified in Part - Sanitized Copy Approved for Release @ 50-Yr 2013/09/03 : CIA-RDP81-01043R002500170003-9

Declassified in Part - Sanitized Copy Approved for Release @ 50-Yr 2013/09/03 : CIA-RDP81-01043R002500170003-9

4-2. Wide Band Response Utilizing Local R-C Feedback

The use of local feedback is one approach to the equalization problem. Actually it is a special class of the more general technique of using feedback to obtain the desired results. Before discussing the specific application to transistor circuits it might be well to discuss the characteristics common to feedback circuits for this type of application.

In this study only local feedback (feedback involving one transistor) was attempted. Although the more general case is also of interest, the problem of analysis is quite difficult and one can run into stability difficulties if feedback around several stages is attempted. It should be pointed out, however, that successful video amplifier circuits have been constructed using both beedback and interstage equalization.[1, 2, 3] However, in almost all cases the design appears to have been based on experimental adjustment of components. Thus a simple usable theory was lacking on this subject.

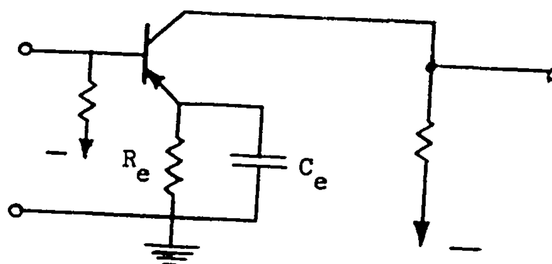

Fig. 4-3 Emitter Feedback Configuration

1. Lo et al, "Transistor Electronics" p. 342 (Prentice Hall, 1955).
2. "Video Pulse Amplifiers Employing Silicon Transistors" R. E. Leslie, High Frequency Transistor Circuits Conference, 1955.
3. "An 80 Volt Output Transistor Video Amplifier" by V. H. Grinich, Trans. PGCT, March 1956.

Declassified in Part - Sanitized Copy Approved for Release @ 50-Yr 2013/09/03 : CIA-RDP81-01043R002500170003-9

Declassified in Part - Sanitized Copy Approved for Release @ 50-Yr 2013/09/03 : CIA-RDP81-01043R002500170003-9

This is probably due to the rather involved transistor equivalent circuit and the many factors which enter into the problem.

The feedback configuration used in this study is shown in Fig. 4-3. A crude statement of the operation of the circuit is that the addition of R_e reduces the midband gain by a certain factor below that available with $R_e = 0$ The capacitor C_e is adjusted so that its shunting effect on R_e begins to be appreciable at the frequency where the gain would fall off due to transistor response or the parasitic capacitances. Since R_e represented degenerative feedback, the effect of C_e at the higher frequencies is to decrease the degeneration or increase the gain. Thus the rise in gain due to C_e can compensate for the fall-off due to the transistor at least over some portion of the desired band. The design procedure for the equalization problem using the local feedback configuration of Fig. 4-3 consists in arriving at values of R_e. and C_e to obtain specified performance.

As a first step in the solution to this problem one needs a network representation of the transistor in the common emitter configuration. Although an analysis based on all the h parameters of the transistor could give a good answer for any given circuit, the algebra is too involved to provide good insight into the problem and to yield a usable design procedure. As a first approximation the equivalent circuit of Fig. 4-4 has been found to yield most

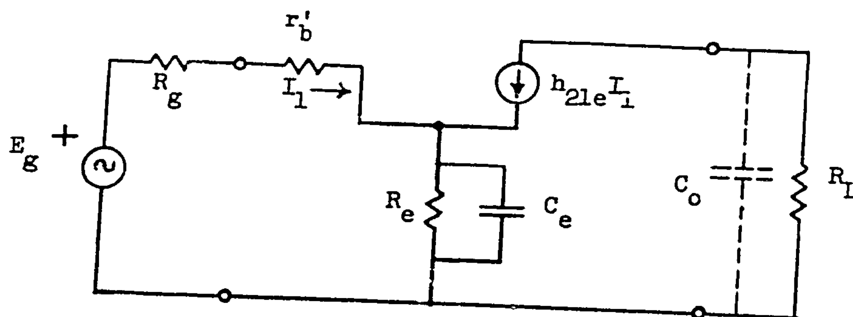

Fig. 4-4 Approximate Equivalent Circuit for Amplifier of Fig. 4-3

Declassified in Part - Sanitized Copy Approved for Release @ 50-Yr 2013/09/03 : CIA-RDP81-01043R002500170003-9

Declassified in Part - Sanitized Copy Approved for Release @ 50-Yr 2013/09/03 : CIA-RDP81-01043R002500170003-9

of the behavior of interest. The transistor is simply represented by h_{21e} with h_{22e} and h_{12e} considered zero. Also h_{11e} is taken as r_b'. Neglect of h_{12} limits the analysis to the case of a low load impedance. The justification for neglecting the diffusion part of h_{11} of the transistor lies in the assumption that Z_e is larger than the internal emitter equivalent T impedance at all frequencies of interest. h_{22} may be neglected if R_L is limited to $R_L \ll \frac{1}{\omega_\alpha C_c}$. The expression for voltage gain can then be found to be

$$\frac{E_o}{E_g} = K_v \doteq \frac{-b_o R_L(1 + ST_e)}{(1 + ST_L)\left[R_b'(1 + ST_e)(1 + ST_b) + b_o R_e\right]} \qquad (4\text{-}7)$$

Where

$$T_e = R_e C_e$$

$$T_L = R_L C_0$$

$$R_b' = R_g + r_b'$$

For $s = 0$, the low frequency gain is

$$K_{vo} \doteq \frac{-b_o R_L}{b_o R_e + R_b'} \doteq \frac{-R_L}{R_e} \qquad (4\text{-}8)$$

when

$$b_o R_e \gg R_b'$$

In order to consider the frequency behavior in detail s is replaced by $j\omega$ in Eq. (4-7) and the square of the magnitude of the resultant expression is found. To simplify the algebra and provide a basis for comparison the quantities in Eq. (4-7) are normalized giving

$$\left|\frac{K_v}{K_{vo}}\right|^2 = \frac{1 + m^2 X^2}{(1 + X^2 T_L^2 \omega_b^2)\left[X^4 m^2 h^2 + X^2\left\{h^2(1 + m)^2 - 2mh\right\} + 1\right]} \qquad (4\text{-}9)$$

Where

$$X = \frac{f}{f_b}$$

$$m = \frac{T_e}{T_b}$$

$$h = \frac{R_b'}{b_o R_e}$$

In a design problem, if the transistor and generator impedance are specified, it remains to choose R_L, R_e and C_e. The factors which enter into a choice of R_L are the following:

1. R_L must remain smaller than $\frac{1}{\omega_\alpha C_c}$ in order for the effects of collector capacitance not to contribute to the response.

2. It may happen that even if R_L satisfies condition 1, the response may still be limited to some extent at least by the shunt capacitance in the output circuit. This is especially true if good high frequency transistors are used.

3. The choice of R_L in an output stage must be consistent with the power handling capacity of the transistor as well as meet the requirements of output swing as closely as possible. This usually requires large R_L which conflicts with the frequency response requirements.

Once R_L is chosen based on the above considerations, the next task is the choice of R_e. This is straightforward since from Eq. (4-8)

Declassified in Part - Sanitized Copy Approved for Release @ 50-Yr 2013/09/03 : CIA-RDP81-01043R002500170003-9

Declassified in Part - Sanitized Copy Approved for Release @ 50-Yr 2013/09/03 : CIA-RDP81-01043R002500170003-9

$$R_e = \frac{R_L}{|K_{vo}|} \tag{4-10}$$

Where if K_{vo} is specified R_e may easily be found. Once R_e is determined the quantity h is fixed and all that remains is a choice of C_e (or m). As a first approach we neglect T_L (this is a reasonable assumption for low values of load impedance and even a mediocre high frequency transistor). Under these conditions, no rise in the response will occur if the coeficients of the X^2 terms in Eq. (4-9) are equated in numerator and denominator.

$$m^2 = h^2 (1 + m)^2 - 2mh$$

This may be solved for m, and subject to the condition that $h \ll 1$

$$m \doteq .414h \tag{4-11}$$

or

$$C_e = .414 \frac{R_b'}{R_e^2 \omega_\alpha}$$

The 3 db bandwidth f_o, (to which there corresponds a value of X called X_o) may be found from

$$\frac{X_o^4 m^2 h^2}{1 + m^2 X_o^2} = 1$$

Eq. (4-11) may be used to eliminate m giving

$$X_o^4 - \frac{X_o^2}{h^2} - \frac{1}{(.414\ h)^2} = 0 \tag{4-12}$$

The solution for X_o is

$$X_o = \frac{1.73}{h}$$

or

$$f_o = 1.73\ f_\alpha \frac{R_e}{R_b'} \tag{4-13}$$

It is of interest at this point to see the effect on the bandwidth of making $C_e = 0$ while retaining R_e. From Eq. (4-9) (again neglecting T_L) the bandwidth denoted by f_{oo} is

$$f_{oo} = \frac{f_b}{h} = f_\alpha \frac{R_e}{R_b'} \tag{4-14}$$

Comparison of this expression with Eq. (4-13) shows that proper adjustment of C_e results in a 73% improvement of the circuit bandwidth over having $C_e = 0$.

Using Eq. (4-14), the expression for C_e given by Eq. (4-11) may be written as

$$C_e = \frac{.414}{2\pi R_e f_{oo}} \tag{4-11a}$$

Declassified in Part - Sanitized Copy Approved for Release @ 50-Yr 2013/09/03 : CIA-RDP81-01043R002500170003-9

Declassified in Part - Sanitized Copy Approved for Release @ 50-Yr 2013/09/03 : CIA-RDP81-01043R002500170003-9

4.3 **Effect of Load Capacitance**

As seen above a simple usable theory can result if $\bar{R}_L$ is made much smaller than $\frac{1}{\omega_\alpha C_c}$. However, even under these conditions parasitic shunt capacitance can limit the response to a marked extent especially if a good high frequency transistor is used. The load impedance to a first approximation adds a -6db per octave term in the denominator of the response function as can be seen from Eq. (4-7). As an aid in evaluating the importance of the load time constant vs. the transistor parameters in limiting the response a curve has been prepared (see Fig. 4-5) which shows the bandwidth of one part of the circuit when the overall bandwidth and the bandwidth of the other part is known. The curve is based on a simple response of the form

$$\left|\frac{K}{K_o}\right|^2 = \frac{1}{\left[1 + (\frac{f}{f_1})^2\right]\left[1 + (\frac{2}{f_2})^2\right]} \qquad (4\text{-}15)$$

This quantity becomes $\frac{1}{2}$ at a frequency f_o, the overall 3db bandwidth. One of the bandwidths say f_2 is related to f_o and the other (f_1) by

$$f_2 = f_o \sqrt{\frac{f_1^2 + f_o^2}{f_1^2 - f_o^2}}$$

In a typical problem f_o is measured and f_1 calculated from the load time constant. The curve then gives f_2, i.e. the bandwidth neglecting the load time constant. The curve shows for example that if f_1 is larger than 3.4 times f_o, f_2 is equal to f_o to within 10°/o. Although the form of response of the transistor amplifier is not the same as that of Eq. (4-15), the curve of Fig. 4-5 does give a good idea of what can be expected in many cases. Of course this plot can be used in many applications in electronics other than transistor circuits.

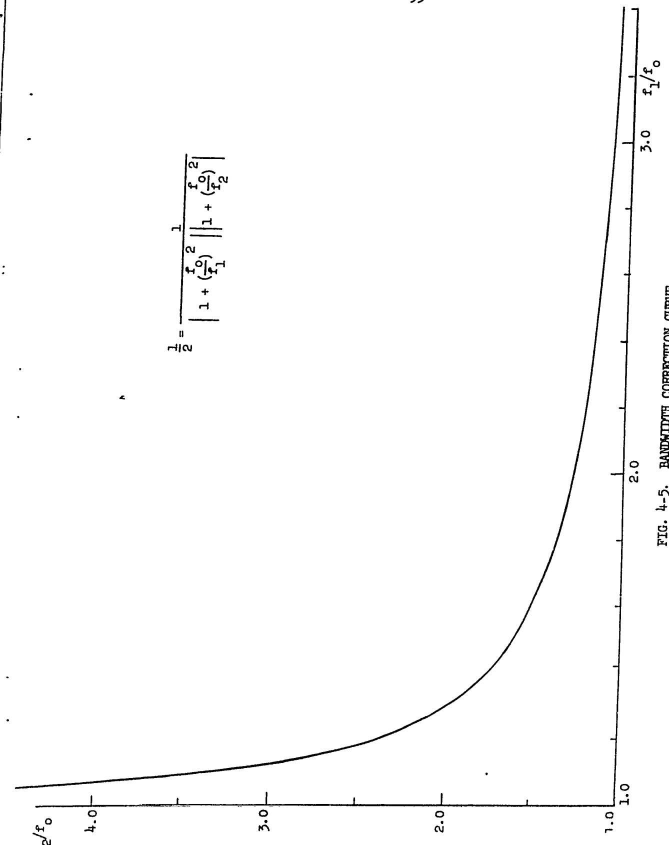

FIG. 4-5. BANDWIDTH CORRECTION CURVE

Declassified in Part - Sanitized Copy Approved for Release @ 50-Yr 2013/09/03 : CIA-RDP81-01043R002500170003-9

Declassified in Part - Sanitized Copy Approved for Release @ 50-Yr 2013/09/03 : CIA-RDP81-01043R002500170003-9

4.4 Experimental Results with R-C Local Feedback Equalization

A test program has been in progress in order to obtain experimental results using the theory developed earlier in this chapter. It is recalled that the philosphy used in working out the equations was to find the simplest usable design procedure and it is expected that only approximate correlation of theory and experiment will result.

The procedure followed was to first decide on the low-frequency gain K_{vo} required. Then R_L, the a-c load resistance (not the bias resistor) was chosen to be less than $\frac{1}{\omega_\alpha C_c}$ for the transistor used. Knowing R_L and K_{vo}, R_e was then calculated using Eq. (4-10). The circuit was then constructed and the bandwidth f_{oo} was measured. From this R_b' was calculated using Eq. (4-14). C_e was then determined from Eq. (4-11) and connected in the circuit. The bandwidth f_o was then measured and the result checked against Eq. (4-13).

Since transistors were used with alpha cut-off frequencies of the order of 10 Mc and collector capacitances of 5μμf, $\frac{1}{\omega_\alpha C_c}$ was about 3000 ohms. The load resistor was in most cases kept at 1000 ohms. It should be mentioned that some improvement in bandwidth over that reported here is possible if shunt peaking is used in the output circuit.

The results of following the design procedure is shown in some representative cases in Table 4-1. It is seen that in every case the values of C_e as calculated resulted in a marked improvement in bandwidth and the improved bandwidths corresponded at least approximately with predicted values. A check was made of the response over the whole band in each case and in no instance was a peak in the response found to exist. R_b' included in every case a 100 ohm generator resistance.

It is to be expected that the best theoretical and experimental agreement would occur in low frequency units since here other factors like output shunt capacitance have relatively little effect.

Table 4-1 Transistor Video Amplifiers Using R-C Local Feedback

Transistor	f_α(Mc)	R_L	Measured f_{oo}(Mc)	Calculated R_b'	Calculated C_e(μμf)	Measured f_o(Mc)	Calculated $f_o = 1.73 f_{oo}$	K_{vo}	Remarks
2N136 No. 1	2.5	1000	1.53	163	430	2.60	2.65	6.4	
2N136 No. 1	3.47	1000	2.08	167	320	4.24*	3.60	6.5	10 volt bias
2N136 No. 1	2.5	2200	1.14	219	58*	2.26	1.98	12.1	
2N78 No. 1	9.0	1000	1.87	481	350	4.9	3.23	5.9	Grown Junction unit
2N113 No. 6	11.0	1000	2.5	440	245	4.77*	4.34	6.8	
2N113 No. 6	11.0	2200	1.62	680	415	2.78*	2.8	12.7	

*Indicates measured data corrected for output capacitance

$R_b' = 100 + r_b'$

Declassified in Part - Sanitized Copy Approved for Release @ 50-Yr 2013/09/03 : CIA-RDP81-01043R002500170003-9

Declassified in Part - Sanitized Copy Approved for Release @ 50-Yr 2013/09/03 : CIA-RDP81-01043R002500170003-9

Another point of importance is that the design procedure is based on certain simplifying assumptions which were not satisfied in some of the cases listed. However, since the data used to enter the calculations was found by measurement, the value of C_e tended to be in a direction so as to provide the needed equalization even when the response was different than the form on which the theory was based.

The results on the grown junction transistors can be expected to be in appreciable error due to the fact that the theory assumed an r_b' which is independent of frequency. Since the low frequency r_b' is usually larger for grown junction transistors than alloy junction units the theoretical performance based on a constant r_b' tend to show the grown junction transistor in an unfavorable light. Actually because z_b' decreases with frequency * it can be expected that the measured bandwidth would be better than the calculated. This was found to be the case. Note also the effect of increasing the collector bias voltage. Since this narrows the base width due to the fact that the collector transistion region widens with bias voltage, f_α increases. However, it is expected that r_b' will increase due to the narrowing of the base width. In most cases the increase in f_α dominates the increase in r_b' and the overall result of a higher collector bias voltage is a favorable increase in the frequency response.

* Pritchard and Coffey "Small Signal Parameters of Grown Junction Transistors at High Frequencies", Convention Record, IRE Part III, 1954.

4.5 Common Emitter-Common Base Circuit

Fig. 4-6 shows the circuit used. The first transistor being in the common emitter configuration tends to limit the response so a good high frequency transistor (SB-100) was selected here. The common base circuit has a wide bandwidth (its alpha cut-off frequency) and it is useful as an output stage because of its low distortion properties. An idea of the R-C interstage necessary may be found from the following reasoning. Assuming the transistors to behave as simple frequency dependent current amplifiers, the transfer function of voltage is

$$\frac{E_o}{E_g} = \frac{b_o}{1 + sT_{b1}} \; \frac{R_s}{R_s + \dfrac{R_e}{1 + sT_e}} \; \frac{\alpha_{02}}{1 + sT_{\alpha 2}} \; \frac{R_L}{R'_{b1} + \dfrac{R_1}{1 + sT_{b1}}} \qquad (4\text{-}16)$$

Where

$T_e = R_e C_e$

$T_{\alpha 2}$ = reciprocal of angular alpha cut-off frequency of T-2

α_{02} = low frequency alpha of T-2 ($\doteq 1$)

$T_L = R_L C_o$ the load time constant

Eq. (4-16) may be simplified to

$$\frac{E_o}{E_g} = K_{vo} \; \frac{1 + sT_e}{1 + sT_e \dfrac{R_s}{R_s + R_e}} \; \frac{1}{1 + s\dfrac{R'_{b1} T_{b1}}{R_1 + R'_{b1}}} \; \frac{1}{1 + sT_{\alpha 2}} \; \frac{1}{1 + sT_L} \qquad (4\text{-}17)$$

The problem now consists in finding T_e for optimum performance. In the above equation the rising input impedance with frequency of the common base circuit

Declassified in Part - Sanitized Copy Approved for Release @ 50-Yr 2013/09/03 : CIA-RDP81-01043R002500170003-9

Declassified in Part - Sanitized Copy Approved for Release @ 50-Yr 2013/09/03 : CIA-RDP81-01043R002500170003-9

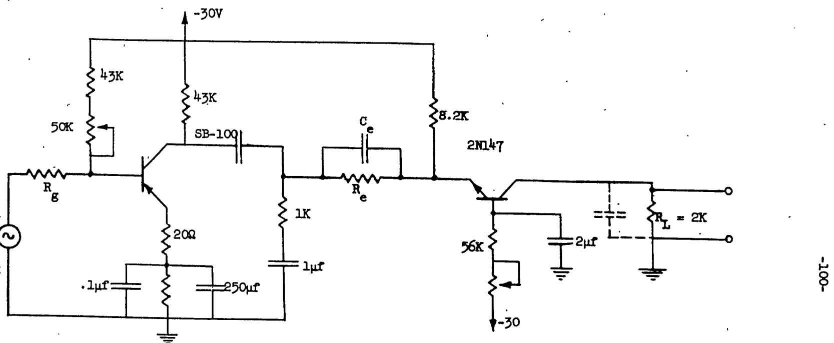

FIG. 4-6. CIRCUIT OF G.E. - G.B. AMPLIFIER

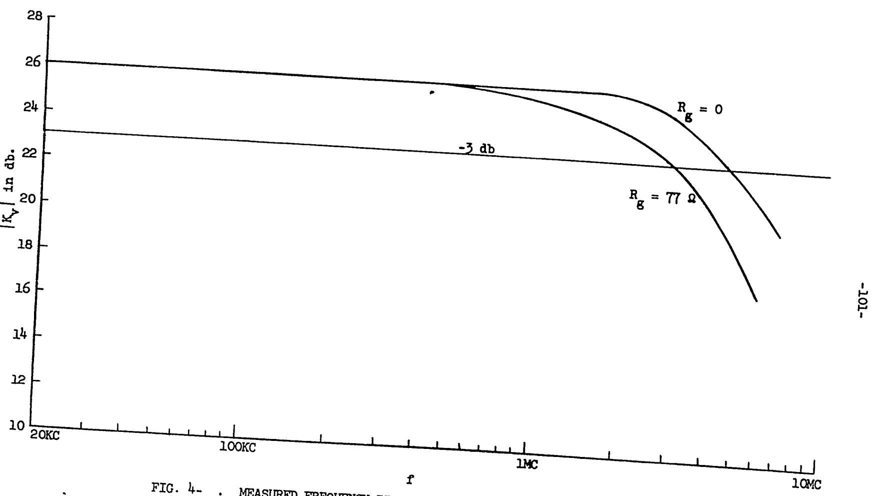

FIG. 4- . MEASURED FREQUENCY RESPONSE OF G.B. - G.E. AMPLIFIER WITH INTERSTAGE

Declassified in Part - Sanitized Copy Approved for Release @ 50-Yr 2013/09/03 : CIA-RDP81-01043R002500170003-9

Declassified in Part - Sanitized Copy Approved for Release @ 50-Yr 2013/09/03 : CIA-RDP81-01043R002500170003-9

has been neglected. This will limit the usefulness of Eq. 4-16 which should not be used for too small a value of R_e. The choice of T_e depends of course, on the pole locations of Eq.(4-17). If the output time constant is limiting the response then T_e should be made nearly equal to T_L and then by arrangement of the factor $\frac{R_s}{R_s + R_e}$ a direct gain bandwidth trade is accomplished (assuming the other two poles to correspond to very high frequencies).

In the circuit of Fig. 4-7 the load time-constant (including the output meter) was .07 μ seconds. R_L was limited to 2K to minimize the output capacitance and still give reasonable gain and output swing. A factor of two was allowed to be lost in the interstage. R_e was chosen as 1000 ohms which is small enough to minimize the effect of the collector capacitance of the first stage and large enough to minimize the effect of the rising input impedance of the common base circuit. T_e was first adjusted to .07 μ seconds, but it was found experimentally that increasing it to .1μ seconds improved the bandwidth without giving a peak in the response. The circuit response is shown in Fig. 4-8 for two values of R_b'. One of these correspond to $R_g = 0$, the other to $R_g = 77\ \Omega$.

CHAPTER 5

Compensation Using RL Networks

5-1. Compensated Amplifiers using Simple RL Networks.

The purpose of this section is to discuss the design of single-and dual-stage grounded-emitter amplifiers using simple series RL networks for compensation in the output and interstage circuits. Although the theory is readily extended to include the analysis of cascade amplifiers having more than two stages, it will be seen that such amplifiers using these simple networks have severe limitations on the available gain and bandwidth.

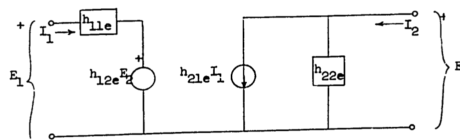

Fig. 5-1. Circuit representation of the h-parameters for a grounded emitter amplifier.

An important consideration in the design procedure is the effect of the internal feedback in the transistor. In Figure 5-1 we show the h-parameter equivalent circuit of a grounded emitter amplifier. Here, the voltage generator $h_{12e}E_2$ affects the voltage gain $K_v = E_2/E_1$ of the amplifier stage. However, we note that this generator may be moved to the position shown in Figure 5-2, without affecting the electrical performance of the amplifier. The gain $K_v' = E_2/E_1$ is then that of the transistor with $h_{12e} = 0$, i.e., with no internal feedback. An examination of Figure 5-2 shows that the circuit is that of an amplifier of gain K_v' with series voltage feedback at the input and a feedback factor $\beta = h_{12e}$. Thus the relation between K_v and K_v' is

Declassified in Part - Sanitized Copy Approved for Release @ 50-Yr 2013/09/03 : CIA-RDP81-01043R002500170003-9

Declassified in Part - Sanitized Copy Approved for Release @ 50-Yr 2013/09/03 : CIA-RDP81-01043R002500170003-9

readily written as

$$K_v = \frac{K'_v}{1 + h_{12e}K'_v} \qquad (5\text{-}1)$$

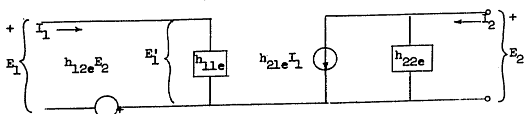

Fig. 5-2. This circuit is electrically equivalent to that of Fig. 5-1.

and we see that K_v may be considered as essentially equal to K'_v if

$$|h_{12e}K'_v| \ll | \qquad (5\text{-}2)$$

This requirement is substantially satisfied in a wide-band grounded-emitter amplifier. We shall see that, just as in the case of vacuum tube amplifiers, the attainment of wide bandwidths results in a relatively low value of voltage gain, usually in the range of 5 to 15. Thus, even when h_{12e} has increased to a value of, say, 10^{-2} at high frequencies, the quantity $h_{12e}K'_v$ will still be considerably less than unity. It should be kept in mind, however, that for transistors in which h_{12e} is abnormally large, Eq. (5-2) does not hold and an exact analysis is required for accurate results. Otherwise, the problem may be greatly simplified by neglecting the internal feedback in the grounded-emitter stage.

5-2. Single Stage Amplifier with RL Network in Output Circuit.

Figure 5-3 shows a single stage grounded emitter amplifier which feeds

a load consisting of a capacitance C_L in parallel with a high resistance R. This may be the grid circuit of a high-level vacuum tube video amplifier, or of a cathode ray tube. As in the vacuum tube case, the load resistance R_3 is of necessity much smaller than R, so that R may be omitted from the analysis. The stage is fed from a generator having a source resistance R_s and an open circuit voltage E, the quantity of interest being the voltage gain $K_v = E_2/E$.

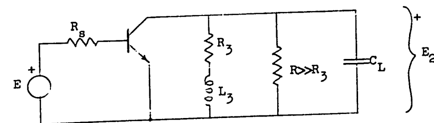

Fig. 5-3. Grounded emitter amplifier with load consisting of C_L and R, and compensating network R_3-L_3. Bias connections have been omitted for simplicity.

In figure 5-4, the transistor has been replaced by its approximate equivalent circuit in terms of h_{11e}, h_{21e}, and y_{22e}. The latter quantity is used as the termination on the input side of the transistor is much closer to short-circuit than open-circuit conditions. This follows from the fact that a low value of R_s is essential if wide bandwidths are to be obtained.

The voltage gain of the stage may be conveniently expressed as the current gain, h_{21e}, times the ratio of the total output circuit impedance $(\frac{1}{y_{22e} + Y_3})$ to the input impedance, $h_{11e}+R_s$. Thus we have

$$K_v = \frac{E_2}{E} = \frac{-h_{21e}}{(h_{11e} + R_s)(y_{22e} + Y_3)} \qquad (5\text{-}3)$$

where Y_3 is the load admittance due to R_3, L_3, and C_L.

Declassified in Part - Sanitized Copy Approved for Release @ 50-Yr 2013/09/03 : CIA-RDP81-01043R002500170003-9

Declassified in Part - Sanitized Copy Approved for Release @ 50-Yr 2013/09/03 : CIA-RDP81-01043R002500170003-9

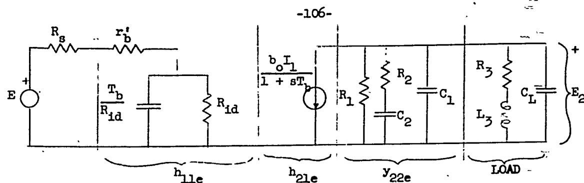

Fig. 5-4. Fig. 5-3 with the transistor replaced by its approximate equivalent circuit.

In general, $R_1 \gg R_3$, so that it may be neglected. Also, the source resistance R_s effectively adds to r_b', so that the effective input impedance seen by the generator may be expressed in the form

$$h_{11e} + R_s = R_s + r_b' + \frac{R_{id}}{1 + sT_b} = R_i' \frac{1 + s\gamma' T_b}{1 + sT_b} \qquad (5\text{-}4)$$

where

$$R_i' = r_b' + R_s + R_{id} \quad ; \quad \gamma' = \frac{r_b' + R_s}{R_i'} \qquad (5\text{-}5)$$

The ratio h_{21e}/h_{11e} is then

$$\frac{h_{21e}}{h_{11e}} = \frac{\dfrac{b_o}{1 + sT_b}}{R_i' \dfrac{1 + s\gamma' T_b}{1 + sT_b}} = \frac{b_o}{R_i'} \frac{1}{1 + s\gamma' T_b} \qquad (5\text{-}6)$$

which shows that the input circuit will contribute a real-axis pole to K_v at $\frac{\omega_b}{\gamma'}$, and demonstates the importance of a low value of R_s. However, the improvement as R_s is reduced diminishes as R_s approaches r_b', so that a compromise is necessary in this respect.

Eq. (5-6) may be substituted into the expression for K_v to give

$$K_v = \frac{-b_o}{R_i'(1 + s\gamma' T_b)} \frac{1}{(y_{22e} + Y_3)} \qquad (5\text{-}7)$$

The admittance $y_{22e} + Y_3$ is shown in Figure 5-5, where the shunt capacitances

C_L and C_1 are represented by a single capacitance C. We see that, for the uncompensated case where L = 0, the load admittance is Y_3 at low frequencies, becoming $Y_3 + Y_2$ at higher frequencies where $\omega C_2 R_2 \gg 1$. While the exact frequency range in which this occurs will depend upon C_2, R_3, and R_2, this effect cannot be disregarded in the design of an amplifier where the best possible performance is desired. That is, if the bandwidth is specified, R_3 should be as large as possible, to give the greatest midband gain consistent with other requirements on the response characteristic. The latter may, for example, require a response which has maximum flatness, i.e., which never exceeds its low frequency value for any frequency. Thus, although considerable complication results from its inclusion, y_{22e} must be taken into account in order to design for optimum results.

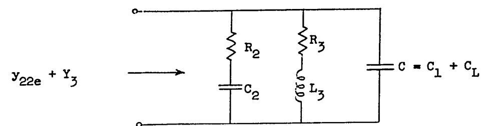

Fig. 5-5. The total output circuit admittance $y_{22e} + Y_3$.

The general expression for the voltage gain K_v in terms of the circuit parameters is

$$\frac{K_v}{K_{vo}} = \frac{(1+sT_2)(1+sT_3)}{(1+s\gamma' T_b)\left\{1+s\left[T_2+R_3(C_2+C)\right]+s^2\left[L_3(C_2+C)+T_2CR_3\right]+s^3CL_3T_2\right\}} \qquad (5\text{-}8)$$

Declassified in Part - Sanitized Copy Approved for Release @ 50-Yr 2013/09/03 : CIA-RDP81-01043R002500170003-9

Declassified in Part - Sanitized Copy Approved for Release @ 50-Yr 2013/09/03 : CIA-RDP81-01043R002500170003-9

where $T_2 = R_2C_2$, $T_3 = L_3/R_3$, and the low-frequency voltage gain K_{vo} is given by

$$K_{vo} = -\frac{b_o R_3}{R_i'} \qquad (5\text{-}9)$$

As R_3 and L_3 are the only adjustable parameters in Eq. 5-8, our control over the form of the response is necessarily limited. If we set

$$R_3 = R_2 = \sqrt{\frac{L_3}{C}} \qquad (5\text{-}10)$$

then the general expression simplifies to,

$$\frac{K_v}{K_{vo}} = \frac{1}{(1+s\gamma' T_b)(1+sT_L)};\ T_L = R_2C \qquad (5\text{-}11)$$

The term $(1+sT_L)$ in Eq. 5-11 is of the same form as that obtained for the vacuum tube amplifier with a parallel RC load. Thus we have a gain-bandwidth trade as far as the effect of the output circuit is concerned, but the added term in Eq. 5-11 imposes a fundamental limitation on the response.

This term commonly corresponds to a frequency in the range of 1 to 3 megacycles, while that corresponding to T_L is generally much higher. Thus the simple form of Eq. 5-11 is of very limited value, and the removal of the term $(1+s\gamma' T_b)$ is highly desirable even if a relatively complicated design procedure is involved.

An examination of Eq. 5-8 shows that either the term $(1+sT_2)$ or $(1+sT_3)$ could be used to cancel that containing $\gamma' T_b$ in the denominator. The former, however, represents a characteristic of the transistor itself and is not subject to control for a given transistor. The alternate choice is to set $\gamma' T_b = T_3$. This determines the ratio L_3/R_3, so that R_3 may be considered as the only remaining adjustable parameter.

For this case, Eq. 5-8 may be re-written in the form

$$\frac{K_v}{K_{vo}} = \frac{1+sT_2}{1+s\left[T_2+R_3(C_2+C)\right] + s^2R_3\left[\gamma' T_b(C+C_2)+T_2C\right] + s^3R_3C\gamma' T_bT_2} \qquad (5\text{-}12)$$

where we have a first power term in s in the numerator and a term in s^3 in the denominator. In general, for arbitrary values of R_3, Eq. 5-12 will not be a desirable form of response, i.e., peaks may exist in the response which result in ringing when a transient input signal is applied. The value of R_3 for maximum flatness may be calculated as

$$R_3 = 2\,\frac{\gamma' T_b - T_2}{C+C_2} \qquad (5\text{-}13)$$

In general, values of R_3 less than this will provide an increased bandwidth, but the response characteristic itself may or may not be flat, depending on the values of the other circuit parameters. Thus, the use of a simple shunt RL circuit in the output offers the possibility of increasing the bandwidth, but offers no means by which specified frequency characteristics may be met. The latter requirement may be met by a more complex network with added degrees of freedom, but here, as in the present case, the transistor itself will impose limitations on the performance available with a given unit.

Referring back to Eq. (5-13) the time constant $\gamma' T_b$ is in general larger than T_2, so that the value of R_3 required is positive. In fact, the value of R_3 as obtained from Eq. (5-13) if frequently large enough so that the voltage gain K_v is quite high. It should be kept in mind that the condition under which we may neglect the internal feedback in the transistor requires $|h_{12e}K_v| \ll 1$, and this will not be true for large values of K_v. Thus, this analysis does not yield accurate results under these conditions. It should be noted that this is of secondary importance, however, as the bandwidth is also reduced to low values. This point is illustrated in the experimental

Declassified in Part - Sanitized Copy Approved for Release @ 50-Yr 2013/09/03 : CIA-RDP81-01043R002500170003-9

Declassified in Part - Sanitized Copy Approved for Release @ 50-Yr 2013/09/03 : CIA-RDP81-01043R002500170003-9

results to be given.

5-3. Exper___ntal Single Stage Amplifiers

In the experimental amplifiers, it is desirable to provide for ease of measurement and rapid change of circuit parameters, in both the amplifier and power supply circuits. (The latter is necessary due to the opposite supply polarities needed for NPN and PNP transistors). This flexibility was provided through the use of the DuMont K-100 Universal Breadboard Chassis Kit. This consists of a framework supported by two end pieces, the former being used to support phenolic "chassis" which are 2 by 4 inches in size. Terminal lugs may be placed in pre-drilled holes in the chassis for electrical connections, while additional holes may be drilled to support peaking coils and other small components.

A chassis with power supply components mounted at the left-hand end and a typical amplifier stage at the right is shown in Figure 5-6. Potentiometers for adjusting the various bias voltages are mounted at the left-hand end of the assembly.

The video amplifier stage in Figure 5-6 is shown actual size in Figure 5-7. Electrical connections to the transistor are made by means of minature Fahenstock clips, the positioning of these being the same as those in the bridge mount described in Chapter 3. A chassis in which the general parts layout is similar, but which uses Alden terminals, is shown in Figure 5-8, also actual size.

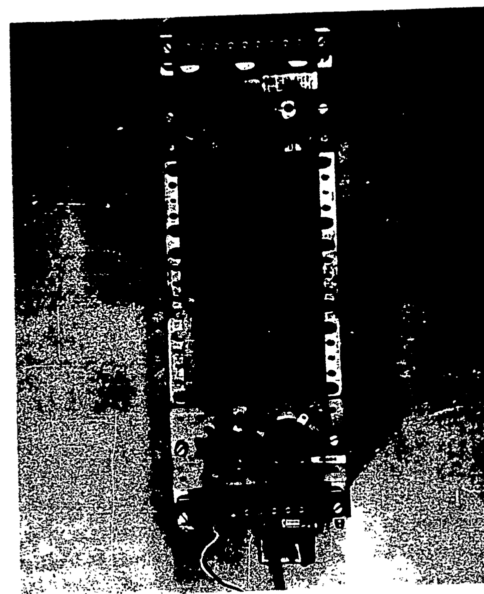

Figure 5-6. DuMont K-100 Chassis Breadboard, with power supply components at the left and video amplifier stage at the right.

Declassified in Part - Sanitized Copy Approved for Release @ 50-Yr 2013/09/03 : CIA-RDP81-01043R002500170003-9

Declassified in Part - Sanitized Copy Approved for Release @ 50-Yr 2013/09/03 : CIA-RDP81-01043R002500170003-9

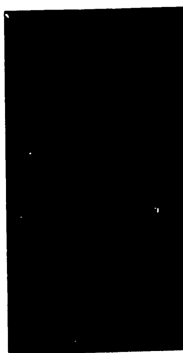

Figure 5-7. Amplifier chassis using minature Fahenstock clips for transistor connections. Actual size photographs.

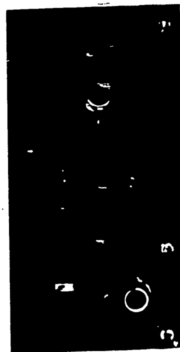

Figure 5-8. Similar to Fig. 5-7, except that Alden clips are used for connections. Actual size photographs.

The type 651DT diode terminal is used for the transistor leads, due to the small wire size, while the type 653T is used for all other connections. These terminals have the advantage that components may be readily changed, a feature of value for electrolytic capacitors where the polarity must be observed in going from NPN to PNP transistor types. It also permits very rapid exchange of the individual chassis on the framework, due to the ease with which the power supply connections may be made.

5-3. Experimental Results.

The circuit for the single-stage amplifier is shown in Figure 5-9.

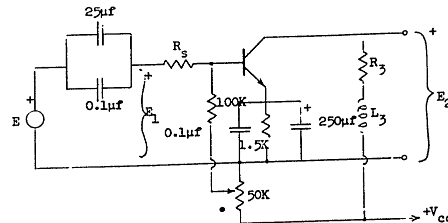

Fig. 5-9. Circuit diagram for the single stange amplifier showing bias connections. The 0.1 mfd. ceramic capacitors are used in parallel with electrolytic units to assure good high-frequency performance.

In taking the response characteristic, the voltage E_1 was held constant so that the effective source resistance for the transistor was R_s. In Figure 5-10 we show the equivalent circuit of Figure 5-4, with the element values labelled for the transistor used, type 2N113-2, in taking the response curves shown later. (The last numeral is for purposes of identification in the laboratory and is not part of the manufacturer's designation.

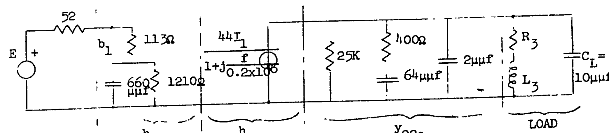

Fig. 5-10. The equivalent circuit for the single stage amplifier, with parameter values for the type 2N113-2 labelled.

Declassified in Part - Sanitized Copy Approved for Release @ 50-Yr 2013/09/03 : CIA-RDP81-01043R002500170003-9

Declassified in Part - Sanitized Copy Approved for Release @ 50-Yr 2013/09/03 : CIA-RDP81-01043R002500170003-9

For this transistor the value of R_3 for maximum flatness (Eq. 5-13) is about 3900 ohms. This value gives a calculated value for K_v of 125, as compared with a measured value of 115. This difference is due to neglecting the 25K shunt resistance in y_{22e}, but is of minor importance in this case.

The measured response characteristic under these conditions is shown in Figure 5-11. The 3 db frequency for L = 0 is 325 kilocycles, while with $L_3 = \gamma' T_b R_3$ the response is improved somewhat, but the new 3 db frequency is only 450 kc. It should be noted that the value of K_{vo} here is so high that neglecting the effect of h_{12e} at high frequencies introduces serious errors so that the preceeding design theory does not provide an accurate answer. On the other hand, the bandwidths attained are well below those required in the majority of wide-band amplifier applications, this being primarily due to the effect of the 64 mmfd. capacitor in y_{22e}. In order to extend the bandwidth, it is necessary to reduce R_3, as was previously mentioned.

Figure 5-12 shows the response of this circuit with $R_3 = R_2 = 400$ ohms and various values of L_3. The midband voltage gain K_{vo} is now calculated to be 12.7, as compared with a measured value of 13.2. For $L_3 = 0$, the measured response is 3 db. down at 1.5 megacycles, showing the effect of the input circuit on the response, as the frequency corresponding to $\gamma' T_b$ is 1.65 megacycles. It should be noted that the response does not drop off at 12 db per octave due to the effect of the term $(1+sT_2)$ in the numerator of Eq. 5-12. This corresponds to a frequency of 6.2 megacycles and tends to reduce the roll-off in the response as this frequency is approached. This point is to be emphasized, as the general appearance of this curve suggests a cutoff due to a single RC or RL time constant.

That this could not be the case is shown by the curve corresponding to $L_3 = \gamma' T_b R_3$. For this case there is a gradual reduction in the high freq-

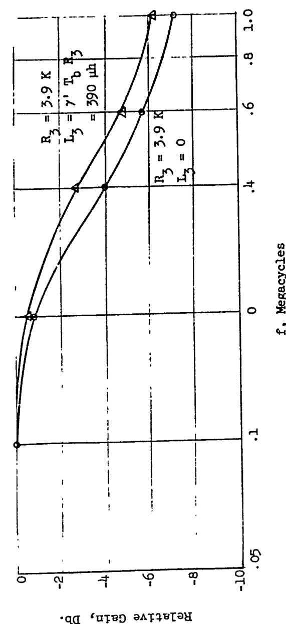

Fig. 5-11. Voltage Gain Response Characteristic for the Circuit of Figure 5-10. Transistor biased at $V_{ce} = -5$ volts, $I_c = -1$ milliampere.

Declassified in Part - Sanitized Copy Approved for Release @ 50-Yr 2013/09/03 : CIA-RDP81-01043R002500170003-9

Declassified in Part - Sanitized Copy Approved for Release @ 50-Yr 2013/09/03 : CIA-RDP81-01043R002500170003-9

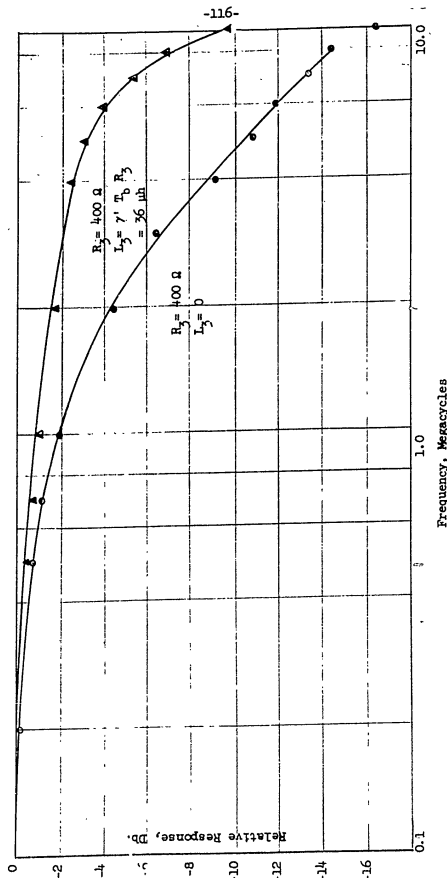

Fig. 5-12. Voltage Gain Response Characteristic of the Circuit of Figure 5-10 with R_3 = 400 ohms for the uncompensated condition (L_3 = 0) and that corresponding to $L_3 = \gamma' T_b R_3$. Bias conditions same as for Fig. 5-11.

uency response, with the 3 db. point occurring at about 5 megacycles. This represents an improvement by a factor of 3.3 to 1 in the high-frequency cut-off, with no loss in midband gain. It will be recalled that the simple shunt-peaking circuit in the vacuum tube case provides an improvement of 1.8 to 1 for no peak in the response, so that the effects here are due to a more complex network. It is worth noting that a somewhat larger value of L_3 than that specified by Eq. 5-12 would provide improved high frequency response. Unfortunately, the analytic determination of this value would involve every term in the expression for the voltage gain, so that this is best determined by final adjustment of L_3 in the circuit.

The above amplifier with a low-frequency gain of 13.2 and a bandwidth of 5 megacycles has a gain-bandwidth product of 66 megacycles, which compares favorably with many vacuum-tube amplifiers. The fundamental reason for this is the fact that the quantity which here corresponds to g_m of the vacuum tube (at low frequencies only) is b_o/R_i' which is 44/1370 or 31,000 micromhos. This is much larger than g_m for the usual pentode used as a video amplifier, a typical value being 5,000 micromhos. On the other hand, the low value of R_3 complicates the problem of obtaining a high output voltage swing from the stage, so that this is a disadvantage where linearity or large swings are important.

5-5. Interstage Equalization

A two-stage amplifier with a simple RL network in the interstage is shown in Figure 5-13.

Declassified in Part - Sanitized Copy Approved for Release @ 50-Yr 2013/09/03 : CIA-RDP81-01043R002500170003-9

Declassified in Part - Sanitized Copy Approved for Release @ 50-Yr 2013/09/03 : CIA-RDP81-01043R002500170003-9

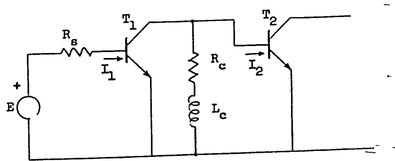

Fig. 5-13. Two stage amplifier with series RL network in the interstage. The current gain $K_i' = I_2/I_1$ may be used as a transfer function. (DC bias networks are not shown).

In analyzing the performance of a network of this type, either the voltage or current gain could be used. However, if we are interested in the overall voltage gain K_v, this may be expressed as $K_v = K_i Z_L/Z_{in}$, where K_i is the overall current gain, and Z_L and Z_{in} the effective load and input impedances, respectively. The current transfer $K_i' = I_2/I_1$ will be considered here, as the overall current gain is just the product of those for the individual stages in the amplifier.

It was shown previously that the use of a shunt resistance R_c in the interstage extends the bandwidth as R_c is reduced, but that a constant-gain bandwidth product is not obtained. We will now show that this may be done for the RL interstage under certain conditions.

The expression for K_i' as obtained from the approximate equivalent circuit is

$$K_i' = \frac{-b_{01}R_c(1+sT_c)(1+sT_{b2})}{(1+sT_{b1})\left[R_c(1+sT_c)(1+sT_{b2})+R_2(1+s\gamma_2 T_{b2})\right]} \qquad (5\text{-}14)$$

where the subscripts 1 and 2 identify the parameter as being for T1 and T2, and the time constant $T_c = L_c/R_c$. Eq. 5-14 is derived under the assumption that the effect of y_{22e} may be neglected compared to the low impedance level of the RL network, an approximation which is generally valid when wide bandwidths are attained.

We see that if the transistors have equal b-cutoff frequencies, then $T_{b1} = T_{b2}$, and Eq. 5-14 will simplify to

$$K_i' = -b_{01}R_c \frac{1+sT_c}{R_c(1+sT_c)(1+sT_{b2})+R_2(1+sT_{b2})} \qquad (5\text{-}15)$$

This may, in turn, be reduced to a transfer function having a single real-axis pole by setting

$$T_c = \gamma_2 T_{b2} \qquad (5\text{-}16)$$

for which case K_i becomes

$$K_i = \frac{-b_{01}m}{1+smT_{b2}} \quad \text{where} \quad m = \frac{R_c}{R_c+R_2} \qquad (5\text{-}17)$$

The angular cutoff frequency for (5-17) is ω_{b2}/m, while its low-frequency value is $-b_{01}m$. We see that the product of these two quantities is constant, so that there is a direct gain-bandwidth exchange. The point illustrated by this case is an interesting one, although of limited practical application due to the restriction that the b-cutoff frequencies must be equal. Eq. 5-14 can always be used in the general case to obtain the overall K_v.

5-6. Two-Stage Amplifier with Interstage and Output Equalization.

Figure 5-14 shows a two-stage amplifier with simple RL compensating networks in both the interstage and output circuits. The overall voltage gain for this system can easily be obtained from the results of the preceeding sections.

Declassified in Part - Sanitized Copy Approved for Release @ 50-Yr 2013/09/03 : CIA-RDP81-01043R002500170003-9

Declassified in Part - Sanitized Copy Approved for Release @ 50-Yr 2013/09/03 : CIA-RDP81-01043R002500170003-9

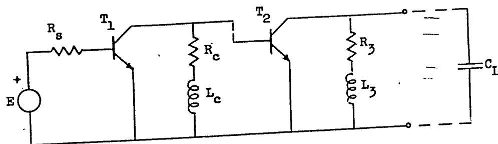

Fig. 5-14. Two stage amplifier with interstage and output networks. Bias components are omitted in this drawing.

The expression for the voltage gain is

$$K_v = \frac{\lambda b_{01} b_{02}}{R'_{i1}} \; \frac{1+sT_c}{(1+s\gamma'_1 T_{b1})\left\{1+s\left[\lambda(T_c+T_{b2})+(1-\lambda)\gamma_2 T_{b2}\right]+s^2\lambda T_c T_{b2}\right\}} \; \frac{1}{y_{22e}+Y_3} \qquad (5\text{-}18)$$

$\lambda = \dfrac{R_c}{R_{i2}+R_c}$ and the low frequency gain is

$$K_{vo} = \frac{b_{01} b_{02} R_c R_3}{R'_{i1}(R_c+R_{i2})} \qquad (5\text{-}19)$$

Here, R_{i2} is the low-frequency value of h_{11e} for T_2, and $T_c = L_c/R_c$ as before. With reference to Section 5-1, the form for $y_{22e} + Y_3$ is:

$$\frac{1}{y_{22e}+Y_3} = \frac{(1+sT_2)(1+sT_3)}{1+s\left[T_2+R_3(C_2+C)\right]+s^2\left[L_3(C_2+C)+T_2 C R_3\right]+s^3 C L_3 T_2} \qquad (5\text{-}20)$$

Thus the general form for K_v for the two-stage amplifier is very complicated, having highest order terms of s^6 and s^3 in denominator and numerator, respectively. An examination of this expression shows, as may be expected, that low values of R_c are essential for good high frequency response.

The adjustable zeros of K_v are T_c and T_3, T_2 being determined by the

particular transistor used. These may be chosen so as to cancel out the term in square brackets in the denominator of Eq. 5-18. That is, we set

$$(1+sT_3)(1+sT_c) = 1+s\,\lambda(T_c+T_{b2})+(1-\lambda)\gamma_2 T_{b2} + s^2\lambda T_c T_{b2} \qquad (5\text{-}21)$$

and equate the coefficients of like powers of s on each side. The results are

$$T_c = \gamma_2 T_{b2} \quad \text{and} \quad T_3 = \lambda T_{b2} \qquad (5\text{-}22)$$

This is a practical approach to the problem, as the largest time constants are those within the square brackets, and their effect upon the response will be most serious. It should be noted that this does not compensate for the factor $(1+s\gamma'_1 T_{b1})$, which, for reasonable values of R_3, is the limiting factor.

The measured and calculated voltage gain as a function of frequency for a two-stage amplifier under these conditions is shown in Figure 5-15. Here the frequency corresponding to $\gamma'_1 T_{b1}$ is 2.7 megacycles, and the low-frequency voltage gain $K_{vo} = 15$. The low frequency gain is nearly the same as that obtained for the single-stage amplifier discussed previously, but the response is much poorer.

An alternate approach which yields better performance is to adjust the zeros at T_c and T_3 so that

$$(1+s\,T_c)(1+s\,T_3)(1+s\,T_2) = (1+s\,\gamma'_1 T_{b1})\left[1+s\left\{\lambda(T_c+T_{b2})+(1-\lambda)\gamma_2 T_{b2}\right\}+s^2\lambda T_c T_{b2}\right]$$

To meet this condition we may set

$$T_c = \gamma'_1\, T_{b1} \qquad (5\text{-}23)$$

and the requirements for T_2 (which is fixed by the transistor used) and T_3 are

Declassified in Part - Sanitized Copy Approved for Release @ 50-Yr 2013/09/03 : CIA-RDP81-01043R002500170003-9

Declassified in Part - Sanitized Copy Approved for Release @ 50-Yr 2013/09/03 : CIA-RDP81-01043R002500170003-9

$$T_2 T_3 = \lambda T_{b2} \gamma_1' T_{b1} \tag{5-24}$$

$$T_2 + T_3 = \lambda(\gamma_1' T_{b1} + T_{b2}) + (1-\lambda)\gamma_2 T_{b2} \tag{5-25}$$

Since both T_3 and λ are parameters which may be chosen at will, these may be solved for T_3 and λ, subject to the restrictions that $T_3 > 0$ and $0 \leq \lambda \leq 1$. Subject to the approximation that $\gamma_1' T_{b1} - \gamma_2 T_{b2} \ll T_{b2}$, the result is

$$\lambda = \frac{T_2}{T_{b2}} \cdot \frac{\gamma_2 T_{b2} - T_2}{\gamma_1' T_{b1} - T_2} \tag{5-26}$$

$$T_3 = \gamma_1' T_{b2} \frac{\gamma_2 T_{b2} - T_2}{\gamma_1' T_{b1} - T_2} \tag{5-27}$$

Due to the complex way in which the time constants enter in, it is difficult to draw general conclusions from these expressions. However, since $T_2 \ll T_{b2}$ will again be small so that the overall K_v is relatively low. The advantage of this design is that the effect of the input circuit is considered, so that the response characteristic is of the form

$$\frac{K_v}{K_{ro}} = \frac{1}{1 + s\left[T_2 + R_3(C_2+C)\right] + s^2\left[L_3(C_2+C) + T_2 C R_3\right] + s^3 C L_3 T_2} \tag{5-28}$$

in which the response may be controlled, within limits, by the choice of R_3.

5-7. Summary

Video amplifiers having reasonable bandwidths and low-frequency voltage gains may be constructed using commercially available transistors. However, the use of simple RL compensating networks does not give the same degree of control over the response as in the vacuum-tube case, as certain parameters must be specified to equalize for the most serious loss in the transistor itself. Thus the design problem will generally require more complex networks for control of the gain, bandwidth, and shape of the response curve, within the limits imposed by the transistor itself.

APPENDIX

Some Characteristics of Transistors Under Hushed Biasing Conditions

During the time the study described in the body of this report was in progress, it came to our attention that a significant improvement in the performance of transistors with respect to their noise properties could be realized by operating at very low values of collector bias voltage. A report on this mode of operation was given by Volkers and Pederson*. They used a common emitter circuit with zero collector to base voltage and .11 emitter to base voltage. The theory of excess noise (noise beyond that contributed by the resistances in the transistor and circuit) is still in a somewhat primitive state and will not be discussed here. In fact interest here is not even centered on the noise properties of transistors. Instead experimental results on transistor circuit behavior under bias conditions reported to give good noise characteristics will be presented. Particular emphasis is on the gain and frequency response of a junction transistor with very low bias voltage. This aspect of the problem is not treated in detail in the work found to date on the hushing principle.

The results of the brief study conducted are summarized in Fig. A-1 for a typical alloy junction transistor (2N136) and Fig. A-2 for a grown junction transistor (2N78). In both cases although the power gain is reduced from the value possible under normal bias

* W. K. Volkers and N. E. Pederson, "The Hushed Transistor Amplifier" TR 54 Millivac Instrument Corporation.

Declassified in Part - Sanitized Copy Approved for Release @ 50-Yr 2013/09/03 : CIA-RDP81-01043R002500170003-9

Declassified in Part - Sanitized Copy Approved for Release @ 50-Yr 2013/09/03 : CIA-RDP81-01043R002500170003-9

conditions, considerable power gains are possible without serious degradation in the frequency response under conditions of "hushing". The ordinate should really be labelled volt ampere gain for the specified load since the input impedance is complex over a large portion of the frequency range. However, since the input power was even less than the input volt-ampere product the curves give a pessimistic picture of the performance under hushed conditions.

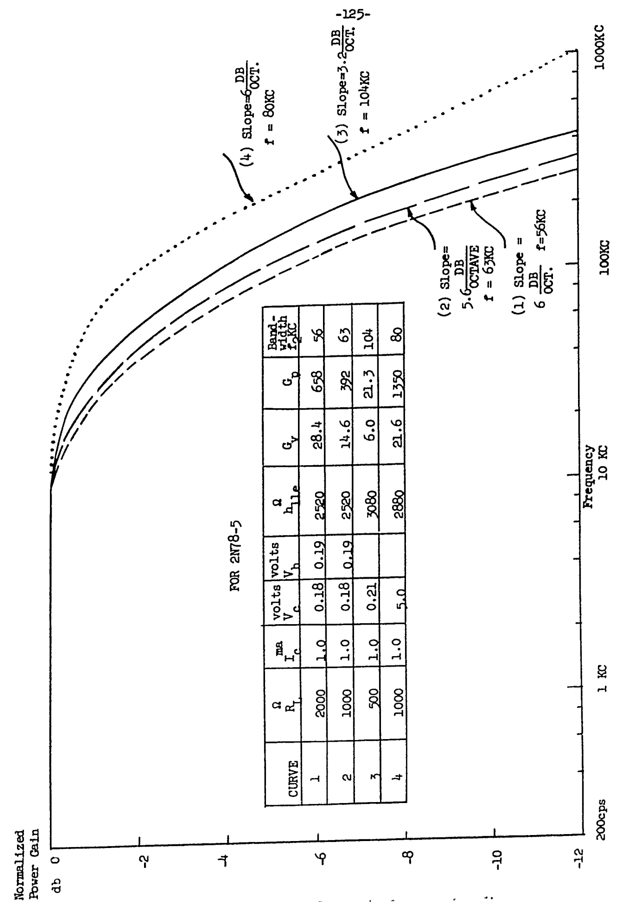

FOR 2N78-5

CURVE	Ω R_L	ma I_c	volts V_c	volts V_b	Ω h_{11e}	G_v	G_p	Band-width f_2KC
1	2000	1.0	0.18	0.19	2520	28.4	658	56
2	1000	1.0	0.18	0.19	2520	14.6	392	63
3	500	1.0	0.21		3080	6.0	21.3	104
4	1000	1.0	5.0		2880	21.6	1350	80

Declassified in Part - Sanitized Copy Approved for Release @ 50-Yr 2013/09/03 : CIA-RDP81-01043R002500170003-9